

Perturbation Analysis of Randomized SVD and its Applications to Statistics

Yichi Zhang* and Minh Tang†

Abstract

Randomized singular value decomposition (RSVD) is a class of computationally efficient algorithms for computing the truncated SVD of large data matrices. Given an $m \times n$ matrix $\widehat{\mathbf{M}}$, the prototypical RSVD algorithm outputs an approximation of the k leading left singular vectors of $\widehat{\mathbf{M}}$ by computing the SVD of $\widehat{\mathbf{M}}(\widehat{\mathbf{M}}^\top \widehat{\mathbf{M}})^g \mathbf{G}$; here $g \geq 1$ is an integer and $\mathbf{G} \in \mathbb{R}^{n \times \tilde{k}}$ is a random Gaussian sketching matrix with $\tilde{k} \geq k$. In this paper we derive upper bounds for the ℓ_2 and $\ell_{2,\infty}$ distances between the exact left singular vectors $\widehat{\mathbf{U}}$ of $\widehat{\mathbf{M}}$ and its approximation $\widehat{\mathbf{U}}_g$ (obtained via RSVD), as well as entrywise error bounds when $\widehat{\mathbf{M}}$ is projected onto $\widehat{\mathbf{U}}_g \widehat{\mathbf{U}}_g^\top$. These bounds depend on the singular values gap and number of power iterations g , and smaller gap requires larger values of g to guarantee the convergences of the ℓ_2 and $\ell_{2,\infty}$ distances. We apply our theoretical results to settings where $\widehat{\mathbf{M}}$ is an additive perturbation of some unobserved signal matrix \mathbf{M} . In particular, we obtain the nearly-optimal convergence rate and asymptotic normality for RSVD on three inference problems, namely, subspace estimation and community detection in random graphs, noisy matrix completion, and PCA with missing data.

Keywords: $2 \rightarrow \infty$ norm, randomized SVD, community detection, matrix completion

Contents

| | | |
|----------|--|-----------|
| 1 | Introduction | 2 |
| 1.1 | Notation | 5 |
| 1.2 | Randomized SVD | 6 |
| 2 | Theoretical results | 7 |
| 2.1 | Refined bounds for low-rank setting | 12 |
| 2.2 | Comparison with existing results | 14 |
| 3 | Random graph inference | 16 |
| 3.1 | Subspace perturbation error bounds | 17 |
| 3.2 | Lower bound and phase transition sharpness | 19 |
| 3.3 | Exact recovery for stochastic blockmodels | 20 |
| 3.4 | Row-wise normal approximation | 22 |
| 4 | Numerical studies | 23 |
| 4.1 | Phase transition | 23 |
| 4.2 | Limiting distribution | 24 |
| 4.3 | Subpopulation discovery of large immune population | 24 |

*Department of Statistics, Indiana University Bloomington. Email: yiczhan@iu.edu

†Department of Statistics, North Carolina State University.

| | |
|--|-----------|
| S1 Additional results for random graph inference | 34 |
| S1.1 Examples of error rates under different parameter regimes | 34 |
| S1.2 Additional numerical results for exact recovery | 35 |
| S2 Matrix completion with noises | 36 |
| S2.1 Theoretical results | 36 |
| S2.2 Real data application: Distance matrix completion | 39 |
| S3 PCA with missing data | 42 |
| S3.1 Computational refinement and theoretical results | 42 |
| S3.2 Extension: HeteroPCA with RSVD approximation | 45 |
| S3.3 Numerical experiments | 47 |
| S3.4 Additional results for Section 4.3 | 49 |
| S4 Distributed estimation for multi-layer networks | 49 |
| S5 Future directions | 51 |
| S6 Proofs for Section 2 | 55 |
| S6.1 Primary | 55 |
| S6.2 Technical lemmas | 56 |
| S6.3 Proof of Theorem 1 | 59 |
| S6.4 Proof of Theorem 2 | 60 |
| S6.4.1 Bounding $\ \mathbf{T}_1\ _{2,\infty}$ | 61 |
| S6.4.2 Bounding $\ \mathbf{T}_2\ _{2,\infty}$ | 63 |
| S6.4.3 Bounding $\ \mathbf{T}_3\ _{2,\infty}$ | 65 |
| S6.4.4 Putting all pieces together | 65 |
| S6.4.5 Bounding $\ (\hat{\mathbf{U}}_g \hat{\mathbf{U}}_g^\top - \hat{\mathbf{U}} \hat{\mathbf{U}}^\top) \hat{\mathbf{M}}\ _{\max}$ | 65 |
| S6.5 Proof of Corollary 2 | 66 |
| S6.6 Proof of Corollary 3 | 68 |
| S7 Proofs for Section 3, Section S2 and Section S3.1 | 70 |
| S7.1 Proof of Theorem 3 | 70 |
| S7.2 Proof of Theorem S6 and Corollary S4 | 72 |
| S7.2.1 Bounding $\ \mathbf{E}\ $ | 73 |
| S7.2.2 Bounding $d_2(\hat{\mathbf{U}}_g, \mathbf{U})$, $d_{2 \rightarrow \infty}(\hat{\mathbf{U}}_g, \mathbf{U})$ and $\ \hat{\mathbf{T}}_g - \mathbf{T}\ _F$ | 74 |
| S7.2.3 Entrywise limiting distribution | 74 |
| S7.2.4 Confidence interval | 75 |
| S7.3 Proof of Theorem S7 | 80 |

1 Introduction

Spectral methods are popular in statistics and machine learning as they provide simple algorithms with strong theoretical guarantees for a diverse number of inference problems including network analysis (Rohe et al., 2011), matrix completion and denoising (Achlioptas and McSherry, 2007; Chatterjee, 2015), covariance estimation/principal component analysis (PCA), non-linear dimension reduction and manifold learning (Belkin and Niyogi, 2003), ranking (Chen et al., 2019), etc. A common unifying theme for spectral algorithms is, given a $\hat{\mathbf{M}}$ of dimensions

$m \times n$, first compute a factorization of $\widehat{\mathbf{M}}$ via singular value decomposition (SVD), keep only the k leading singular values and singular vectors, and finally perform inference using the truncated SVD representation. The value k is usually chosen to be as small as possible while still preserving most of the information.

For many inference problems in statistics, the observed matrix $\widehat{\mathbf{M}}$ is generally noisy due to sampling and/or perturbation errors, i.e., $\widehat{\mathbf{M}}$ is generated from a “signal-plus-noise” model $\widehat{\mathbf{M}} = \mathbf{M} + \mathbf{E}$ where \mathbf{M} is assumed to be the underlying true signal matrix with certain structure such as being (approximately) low rank and/or sparse, and \mathbf{E} is the unobserved perturbation noise. Let $\widehat{\mathbf{U}}$ and \mathbf{U} be the leading singular vectors of $\widehat{\mathbf{M}}$ and \mathbf{M} , respectively. As $\widehat{\mathbf{M}}$ is a noisy realization of \mathbf{M} , $\widehat{\mathbf{U}}$ will also be a noisy estimate of \mathbf{U} and thus the main aim now is to bound the distance between $\widehat{\mathbf{U}}$ and \mathbf{U} or between $\widehat{\mathbf{U}}\widehat{\mathbf{U}}^\top\widehat{\mathbf{M}}$ and \mathbf{M} .

Error bounds for $\widehat{\mathbf{U}}$ is a fundamental topic in matrix perturbation theory. Classical results include the Davis–Kahan and Wedin’s Theorems (Davis and Kahan, 1970; Wedin, 1972) for eigenvectors and singular vectors subspaces; these results make minimal assumptions on \mathbf{E} . The last decade has witnessed further study of matrix perturbations from more statistical perspectives by introducing additional assumptions on \mathbf{E} and \mathbf{M} such as (1) the entries of \mathbf{E} are independent random variables and/or (2) the leading singular vectors of \mathbf{M} has bounded coherence. Examples include more refined matrix concentration inequalities (Tropp, 2012; Oliveira, 2010), rate-optimal subspace perturbation bound (Cai and Zhang, 2018), and $\ell_{2,\infty}$ perturbation bounds (Abbe et al., 2020; Damle and Sun, 2020; Fan et al., 2018; Eldridge et al., 2018; Mao et al., 2021; Cape et al., 2019a,b; Lei, 2019). In particular, error bounds for $\widehat{\mathbf{U}}$ in $\ell_{2,\infty}$ norm (see Section 1.1 for a definition) yields finer and more uniform control between \mathbf{U} and $\widehat{\mathbf{U}}$, and thus can be used to derive limiting distributions for the rows of $\widehat{\mathbf{U}}$ and entrywise confidence intervals for $\widehat{\mathbf{U}}\widehat{\mathbf{U}}^\top\widehat{\mathbf{M}} - \mathbf{M}$; see Chen et al. (2021) for a recent survey with several illustrative examples.

While $\widehat{\mathbf{U}}$ has many desirable statistical properties, its computation can be quite challenging when the dimensions of $\widehat{\mathbf{M}}$ are large. Indeed, many classical algorithms for SVD, such as those based on pivotal QR decompositions and/or Householder transformations, require $O(mn \min\{m, n\})$ floating-point operations (flops) and return the full set of $\min\{m, n\}$ singular values and vectors, even when only the leading $k < m$ of them are desired; see Sections 5.4 and 8.3 of Golub and Van Loan (2013). These algorithms also require random access to the entries of $\widehat{\mathbf{M}}$ and are thus very inefficient when $\widehat{\mathbf{M}}$ is too large to store in RAM due to the need for frequent data transfer between slow and fast memory. Recently in the numerical linear

algebra community, randomized SVD (RSVD) (Rokhlin et al., 2010; Halko et al., 2011; Musco and Musco, 2015) had been widely studied with the aim of providing fast, memory efficient, and accurate approximations for the truncated SVD of large data matrices. The prototypical RSVD algorithm (Halko et al., 2011) first sketches $\widehat{\mathbf{M}}$ into a smaller matrix $\mathbf{Y} = \widehat{\mathbf{M}}(\widehat{\mathbf{M}}^\top \widehat{\mathbf{M}})^g \mathbf{G} \in \mathbb{R}^{m \times \tilde{k}}$ where $\mathbf{G} \in \mathbb{R}^{n \times \tilde{k}}$ is a random matrix, and then uses the k leading left singular vectors of \mathbf{Y} , namely $\widehat{\mathbf{U}}_g$, as an approximation to $\widehat{\mathbf{U}}$. The parameters g and \tilde{k} are user-specified, with g usually a small integer and \tilde{k} being slightly larger than k . There are numerous choices for \mathbf{G} including Gaussian, Rademacher, comcolumn-subsampling, and random orthogonal matrices; see Mahoney (2011); Woodruff (2014); Kannan and Vempala (2017) and the references therein.

The *sketch-and-solve* strategy of RSVD yields an algorithm with computational complexity of $O(mn\tilde{k})$ flops and furthermore these mainly involve the matrix-matrix products $\widehat{\mathbf{M}}\mathbf{X}$ and $\widehat{\mathbf{M}}^\top \mathbf{X}$, where \mathbf{X} is of dimensions $m \times \tilde{k}$ or $n \times \tilde{k}$, which are highly-optimized operations on almost all computing platforms. RSVD is also “pass efficient” (Drineas et al., 2006; Halko et al., 2011) and requires at most $(2g + 1)$ passes through the data; this dramatically reduces memory storage (Golub and Van Loan, 2013; Lopes et al., 2020). Finally, RSVD allows for data compression (Cormode et al., 2011) and can be adapted to a streaming setting (Tropp et al., 2019). Many recent works have replaced classical SVD with RSVD; see e.g., Tsiligkaridis and Hero (2013); Davenport and Romberg (2016); Tsuyuzaki et al. (2020); Zhang et al. (2018); Kumar et al. (2019); Hie et al. (2019) for examples in covariance matrix estimation, matrix completion, and network embeddings.

Existing theoretical results for RSVD, such as those in Rokhlin et al. (2010); Halko et al. (2011); Saibaba (2019); Lopes et al. (2020), focused exclusively on the setting where $\widehat{\mathbf{M}}$ is assumed to be noise-free, i.e., these results either bound $\|\sin \Theta(\widehat{\mathbf{U}}_g, \widehat{\mathbf{U}})\|$ or $\|(\mathbf{I} - \widehat{\mathbf{U}}_g \widehat{\mathbf{U}}_g^\top) \widehat{\mathbf{M}}\|$ where $\|\cdot\|$ denote some unitarily invariant (UI) norm. In particular these error bounds for $\widehat{\mathbf{U}}_g$ decreases as g (the number of power iterations) and/or \tilde{k} (the sketching dimensions) increases. However, if $\widehat{\mathbf{M}}$ is noisy then its leading singular vectors $\widehat{\mathbf{U}}$ will also be a noisy estimate of \mathbf{U} . Under this perspective, the main aim now should be to bound the difference between $\widehat{\mathbf{U}}_g$ and \mathbf{U} , and we thus need to balance between the approximation error of $\widehat{\mathbf{U}}_g$ to $\widehat{\mathbf{U}}$, and the estimation error of $\widehat{\mathbf{U}}$ to \mathbf{U} . This is straightforward and generally leads to sharp bounds when both approximation and estimation errors are in terms of UI norms. However, if results for $\widehat{\mathbf{U}}$ use $\ell_{2,\infty}$ or entrywise norms while those for $\widehat{\mathbf{U}}_g$ use UI norms then their combinations will surely be sub-optimal. In other words, more refined results for $\widehat{\mathbf{U}}$, such as row-wise limiting

distributions of $\hat{\mathbf{U}}$ and entrywise concentration for $\hat{\mathbf{U}}\hat{\mathbf{U}}^\top\hat{\mathbf{M}} - \mathbf{M}$, do not extend directly to that for $\hat{\mathbf{U}}_g$ and $\hat{\mathbf{U}}_g\hat{\mathbf{U}}_g^\top\hat{\mathbf{M}} - \mathbf{M}$.

This paper addresses the above-mentioned gap, i.e., we derive, under minimal assumptions, upper bounds for the $\ell_{2,\infty}$ difference between $\hat{\mathbf{U}}_g$ and $\hat{\mathbf{U}}$, as well as entrywise concentration for $(\hat{\mathbf{U}}_g\hat{\mathbf{U}}_g^\top - \hat{\mathbf{U}}\hat{\mathbf{U}}^\top)\hat{\mathbf{M}}$. As a by-product of our analysis we also obtain bounds for $\|\sin\Theta(\hat{\mathbf{U}}_g, \hat{\mathbf{U}})\|$ comparable to those in the RSVD literature but with a markedly simple proof. In the setting where $\hat{\mathbf{M}}$ is generated under a “signal-plus-noise” model, we show that the ℓ_2 and $\ell_{2,\infty}$ bounds between $\hat{\mathbf{U}}_g$ and \mathbf{U} exhibit a phase-transition phenomenon in that if the signal-to-noise ratio (SNR) decreases then g need to increase to guarantee sharp convergence rates and asymptotic normality. Precise values of g where this transition occurs can also be determined provided that $\hat{\mathbf{M}}$ satisfy a certain trace growth conditions. Finally we apply our theoretical results to three inference problems: subspace estimation and community detection in random graphs, matrix completion, and PCA with missing data. By combining our results for $\hat{\mathbf{U}}_g$ with existing results for $\hat{\mathbf{U}}$, we show that $\hat{\mathbf{U}}_g$ has the same theoretical guarantees as $\hat{\mathbf{U}}$, thus our results provide a bridge between the numerical linear algebra and statistics communities.

Empirically, the effectiveness of RSVD has been demonstrated across a wide range of application domains, including single-cell RNA sequencing (scRNA-seq) (Hie et al., 2019; Tsuyuzaki et al., 2020), geophysical imaging (Kumar et al., 2019), and large-scale network analysis (Zhang et al., 2018). Thus, the primary objective of our numerical studies is not to extend the scope of RSVD’s empirical use, but rather to illustrate the theoretical insights developed in this paper and showcase the statistical validation of RSVD in applications. We conduct simulations and real-data analyses using RSVD for random graph inference, PCA, and matrix completion. These empirical studies consistently support our theoretical predictions, namely that to achieve sharp convergence rates and asymptotic normality under certain SNR regimes requires sufficiently large g and \tilde{k} . We present the random graph simulations and scRNA-seq data analysis in the main text; the remaining numerical results are included in the Supplementary File.

1.1 Notation

Let a be a positive integer. We write $[a]$ to denote the set $\{1, \dots, a\}$. For two non-negative sequences $\{a_n\}_{n \geq 1}$ and $\{b_n\}_{n \geq 1}$, we write $a_n \lesssim b_n$, $b_n \gtrsim a_n$, $a_n = O(b_n)$ or $b_n = \Omega(a_n)$ if there exists a constant $c > 0$ not depending on n such that $a_n \leq cb_n$ for all but finitely many $n \geq 1$. We write $a_n \asymp b_n$ if $a_n \lesssim b_n$ and $a_n \gtrsim b_n$. We write $a_n = o(b_n)$ or $b_n = \omega(a_n)$ if

$\lim_{n \rightarrow \infty} a_n/b_n = 0$. The set of $d \times d'$ matrices with orthonormal columns is denoted as $\mathbb{O}_{d \times d'}$ when $d \neq d'$ and is denoted as \mathbb{O}_d otherwise. Let \mathbf{N} be an arbitrary matrix. We denote the i th row of \mathbf{N} by $[\mathbf{N}]_i$, and the ij th entry of \mathbf{N} by $[\mathbf{N}]_{ij}$. We write $\text{tr } \mathbf{N}$ and $\text{rk}(\mathbf{N})$ to denote the trace and rank of a matrix \mathbf{N} , respectively, and write $\sigma_k(\mathbf{N})$ as the k th largest singular value of \mathbf{N} . The spectral and Frobenius norm of \mathbf{N} are denoted as $\|\mathbf{N}\|$ and $\|\mathbf{N}\|_F$, respectively. The maximum (in modulus) of the entries of \mathbf{N} is denoted as $\|\mathbf{N}\|_{\max}$. In addition we denote the $2 \rightarrow \infty$ norm of \mathbf{N} by $\|\mathbf{N}\|_{2,\infty} = \max_{\|\mathbf{x}\|=1} \|\mathbf{N}\mathbf{x}\|_\infty = \max_i \|[\mathbf{N}]_i\|$, i.e., $\|\mathbf{N}\|_{2,\infty}$ is the maximum of the ℓ_2 norms of the rows of \mathbf{N} . We have the relationships $n^{-1/2}\|\mathbf{N}\| \leq \|\mathbf{N}\|_{2,\infty} \leq \|\mathbf{N}\|$ and $\|\mathbf{N}\|_{\max} \leq \|\mathbf{N}\|_{2,\infty} \leq d^{1/2}\|\mathbf{N}\|_{\max}$, where n and d are the number of rows and columns of \mathbf{N} , respectively. For two matrices $\mathbf{U}_1 \in \mathbb{O}_{n \times d}$ and $\mathbf{U}_2 \in \mathbb{O}_{n \times d}$, we define their ℓ_2 and $\ell_{2,\infty}$ distances as

$$d_2(\mathbf{U}_1, \mathbf{U}_2) := \inf_{\mathbf{W} \in \mathbb{O}_d} \|\mathbf{U}_1 - \mathbf{U}_2 \mathbf{W}\|, \quad d_{2,\infty}(\mathbf{U}_1, \mathbf{U}_2) := \inf_{\mathbf{W} \in \mathbb{O}_d} \|\mathbf{U}_1 - \mathbf{U}_2 \mathbf{W}\|_{2,\infty}.$$

Note that $d_2(\mathbf{U}_1, \mathbf{U}_2) \leq \sqrt{2} \|\sin \Theta(\mathbf{U}_1, \mathbf{U}_2)\|$ where $\sin \Theta(\mathbf{U}_1, \mathbf{U}_2)$ is the diagonal matrix whose elements are the singular values of $(\mathbf{I} - \mathbf{U}_1 \mathbf{U}_1^\top) \mathbf{U}_2$.

1.2 Randomized SVD

Let $\widehat{\mathbf{M}}$ be a $m \times n$ matrix and suppose that we want to compute the singular vectors $\widehat{\mathbf{U}}^{(k)}$ associated with the k largest singular values of $\widehat{\mathbf{M}}$. One popular and widely used approach for computing $\widehat{\mathbf{U}}^{(k)}$ is via randomized subspace iteration. More specifically we first sample an $n \times \tilde{k}$ matrix \mathbf{G} whose entries are iid standard normals and compute $\mathbf{Y}_g = \widehat{\mathbf{M}}^g \mathbf{G}$ if $\widehat{\mathbf{M}}$ is symmetric and $\mathbf{Y}_g = \widehat{\mathbf{M}}(\widehat{\mathbf{M}}^\top \widehat{\mathbf{M}})^g \mathbf{G}$ otherwise, where g is a positive integer. Let $\widehat{\mathbf{U}}_g^{(k)}$ be the $n \times k$ matrix whose columns form an orthonormal basis for the k leading left singular vectors of \mathbf{Y}_g . Then $\widehat{\mathbf{U}}_g^{(k)}$ is an approximation to $\widehat{\mathbf{U}}^{(k)}$ and we can take $\widehat{\mathbf{U}}_g^{(k)} \widehat{\mathbf{U}}_g^{(k)\top} \widehat{\mathbf{M}}$ as a low rank approximation to $\widehat{\mathbf{M}}$; see Algorithm 1 for a formal description. The value of \tilde{k} , the number of columns of \mathbf{G} , is often chosen to be slightly larger than k in order to increase the probability that the column space of \mathbf{Y}_g is closely aligned with $\widehat{\mathbf{U}}^{(k)}$, and empirical observations suggest that $5 \leq \tilde{k} - k \leq 10$ is sufficient for most practical applications (Halko et al., 2011). Algorithm 1 is algebraically equivalent to a version wherein one periodically orthonormalizes $\widehat{\mathbf{M}}(\widehat{\mathbf{M}}^\top \widehat{\mathbf{M}})^{g'} \mathbf{G}$ (via QR decomposition) for $g' < g$ before computing $\widehat{\mathbf{M}}(\widehat{\mathbf{M}}^\top \widehat{\mathbf{M}})^{g'+1} \mathbf{G}$; see e.g., Remark 4.3 of Halko et al. (2011). This extra orthonormalization leads to more numerically stable outputs but has no impact on the theoretical results. For more discussion on randomized subspace

Algorithm 1: RSVD

Input: $\widehat{\mathbf{M}} \in \mathbb{R}^{m \times n}$, rank $k \geq 1$, sketching dimension $\tilde{k} \geq k$, power iterations $g \geq 1$.

- 1 Generate a $n \times k$ sketching matrix \mathbf{G} whose elements are iid standard normals;
- 2 If $\widehat{\mathbf{M}}$ is symmetric, compute $\widehat{\mathbf{M}}^g \mathbf{G}$ by iterating $\widehat{\mathbf{M}}\mathbf{G}, \widehat{\mathbf{M}}(\widehat{\mathbf{M}}\mathbf{G}), \dots, \widehat{\mathbf{M}}(\widehat{\mathbf{M}}^{g-1}\mathbf{G})$,
otherwise, compute $\widehat{\mathbf{M}}(\widehat{\mathbf{M}}^\top \widehat{\mathbf{M}})^g \widehat{\mathbf{G}}$ by iterating $\widehat{\mathbf{M}}\mathbf{G}, \widehat{\mathbf{M}}^\top(\widehat{\mathbf{M}}\mathbf{G}), \dots, \widehat{\mathbf{M}}(\widehat{\mathbf{M}}^\top \widehat{\mathbf{M}})^g \widehat{\mathbf{G}}$;
- 3 Obtain the *exact* SVD of either $\widehat{\mathbf{M}}^g \mathbf{G}$ or $\widehat{\mathbf{M}}(\widehat{\mathbf{M}}^\top \widehat{\mathbf{M}})^g \widehat{\mathbf{G}}$ and let $\widehat{\mathbf{U}}_g^{(k)}$ be the $m \times k$ matrix whose columns are the k leading left singular vectors;

Output: Estimated singular vectors $\widehat{\mathbf{U}}_g^{(k)}$ and low-rank $\widehat{\mathbf{U}}_g^{(k)} \widehat{\mathbf{U}}_g^{(k)\top} \widehat{\mathbf{M}}$.

iteration, see Section 4.5 of [Halko et al. \(2011\)](#), Section 11.6 of [Martinsson and Tropp \(2020\)](#), and Section 4.3 of [Woodruff \(2014\)](#), [Musco and Musco \(2015\)](#). Algorithm 1 is known as the PowerRangeFinder and SubspacePowerMethod in [Halko et al. \(2011\)](#); [Woodruff \(2014\)](#); [Musco and Musco \(2015\)](#).

Remark 1. If we set $g = 1$ in Algorithm 1 then we get the “sketched SVD” algorithm described in [Lopes et al. \(2020\)](#); [Mahoney \(2011\)](#). Sketched SVD is very useful when $\widehat{\mathbf{M}}$ is too large to store in fast memory as the procedure only requires one pass through the data. However, as we will show in Section 2 and Section 3, setting $g = 1$ can lead to poor estimates of \mathbf{U} unless $\tilde{k} = \Omega(n) \gg k$. The choice $\tilde{k} = \Omega(n)$ has recently been considered in the context of sketching PCA ([Yang et al., 2021](#)). However, in practice it is preferable to choose \tilde{k} as small as possible, because the Step 3 in Algorithm 1 requires $O(m\tilde{k}^2)$ flops.

2 Theoretical results

Let $\widehat{\mathbf{M}}$ be a $m \times n$ matrix and for any $k \leq \min\{m, n\}$ denote the SVD of $\widehat{\mathbf{M}}$ by

$$\widehat{\mathbf{M}} := \widehat{\mathbf{U}}^{(k)} \widehat{\Sigma}^{(k)} \widehat{\mathbf{V}}^{(k)\top} + \widehat{\mathbf{U}}_{\perp}^{(k)} \widehat{\Sigma}_{\perp}^{(k)} \widehat{\mathbf{V}}_{\perp}^{(k)\top} \quad (2.1)$$

where $\widehat{\Sigma}^{(k)}$ is the diagonal matrix containing the k largest singular values of $\widehat{\mathbf{M}}$, $\widehat{\mathbf{U}}^{(k)} \in \mathbb{R}^{m \times k}$ and $\widehat{\mathbf{V}}^{(k)} \in \mathbb{R}^{n \times k}$ are the corresponding left and right singular vectors. We now present the general upper bounds for $d_2(\widehat{\mathbf{U}}_g^{(k)}, \widehat{\mathbf{U}}^{(k)})$ and $d_{2,\infty}(\widehat{\mathbf{U}}_g^{(k)}, \widehat{\mathbf{U}}^{(k)})$.

Theorem 1. Let $\widehat{\mathbf{M}}$ be given and compute $\widehat{\mathbf{U}}_g^{(k)}$ via Algorithm 1 for some choices of k, g and \tilde{k} where $n \geq \tilde{k} \geq (1 - c_{\text{gap}})^{-2} \{k + (8k \log(1/\vartheta))^{1/2} + 2 \log(1/\vartheta)\}$; here $c_{\text{gap}} \in (0, 1)$ and $\vartheta > 0$ are both arbitrary. Denote by $\hat{\sigma}_i$ the i th largest singular value of $\widehat{\mathbf{M}}$ and let $\|\cdot\|$ be any unitarily

invariant norm. Then for all $g \geq 1$ we have

$$\|\sin \Theta(\hat{\mathbf{U}}_g^{(k)}, \hat{\mathbf{U}}^{(k)})\| = \|(\mathbf{I} - \hat{\mathbf{U}}_g^{(k)} \hat{\mathbf{U}}_g^{(k)\top}) \hat{\mathbf{U}}^{(k)}\| \leq \frac{3n^{1/2} \|(\hat{\Sigma}_\perp^{(k)})^{\tilde{g}}\|}{c_{\text{gap}} \tilde{k}^{1/2} \hat{\sigma}_k^{\tilde{g}}} \quad (2.2)$$

with probability at least $1 - \vartheta - 2e^{-n/2}$, where $\tilde{g} = g$ if $\hat{\mathbf{M}}$ is symmetric and $\tilde{g} = 2g + 1$ otherwise. Let $\hat{\zeta}_k = \hat{\sigma}_{k+1}/\hat{\sigma}_k$. Eq. (2.2) implies

$$d_2(\hat{\mathbf{U}}_g^{(k)}, \hat{\mathbf{U}}^{(k)}) \leq \sqrt{2} \|\sin \Theta(\hat{\mathbf{U}}_g^{(k)}, \hat{\mathbf{U}}^{(k)})\| \leq \frac{3\sqrt{2}n^{1/2} \hat{\zeta}_k^{\tilde{g}}}{c_{\text{gap}} \tilde{k}^{1/2}} \quad (2.3)$$

with probability at least $1 - \vartheta - 2e^{-n/2}$.

Theorem 2. Consider the setting in Theorem 1. Let $\hat{\zeta}_k = \hat{\sigma}_{k+1}/\hat{\sigma}_k$. For any $\delta > 0$ such that $\tilde{k} \geq 2 \log \delta^{-1}$, define

$$r_{2,\infty} = \frac{\sqrt{128}e(k \log \delta^{-1})^{1/2} \hat{\zeta}_k^{\tilde{g}}}{c_{\text{gap}}^2 \tilde{k}^{1/2}} + \frac{18n \|\hat{\mathbf{U}}^{(k)}\|_{2,\infty} \hat{\zeta}_k^{2\tilde{g}}}{c_{\text{gap}}^2 \tilde{k}} + \frac{36n(\log \delta^{-1})^{1/2} \hat{\zeta}_k^{3\tilde{g}}}{c_{\text{gap}}^3 \tilde{k}} \quad (2.4)$$

where $\tilde{g} = g$ if $\hat{\mathbf{M}}$ is symmetric and $\tilde{g} = 2g + 1$ otherwise. Then for all $g \geq 1$ we have

$$d_{2,\infty}(\hat{\mathbf{U}}_g^{(k)}, \hat{\mathbf{U}}^{(k)}) \leq r_{2,\infty} \quad (2.5)$$

with probability at least $1 - 4m\tilde{k}\delta - \vartheta - 2e^{-n/2}$, where ϑ appears in the lower bound condition for \tilde{k} given in Theorem 1. Furthermore, for any $\gamma > 0$ such that $\tilde{k} \geq 2 \log \gamma^{-1}$, define

$$\tilde{r}_{2,\infty} = \frac{\sqrt{128}e(k \log \gamma^{-1})^{1/2} \hat{\zeta}_k^{\tilde{g}}}{c_{\text{gap}}^2 \tilde{k}^{1/2}} + \frac{18n \|\hat{\mathbf{V}}^{(k)}\|_{2,\infty} \hat{\zeta}_k^{2\tilde{g}}}{c_{\text{gap}}^2 \tilde{k}} + \frac{36n(\log \gamma^{-1})^{1/2} \hat{\zeta}_k^{3\tilde{g}}}{c_{\text{gap}}^3 \tilde{k}}, \quad (2.6)$$

where $\tilde{g} = g$ if $\hat{\mathbf{M}}$ is symmetric and $\tilde{g} = 2g + 1$ otherwise. Then for all $g \geq 1$, we have

$$\|(\hat{\mathbf{U}}_g^{(k)} \hat{\mathbf{U}}_g^{(k)\top} - \hat{\mathbf{U}}^{(k)} \hat{\mathbf{U}}^{(k)\top}) \hat{\mathbf{M}}\|_{\max} \leq \hat{\sigma}_1(r_{2,\infty} \tilde{r}_{2,\infty} + \|\hat{\mathbf{U}}^{(k)}\|_{2,\infty} \tilde{r}_{2,\infty} + \|\hat{\mathbf{V}}^{(k)}\|_{2,\infty} r_{2,\infty}), \quad (2.7)$$

with probability at least $1 - 4\tilde{k}(m\delta + n\gamma) - \vartheta - 2e^{-n/2}$.

Remark 2 (Technical ideas behind the $\ell_{2,\infty}$ bound). We briefly discuss the main technical ideas behind the $\ell_{2,\infty}$ bound in Theorem 2. For clarity we focus on the case where $\hat{\mathbf{M}}$ is an $n \times n$ symmetric matrix with eigendecomposition $\hat{\mathbf{U}} \hat{\Lambda} \hat{\mathbf{U}}^\top + \hat{\mathbf{U}}_\perp \hat{\Lambda}_\perp \hat{\mathbf{U}}_\perp^\top$. Note that the eigenvalues in $\hat{\Lambda}$ and $\hat{\Lambda}_\perp$ are ordered by decreasing magnitude, and the superscript “(k)” is omitted for ease

of notations. If $\tilde{k} - k > 0$ then (with probability one) the column space of $\hat{\mathbf{U}}$ coincides with that of $\check{\mathbf{U}}_g$ whose columns are the k leading left singular vectors of $\hat{\mathbf{U}}\hat{\mathbf{\Lambda}}^g\hat{\mathbf{U}}^\top\mathbf{G}$, and bounding $d_{2,\infty}(\hat{\mathbf{U}}_g, \hat{\mathbf{U}})$ reduces to bounding $d_{2,\infty}(\check{\mathbf{U}}_g, \hat{\mathbf{U}})$. Next note that

$$\widehat{\mathbf{M}}^g\mathbf{G} = \hat{\mathbf{U}}\hat{\mathbf{\Lambda}}^g\hat{\mathbf{U}}^\top\mathbf{G} + \hat{\mathbf{U}}_\perp\hat{\mathbf{\Lambda}}_\perp^g\hat{\mathbf{U}}_\perp^\top\mathbf{G}, \quad (2.8)$$

where the second term on the right-hand side of Eq. (2.8) can be viewed as an additive perturbation. Unlike standard settings, the matrices in Eq. (2.8) are highly unbalanced when $\tilde{k} \ll n$ and also strongly correlated (due to their dependency on a common \mathbf{G}). We address these issues as follows. First we extend the deterministic Procrustes analysis in (Cape et al., 2019b) to decompose the difference between $\check{\mathbf{U}}_g$ and $\hat{\mathbf{U}}_g$ into three terms \mathbf{T}_1 , \mathbf{T}_2 , and \mathbf{T}_3 (see Eq. (S6.12) in the Supplementary File). Next we observe that \mathbf{T}_1 can be represented as the product of two *independent* Gaussian matrices depending on \mathbf{G} from which, after some careful analysis that exploit various properties of \mathbf{G} , we obtain a sharp concentration bound for $\|\mathbf{T}_1\|_{2,\infty}$. Finally we bound $\|\mathbf{T}_2\|_{2,\infty}$ and $\|\mathbf{T}_3\|_{2,\infty}$ using a version of the Wedin sin- Θ theorem for unbalanced matrices (Cai and Zhang, 2018).

Remark 3 (Illustrations of the $r_{2,\infty}$ rate). We simplify the $\ell_{2,\infty}$ bound in (2.5) under different parameter regimes for illustration. Assume that $\widehat{\mathbf{M}}$ is symmetric, k is fixed, $\hat{\zeta}_k \asymp n^{-\psi}$, $\tilde{k} \asymp n^\phi$ for some $\psi > 0$ and $\phi \in (0, 1]$, and $\|\hat{\mathbf{U}}^{(k)}\|_{2,\infty} \asymp n^{-1/2}$. Then (2.5) yields

$$d_{2,\infty}(\hat{\mathbf{U}}_g^{(k)}, \hat{\mathbf{U}}^{(k)}) \lesssim \sqrt{\log n} \cdot n^{-\psi g - \phi/2} + n^{1/2 - 2\psi g - \phi} + \sqrt{\log n} \cdot n^{1 - 3\psi g - \phi} \quad (2.9)$$

with high probability. The dominant term in (2.9) depends on the relative magnitudes of ϕ , ψ and g . For $\phi \approx 0$, the first term dominates when ψg is large, i.e., the singular value gap and the number of power iterations are relatively large, the second term dominates when ψg is moderate, and the third term dominates when ψg is small. For $\phi \approx 1$, the second term is always negligible compared to the first term, and furthermore the first term dominates for large ψg and the third term dominates for small ψg . Finally, for any choice of ϕ , we can make $d_{2,\infty}(\hat{\mathbf{U}}_g^{(k)}, \hat{\mathbf{U}}^{(k)})$ arbitrarily small by increasing ψ , or g , or both. See Section S1 of the Supplementary File for concrete examples in the context of random graph inference.

The choice of c_{gap} in Theorem 1 and Theorem 2 provides a trade-off between the magnitudes of $\tilde{k} - k$ and upper bounds for $\hat{\mathbf{U}}_g^{(k)} - \hat{\mathbf{U}}^{(k)}$ in ℓ_2 and $\ell_{2,\infty}$ norms, i.e., if c_{gap} decreases then

the “oversampling” dimension $\tilde{k} - k$ can be made smaller but the upper bounds in Eq. (2.3), Eq. (2.5), and Eq. (2.7) will increase. In our subsequent discussion we will, for ease of exposition, typically set c_{gap} to an arbitrarily small constant and thus omit factors depending on c_{gap} from our bounds. The condition for \tilde{k} in Theorem 1 and Theorem 2 also depend on ϑ , and this allows us to handle settings where m and n are of very different magnitudes. For example, suppose $n \asymp e^{m^\alpha}$ for some $\alpha > 0$. Then $\log n \gg \log m$ and thus the requirement for \tilde{k} when setting $\vartheta = m^{-1}$ is much less stringent compared to when setting $\vartheta = n^{-1}$. In the same vein, the bounds in Theorem 2 include two additional parameters δ and γ so that we can precisely control the magnitude of $r_{2,\infty}$ and $\tilde{r}_{2,\infty}$ in Eq. (2.5) and Eq. (2.7), e.g., if m and n are of very different magnitude then $\log \delta^{-1}$ and $\log \gamma^{-1}$ can also be of different magnitude, while if $m \asymp n$ then we can choose $\log(\delta^{-1}) = \log(\gamma^{-1}) = \log(\vartheta^{-1}) = (c + 2) \log(m + n)$ to guarantee that all of the bounds in Theorem 1 and Theorem 2 hold with probability at least $1 - O((m + n)^{-c})$ where $c > 0$ is any arbitrary constant. Finally, for concreteness we had include explicit constants in our statement of Theorem 1 and Theorem 2 but their values are chosen mainly for ease of exposition and are thus possibly sub-optimal.

Remark 4. For conciseness we only stated Theorem 1 and Theorem 2 for the approximate left singular vectors $\hat{\mathbf{U}}_g^{(k)}$. Results for the approximate right singular vectors $\hat{\mathbf{V}}_g^{(k)}$ are obtained simply by applying the algorithms and theorems to $\hat{\mathbf{M}}^\top$, i.e., we replace n with m in Theorem 1 and swap the roles of m and n (as well as the roles of $\hat{\mathbf{U}}^{(k)}$ and $\hat{\mathbf{V}}^{(k)}$) in Theorem 2. For example, we have

$$d_2(\hat{\mathbf{V}}_g^{(k)}, \hat{\mathbf{V}}^{(k)}) \leq \frac{3\sqrt{2}m^{1/2}}{c_{\text{gap}}\tilde{k}^{1/2}} \left(\frac{\hat{\sigma}_{k+1}}{\hat{\sigma}_k} \right)^{\tilde{g}} \quad (2.10)$$

with probability at least $1 - \vartheta - 2e^{-m/2}$ and

$$d_{2,\infty}(\hat{\mathbf{V}}_g^{(k)}, \hat{\mathbf{V}}^{(k)}) \leq \frac{\sqrt{128}e(k \log \delta^{-1})^{1/2} \hat{\zeta}_k^{\tilde{g}}}{c_{\text{gap}}^2 \tilde{k}^{1/2}} + \frac{18m \hat{\zeta}_k^{2\tilde{g}} \|\hat{\mathbf{V}}^{(k)}\|_{2,\infty}}{c_{\text{gap}}^2 \tilde{k}} + \frac{36m(\log \delta^{-1})^{1/2} \hat{\zeta}_k^{3\tilde{g}}}{c_{\text{gap}}^3 \tilde{k}} \quad (2.11)$$

with probability at least $1 - 4n\tilde{k}\delta - \vartheta - 2e^{-m/2}$.

Remark 5. In this paper we only considered Gaussian sketching matrices as they are (1) most commonly used and (2) lead to simple and precise theoretical results. Other type of \mathbf{G} such as uniform and Rademacher have also been studied in the literature (Mahoney, 2011; Woodruff, 2014; Kannan and Vempala, 2017). We note that any distribution for \mathbf{G} that satisfies Lemma S3 in the Supplementary, will also lead to the same $\sin \Theta$ upper bounds (up to some multiplicative

constants) as those presented in Theorem 1. In contrast, the analysis in Theorem 2 leverage several properties that are intrinsic to normal random variables. We thus leave the extension of Theorem 2 for non-Gaussian \mathbf{G} to future work.

Finally, let \mathbf{M} be a $m \times n$ matrix and, similar to Eq.(2.1), denote its SVD by

$$\mathbf{M} := \mathbf{U}^{(k)} \mathbf{\Sigma}^{(k)} \mathbf{V}^{(k)\top} + \mathbf{U}_{\perp}^{(k)} \mathbf{\Sigma}_{\perp}^{(k)} \mathbf{V}_{\perp}^{(k)\top},$$

where $\mathbf{\Sigma}^{(k)}$ is the diagonal matrix containing the k largest singular values of \mathbf{M} and $\mathbf{U}^{(k)}, \mathbf{V}^{(k)}$ are the corresponding left and singular vectors. Next suppose we only observe $\widehat{\mathbf{M}} = \mathbf{M} + \mathbf{E}$ and want to use $\widehat{\mathbf{U}}_g^{(k)}$ as an estimate for $\mathbf{U}^{(k)}$. Then, by Weyl's inequality, $|\hat{\sigma}_i - \sigma_i| \leq \|\mathbf{E}\|$ for all i , where $\sigma_1 \geq \sigma_2 \geq \dots$ are the singular values of \mathbf{M} . Thus if $\sigma_k > \|\mathbf{E}\|$ then $\hat{\zeta}_k = \hat{\sigma}_{k+1}/\hat{\sigma}_k \leq (\sigma_{k+1} + \|\mathbf{E}\|)/(\sigma_k - \|\mathbf{E}\|)$. Substituting this bound for $\hat{\zeta}_k$ into Theorem 1 and Theorem 2 we directly obtain upper bounds for $d_2(\widehat{\mathbf{U}}_g^{(k)}, \mathbf{U}^{(k)})$ and $d_{2,\infty}(\widehat{\mathbf{U}}_g^{(k)}, \mathbf{U}^{(k)})$ that depend only on $\|\mathbf{E}\|$ and $\{\sigma_k, \sigma_{k+1}\}$.

Corollary 1. *Consider the setting in Theorem 1 and suppose that $\widehat{\mathbf{M}} = \mathbf{M} + \mathbf{E}$ where k is chosen such that $\sigma_k > \|\mathbf{E}\|$. Let*

$$\zeta_k = (\sigma_{k+1} + \|\mathbf{E}\|)/(\sigma_k - \|\mathbf{E}\|),$$

and define $r'_{2,\infty}$ and $\tilde{r}'_{2,\infty}$ as $r_{2,\infty}$ and $\tilde{r}_{2,\infty}$ in Eq. (2.4) and Eq. (2.6) but with ζ_k , $u_{2,\infty} := \|\mathbf{U}^{(k)}\|_{2,\infty} + d_{2,\infty}(\widehat{\mathbf{U}}^{(k)}, \mathbf{U}^{(k)})$, and $v_{2,\infty} := \|\mathbf{V}^{(k)}\|_{2,\infty} + d_{2,\infty}(\widehat{\mathbf{V}}^{(k)}, \mathbf{V}^{(k)})$ in place of $\hat{\zeta}_k$, $\|\widehat{\mathbf{U}}^{(k)}\|_{2,\infty}$, and $\|\widehat{\mathbf{V}}^{(k)}\|_{2,\infty}$ respectively. Then for all $g \geq 1$ we have

$$|d_2(\widehat{\mathbf{U}}_g^{(k)}, \mathbf{U}^{(k)}) - d_2(\widehat{\mathbf{U}}^{(k)}, \mathbf{U}^{(k)})| \leq d_2(\widehat{\mathbf{U}}_g^{(k)}, \widehat{\mathbf{U}}^{(k)}) \leq 3\sqrt{2}c_{\text{gap}}^{-1}(n/\tilde{k})^{1/2}\zeta_k^{\tilde{g}}$$

with probability at least $1 - \vartheta - 2e^{-n/2}$, and

$$|d_{2,\infty}(\widehat{\mathbf{U}}_g^{(k)}, \mathbf{U}^{(k)}) - d_{2,\infty}(\widehat{\mathbf{U}}^{(k)}, \mathbf{U}^{(k)})| \leq d_{2,\infty}(\widehat{\mathbf{U}}_g^{(k)}, \widehat{\mathbf{U}}^{(k)}) \leq r'_{2,\infty},$$

with probability at least $1 - 4m\tilde{k}\delta - \vartheta - 2e^{-n/2}$. Finally, denote $\widehat{\mathbf{\Pi}}_g^{(k)} = \widehat{\mathbf{U}}_g^{(k)} \widehat{\mathbf{U}}_g^{(k)\top}$ and $\widehat{\mathbf{\Pi}}^{(k)} = \widehat{\mathbf{U}}^{(k)} \widehat{\mathbf{U}}^{(k)\top}$. Then we also have

$$|\|\widehat{\mathbf{\Pi}}_g^{(k)} \widehat{\mathbf{M}} - \mathbf{M}\|_{\max} - \|\widehat{\mathbf{\Pi}}^{(k)} \widehat{\mathbf{M}} - \mathbf{M}\|_{\max}| \leq (\sigma_1 + \|\mathbf{E}\|) (r'_{2,\infty} \tilde{r}'_{2,\infty} + u_{2,\infty} \tilde{r}'_{2,\infty} + v_{2,\infty} r'_{2,\infty}) \quad (2.12)$$

with probability at least $1 - 4\tilde{k}(m\delta + n\gamma) - \vartheta - 2e^{-n/2}$. In all of the above bounds we have $\tilde{g} = g$ if $\widehat{\mathbf{M}}$ is symmetric and $\tilde{g} = 2g + 1$ otherwise.

2.1 Refined bounds for low-rank setting

Theorems 1 and Theorem 2 hold for any $\widehat{\mathbf{M}}$, any k , and any g . In particular they implied that if $\widehat{\mathbf{M}} = \mathbf{M} + \mathbf{E}$ and there exists a $c > 1$ such that $1/\zeta_k = (\sigma_k - \|\mathbf{E}\|)/(\sigma_{k+1} + \|\mathbf{E}\|) \geq c$ then the upper bounds in Corollary 1 converge to 0 at rate c^{-g} , and are thus negligible for $g = \Omega(\log(n)/\log(c))$. If \mathbf{M} is low-rank with $\text{rk}(\mathbf{M}) = k_0$, then the bounds in Corollary 1 can be further refined when we choose $k = k_0$, especially when $\|\mathbf{E}\| \ll \sigma_{k_0}$. To reduce notational burden we only present results when $\widehat{\mathbf{M}}$ is symmetric (this is sufficient for our discussion in Section 3) so that the subsequent bounds and probabilities can be stated explicitly in terms of n, \tilde{k} and $\sigma_{k_0}/\|\mathbf{E}\|$. Similar results hold when $\widehat{\mathbf{M}}$ is asymmetric/rectangular and we leave them to the interested reader.

Corollary 2. Assume the setting of Corollary 1 where $\widehat{\mathbf{M}}$ is a symmetric $n \times n$ matrix with $\text{rk}(\mathbf{M}) = k_0$. Denote $E_n = \|\mathbf{E}\|$ and let $\widehat{\mathbf{U}}_g^{(k_0)}$ be computed from $\widehat{\mathbf{M}}$ via Algorithm 1 for some choice of $\tilde{k} \geq (1 - c_{\text{gap}})^{-2}(k_0 + \sqrt{24k_0 \log n} + 6 \log n)$ where $c_{\text{gap}} \in (0, 1)$ is a fixed but arbitrary constant. For any specified $\iota > 0$, let $g_\iota = \frac{\log\{3\sqrt{2}c_{\text{gap}}^{-1}(n/\tilde{k})^{1/2}\iota^{-1}\}}{\log(1/\zeta_{k_0})}$. If $\sigma_{k_0} > 2E_n$ then we have

$$d_2(\widehat{\mathbf{U}}_g^{(k_0)}, \mathbf{U}^{(k_0)}) \leq (1 + \iota \cdot \zeta_{k_0}^{g-g_\iota-1}) \frac{E_n}{\sigma_{k_0}}, \text{ for any } g \geq 1, \quad (2.13)$$

with probability at least $1 - 2n^{-3}$; recall $\zeta_{k_0} = E_n/(\sigma_{k_0} - E_n) < 1$. Furthermore, if $\sigma_{k_0}/E_n \gtrsim n^\epsilon$ for some fixed but arbitrary $\epsilon > 0$ then Eq. (2.13) can be refined to

$$d_2(\widehat{\mathbf{U}}_g^{(k_0)}, \mathbf{U}^{(k_0)}) \leq \begin{cases} O((E_n/\sigma_{k_0})^{g-g_*}) & \text{if } g_* \leq g \leq 1 + g_* \\ (1 + o(1))E_n/\sigma_{k_0} & \text{if } g \geq 1 + g_* + \Delta \end{cases}, \quad (2.14)$$

with probability at least $1 - 2n^{-3}$. Here $g_* = \frac{\log(n/\tilde{k})}{2\log(1/\zeta_{k_0})}$ and $\Delta = \omega(\log^{-1} n)$ is arbitrary; note that $g_* \leq (2\epsilon)^{-1}$ for sufficiently large n .

Remark 6. We now discuss two special cases of Corollary 2.

1. Suppose $cn \leq \tilde{k} \leq (1-c)n$ for some constant $c \in (0, 1)$ and $\sigma_{k_0} = \omega(E_n)$. Then $\frac{\log(n/\tilde{k})}{2\log(1/\zeta_{k_0})} = o(1)$, and setting $\iota = 4\sqrt{2}c_{\text{gap}}^{-1}c^{-1/2}$ in (2.13) we obtain $d_2(\widehat{\mathbf{U}}_g^{(k_0)}, \mathbf{U}^{(k_0)}) = (1 + o(1))E_n/\sigma_{k_0}$ for all $g \geq 1$, with probability at least $1 - 2n^{-3}$. In other words, if we estimate $\mathbf{U}^{(k_0)}$ using

only the leading singular vectors of the sketched matrix $\widehat{\mathbf{M}}\mathbf{G}$ then we need a sketching dimension of $\tilde{k} = \Omega(n)$. A similar phenomenon was observed for PCA using random projections (Yang et al., 2021).

2. Next suppose k_0 is bounded by a finite constant and $\tilde{k} \asymp \log n$. If $\sigma_{k_0}/E_n \gtrsim n^\epsilon$ for some fixed but arbitrary $\epsilon > 0$ then (2.14) implies

$$d_2(\widehat{\mathbf{U}}_g^{(k_0)}, \mathbf{U}^{(k_0)}) \leq (1 + o(1))E_n/\sigma_{k_0} \text{ for all } g \geq 1 + (2\epsilon)^{-1}, \quad (2.15)$$

with probability at least $1 - 2n^{-3}$, as $(2\epsilon)^{-1} - g_* = \omega(\log^{-1} n)$.

Corollary 3. Assume the setting of Corollary 2 with $\sigma_{k_0} > 2E_n$ where $E_n = \|\mathbf{E}\|$. Define

$$g_* = \max \left\{ 1 + \frac{\log(nk_0/\tilde{k}) + \log \log n}{2 \log(\frac{1}{2}\sigma_{k_0}/E_n)}, \frac{1}{3} + \frac{\log(n^{3/2}/\tilde{k}) + \frac{1}{2} \log \log n}{3 \log(\frac{1}{2}\sigma_{k_0}/E_n)}, \frac{1}{2} + \frac{\log(n^{3/2}\|\mathbf{U}^{(k_0)}\|_{2,\infty}/\tilde{k})}{2 \log(\frac{1}{2}\sigma_{k_0}/E_n)} \right\},$$

Suppose also that $d_{2,\infty}(\widehat{\mathbf{U}}^{(k_0)}, \mathbf{U}^{(k_0)}) \leq \|\mathbf{U}^{(k_0)}\|_{2,\infty}$. We then have, for all $g \geq g_*$,

$$d_{2,\infty}(\widehat{\mathbf{U}}_g^{(k_0)}, \mathbf{U}^{(k_0)}) \leq d_{2,\infty}(\widehat{\mathbf{U}}^{(k_0)}, \mathbf{U}^{(k_0)}) + O(n^{-1/2}E_n/\sigma_{k_0}) \quad (2.16)$$

with probability at least $1 - 5n^{-3} - 2e^{-n/2}$, where the hidden factor in $O(n^{-1/2}E_n/\sigma_{k_0})$ only depend on c_{gap} . Furthermore for all $g \geq g_*$ we have

$$\|\widehat{\mathbf{U}}_g^{(k_0)}\widehat{\mathbf{U}}_g^{(k_0)\top}\widehat{\mathbf{M}} - \mathbf{M}\|_{\max} \leq \|\widehat{\mathbf{U}}^{(k_0)}\widehat{\mathbf{U}}^{(k_0)\top}\widehat{\mathbf{M}} - \mathbf{M}\|_{\max} + O(\kappa n^{-1/2}E_n\|\mathbf{U}\|_{2,\infty}), \quad (2.17)$$

with probability at least $1 - 9n^{-3} - 2e^{-n/2}$, where $\kappa = \sigma_1/\sigma_{k_0}$ is the condition number for \mathbf{M} and the hidden factor in $O(n^{-1/2}\kappa E_n\|\mathbf{U}^{(k_0)}\|_{2,\infty})$ only depends on c_{gap} .

If $\sigma_k = \omega(E_n)$ then the terms $O(n^{-1/2}E_n/\sigma_{k_0})$ and $O(\kappa n^{-1/2}E_n\|\mathbf{U}^{(k_0)}\|_{2,\infty})$ in Eq. (2.16) and Eq. (2.17) can be replaced by $o(n^{-1/2}E_n/\sigma_{k_0})$ and $o(\kappa n^{-1/2}E_n\|\mathbf{U}^{(k_0)}\|_{2,\infty})$ provided that $g \geq g_* + \Delta$ where $\Delta > 0$ is any arbitrary constant. Finally if $\sigma_{k_0}/E_n \gtrsim n^\epsilon$ for a fixed but arbitrary $\epsilon > 0$ then the above expression for g_* can be simplified to

$$g_* = \max \left\{ 1 + \frac{\log(nk_0/\tilde{k})}{2 \log(\sigma_{k_0}/E_n)}, \frac{1}{3} + \frac{\log(n^{3/2}/\tilde{k})}{3 \log(\sigma_{k_0}/E_n)}, \frac{1}{2} + \frac{\log(n^{3/2}\|\mathbf{U}^{(k_0)}\|_{2,\infty}/\tilde{k})}{2 \log(\sigma_{k_0}/E_n)} \right\}. \quad (2.18)$$

2.2 Comparison with existing results

For ease of exposition we will fix some choice of k and thus drop the index k from the matrices $\hat{\mathbf{U}}_g^{(k)}$ and $\hat{\mathbf{U}}^{(k)}$. Also, we will implicitly assume that $\tilde{g} = g$ if $\widehat{\mathbf{M}}$ is symmetric and $\tilde{g} = 2g + 1$ otherwise. As we alluded to in the introduction, theoretical analysis of RSVD mostly focused on spectral and Frobenius norms upper bounds for $\sin \Theta(\hat{\mathbf{U}}_g, \hat{\mathbf{U}})$ and $(\mathbf{I} - \hat{\mathbf{U}}_g \hat{\mathbf{U}}_g^\top) \widehat{\mathbf{M}}$ in settings where $\widehat{\mathbf{M}}$ is assumed to be *noise-free*.

Let $\|\cdot\|$ be any unitarily invariant norm. By combining Theorems 4 and 6 in [Saibaba \(2019\)](#), we have

$$\|\sin \Theta(\hat{\mathbf{U}}_g, \hat{\mathbf{U}})\| \leq \frac{C \tilde{k}^{1/2} \|\hat{\Sigma}_\perp^{\tilde{g}}\|}{\hat{\sigma}_k^{\tilde{g}} (1 - \hat{\zeta}_k) (\tilde{k} - k + 1) \eta^{1/(\tilde{k} - k + 1)}} ((n - k)^{1/2} + \tilde{k}^{1/2} + (\log 1/\eta)^{1/2}) \quad (2.19)$$

with probability at least $1 - \eta$, where C is a universal constant. Ignoring constant factors, Eq. (2.2) is similar to Eq. (2.19), with the main difference being that Eq. (2.19) include extra factors $\eta^{1/(\tilde{k} - k + 1)}$ and $(1 - \hat{\zeta}_k)$ in the denominator. Our bound in Eq. (2.2) is therefore sharper than Eq. (2.19) when $\hat{\zeta}_k = \hat{\sigma}_{k+1}/\hat{\sigma}_k \approx 1$ and/or $\eta \rightarrow 0$.

Next, for $(\mathbf{I} - \hat{\mathbf{U}}_g \hat{\mathbf{U}}_g^\top) \widehat{\mathbf{M}}$, let $\Pi_{\mathbf{Y}_g}$ be the orthogonal projection onto the column space of \mathbf{Y}_g where $\mathbf{Y}_g = \widehat{\mathbf{M}}^g \mathbf{G}$ if $\widehat{\mathbf{M}}$ is symmetric and $\mathbf{Y}_g = \widehat{\mathbf{M}} (\widehat{\mathbf{M}}^\top \widehat{\mathbf{M}})^g \mathbf{G}$ otherwise. Then by Corollary 10.10 in [Halko et al. \(2011\)](#) we have for $\tilde{k} \geq k + 2$ that

$$\|(\mathbf{I} - \Pi_{\mathbf{Y}_g}) \widehat{\mathbf{M}}\| \leq \left(1 + \frac{k^{1/2}}{(\tilde{k} - k - 1)^{1/2}} + \frac{e \tilde{k}^{1/2} (\min\{m, n\} - k)^{1/2}}{\tilde{k} - k}\right)^{1/\tilde{g}} \hat{\sigma}_{k+1} \quad (2.20)$$

with high probability. Meanwhile, from Theorem 1 we have by the triangle inequality that

$$\|(\mathbf{I} - \hat{\mathbf{U}}_g \hat{\mathbf{U}}_g^\top) \widehat{\mathbf{M}}\| \leq C (n/\tilde{k})^{1/2} (\hat{\sigma}_{k+1}/\hat{\sigma}_k)^{\tilde{g}} \hat{\sigma}_1 + \hat{\sigma}_{k+1} \quad (2.21)$$

with high probability, where C is a universal constant. Comparing Eq. (2.20) and Eq. (2.21) we see that they both converge to $\hat{\sigma}_{k+1}$ as \tilde{g} increases, but the manner in which they converge can be significantly different. More specifically Eq. (2.20) does not depend on the singular value gap $\hat{\sigma}_{k+1}/\hat{\sigma}_k$ but its rate of convergence becomes slower for larger values of \tilde{g} . In contrast, Eq. (2.21) depends on $(\hat{\sigma}_{k+1}/\hat{\sigma}_k)^{\tilde{g}}$ and converges to $\hat{\sigma}_{k+1}$ rather quickly if $\hat{\sigma}_{k+1} \ll \hat{\sigma}_k$ but arbitrarily slowly when $\hat{\sigma}_{k+1} \approx \hat{\sigma}_k$. For many statistical applications including those in Section 3 and Sections S2-S3.1, \mathbf{M} will be approximately low-rank so that bounds based on Eq. (2.21) are sharper than

those derived from Eq. (2.20).

We now discuss the upper bounds for $d_{2 \rightarrow \infty}(\hat{\mathbf{U}}_g, \hat{\mathbf{U}})$. Perturbation bounds in $\ell_{2,\infty}$ norm is rarely studied in the RSVD literature and among existing results, the one that is perhaps most related to ours is from Proposition 1 in Charisopoulos et al. (2020) wherein the authors approximate the leading eigenvectors of a symmetric $\hat{\mathbf{M}}$ using a subspace iteration procedure similar to that in Algorithm 1 with $\tilde{k} = k$, and they showed that

$$d_{2,\infty}(\hat{\mathbf{U}}_g, \hat{\mathbf{U}}) \leq \frac{1}{\sqrt{1-d_0^2}} \left(\frac{\hat{\sigma}_{k+1}}{\hat{\sigma}_k} \right)^g \left[\sqrt{2}d_0 + C_*(1 + \sqrt{n}\|\hat{\mathbf{U}}\|_{2,\infty})d_{2,\infty}(\hat{\mathbf{U}}_0, \hat{\mathbf{U}}) \right] \quad (2.22)$$

for all $g \geq 1$, where $\hat{\mathbf{U}}_0$ denote any arbitrary initial estimate for $\hat{\mathbf{U}}$ and $d_0 := d_2(\hat{\mathbf{U}}_0, \hat{\mathbf{U}})$. Eq. (2.22) is similar in spirit to ours Eq. (2.5), with the most obvious difference being that Eq. (2.5) include terms with extra factors of $(n/\tilde{k})^{1/2}$ and $(\hat{\sigma}_{k+1}/\hat{\sigma}_k)^{\tilde{g}}$. The main limitation of Eq. (2.22), however, lies in the fact that it depends on the assumption

$$\|\hat{\mathbf{U}}_{\perp} \hat{\Sigma}^g \hat{\mathbf{U}}_{\perp}^{\top}\|_{\infty} \leq C_* \hat{\sigma}_{k+1}^g \|\mathbf{I} - \hat{\mathbf{U}} \hat{\mathbf{U}}^{\top}\|_{\infty} \quad (2.23)$$

for all $g \geq 1$, where $\|\cdot\|_{\infty}$ denote the maximum row-sum (after taking absolute values) of a matrix, and C_* is the constant appearing in Eq. (2.22); see Assumption 1 in Charisopoulos et al. (2020) for more details. The condition in Eq. (2.23) can be restrictive. In particular, for many statistical applications including random graph inference and matrix completion, we have $\hat{\mathbf{M}} = \mathbf{M} + \mathbf{E}$ where \mathbf{M} is low-rank, \mathbf{U} has bounded coherence, and $\|\mathbf{E}\|_{\infty} \gg \|\mathbf{E}\|$. Letting $k = \text{rk}(\mathbf{M})$, we typically have $\|\hat{\mathbf{U}} \hat{\Sigma} \hat{\mathbf{U}}^{\top} - \mathbf{M}\|_{\infty} \ll \|\mathbf{E}\|_{\infty}$ and $\|\hat{\mathbf{U}} \hat{\mathbf{U}}^{\top}\|_{\infty} \asymp 1$ so that

$$\|\hat{\mathbf{U}}_{\perp} \hat{\Sigma}_{\perp}^g \hat{\mathbf{U}}_{\perp}^{\top}\|_{\infty} \geq \|\hat{\mathbf{M}} - \mathbf{M}\|_{\infty} - \|\hat{\mathbf{U}} \hat{\Sigma} \hat{\mathbf{U}}^{\top} - \mathbf{M}\| \gtrsim \|\mathbf{E}\|_{\infty} \gg \|\mathbf{E}\| \asymp \hat{\sigma}_{k+1} \|\mathbf{I} - \hat{\mathbf{U}} \hat{\mathbf{U}}^{\top}\|_{\infty},$$

and hence Eq. (2.23) does not hold for $g = 1$. In contrast, the only assumption we need for Theorem 2 is that \tilde{k} is lower bounded, i.e., $\tilde{k} \geq (1 - c_{\text{gap}})^{-2} \{\sqrt{k} + \sqrt{2 \log \vartheta^{-1}}\}^2$ where c_{gap} and ϑ are both arbitrary. The discrepancies between the above sets of assumptions is mainly because the analysis in Charisopoulos et al. (2020) is for subspace iteration and not *randomized* subspace iteration. More specifically, Charisopoulos et al. (2020) viewed $\hat{\mathbf{U}}_0$ as given but arbitrary and thus they cannot control $\hat{\mathbf{U}}_{\perp} \hat{\Sigma}_{\perp}^{\tilde{g}} \hat{\mathbf{U}}_{\perp}^{\top} \hat{\mathbf{U}}_0$ for all g and all $\hat{\mathbf{U}}_0$ without making (possibly restrictive) assumptions on $\hat{\mathbf{M}}$ itself. In contrast, as we assume that $\hat{\mathbf{U}}_0$ is a random matrix independent of $\hat{\mathbf{M}}$ and only dependent on \mathbf{G} , we can leverage the randomness in $\hat{\mathbf{U}}_0$ to bound $\hat{\mathbf{U}}_{\perp} \hat{\Sigma}_{\perp}^{\tilde{g}} \hat{\mathbf{U}}_{\perp}^{\top} \hat{\mathbf{U}}_0$

conditional on $\widehat{\mathbf{M}}$ and thus alleviate the need to make assumptions on $\widehat{\mathbf{M}}$ (not to mention that, by carefully exploiting the Gaussianity of \mathbf{G} , we also obtain more precise $\ell_{2,\infty}$ error bounds compared to that for some given but arbitrary $\widehat{\mu}_0$). See Remark 2 for more discussions.

Finally we note that Eq. (2.7), Eq. (2.12) and Eq. (2.17) are, to the best of our knowledge, the first set of bounds for entrywise differences between the RSVD-based low-rank approximation $\widehat{\mathbf{U}}_g \widehat{\mathbf{U}}_g^\top \widehat{\mathbf{M}}$ and the truncated exact SVD $\widehat{\mathbf{U}} \widehat{\mathbf{U}}^\top \widehat{\mathbf{M}}$. If $\widehat{\mathbf{M}} = \mathbf{M} + \mathbf{E}$ then these results also yield entrywise bounds for $\mathbf{M} - \widehat{\mathbf{U}}_g \widehat{\mathbf{U}}_g^\top \widehat{\mathbf{M}}$ as well as normal approximations and entrywise confidence intervals for \mathbf{M} ; see Section S2 for more details.

3 Random graph inference

We now apply Corollary 2 and Corollary 3 to estimate the leading eigenvectors for edge-independent random graphs with low-rank edge probabilities matrices. Additional applications to matrix completion and PCA with missing data are presented in Section S2 and Section S3 of the Supplementary File. Let $\widehat{\mathbf{M}} = [\widehat{m}_{ij}]$ be the adjacency matrix of a random graph on n vertices with edge probabilities $\mathbf{M} = [m_{ij}]$, i.e., $\widehat{\mathbf{M}}$ is a symmetric, binary matrix whose upper triangular entries are independent Bernoulli random variables with $\mathbb{P}(\widehat{m}_{ij} = 1) = m_{ij}$. Suppose $\text{rk}(\mathbf{M}) = k_0$ for some constant k_0 , $\|\mathbf{U}^{(k_0)}\|_{2 \rightarrow \infty} \asymp k_0^{1/2} n^{-1/2}$, $\sigma_{k_0} \asymp n\rho_n$, and $\|\mathbf{E}\| \lesssim (n\rho_n)^{1/2}$ with probability at least $1 - n^{-3}$; here $\rho_n \in [0, 1]$ satisfies $n\rho_n = \Omega(\log n)$ as n increases.

The above assumption are quite mild and are satisfied by many random graph models including Erdős–Rényi, stochastic blockmodels and its degree-corrected and/or mixed-membership variants (Holland et al., 1983; Karrer and Newman, 2011; Airolidi et al., 2008), (generalized) random dot product graphs (Rubin-Delanchy et al., 2022), as well as any edge-independent random graph whose edge probabilities are sufficiently homogeneous, i.e., $\max_i \sum_j m_{ij} \asymp \min_i \sum_j m_{ij}$. The factor ρ_n corresponds to the sparsity of $\widehat{\mathbf{M}}$, i.e., with high probability $\widehat{\mathbf{M}}$ has $\Theta(n^2 \rho_n)$ non-zero entries. We note that random graph inference using spectral methods generally require $n\rho_n \gtrsim \log n$ as otherwise the leading eigenvalues and eigenvectors of $\widehat{\mathbf{M}}$ may not yield consistent estimates for the corresponding eigenvalues and eigenvectors of \mathbf{M} . Finally the assumption $\mathbb{P}(\|\mathbf{E}\| \lesssim (n\rho_n)^{1/2}) \geq 1 - n^{-3}$ is chosen mainly for convenience as, under the above conditions, by using standard matrix concentration inequalities (Oliveira, 2010; Tropp, 2012; Lei and Rinaldo, 2015) we can show that for any finite constant $c > 0$ there exists a finite constant $C > 0$ depending only on c such that $\mathbb{P}(\|\mathbf{E}\| \leq C(n\rho_n)^{1/2}) \geq 1 - n^{-c}$.

3.1 Subspace perturbation error bounds

Suppose n is large and we are interested in computing the k_0 leading singular vectors of $\widehat{\mathbf{M}}$ as an estimate for the k_0 leading singular vectors of \mathbf{M} . To save computational time, we will use Algorithm 1 with some choices of $g \geq 1$ and $\tilde{k} \geq k_0$. Then by Corollary 2 we have

$$d_2(\widehat{\mathbf{U}}_g, \mathbf{U}) = O((n\rho_n)^{-1/2}), \quad \text{for all } g \geq 1 + \frac{(1+o(1))\log(n/\tilde{k})}{\log(n\rho_n)} \quad (3.1)$$

with high probability, where the hidden factor in $o(1)$ does not depend on n, \tilde{k} and ρ_n . Note that, for ease of exposition, we omit the dependency on k_0 for all matrices.

Furthermore, under the *strong signal regime* $n\rho_n = \Omega(n^\beta)$ for some fixed but arbitrary $\beta > 0$, by Corollary 2, Eq. (3.1) can be strengthened to

$$d_2(\widehat{\mathbf{U}}_g, \mathbf{U}) = \begin{cases} O((n\rho_n)^{-1/2}) & \text{if } g > 1 + \alpha_* \\ O((n\rho_n)^{-(g-\alpha_*)/2}) & \text{if } \alpha_* \leq g \leq 1 + \alpha_*, \end{cases} \quad (3.2)$$

with probability at least $1 - 3n^{-3}$, where $\alpha_* = \frac{\log(n/\tilde{k})}{\log n\rho_n} \leq \beta^{-1} + o(1)$. Eq. (3.1) and Eq. (3.2) imply a phase transition for $d_2(\widehat{\mathbf{U}}_g, \mathbf{U})$. In particular, the assumptions at the beginning of this section together with the Davis-Kahan theorem imply $d_2(\widehat{\mathbf{U}}, \mathbf{U}) \leq \frac{E_n}{\sigma_{k_0}}$ with high probability. Therefore, under the strong signal regime, if $g \geq 1 + \alpha_*$ then $d_2(\widehat{\mathbf{U}}_g, \mathbf{U})$ is asymptotically equivalent to $d_2(\widehat{\mathbf{U}}, \mathbf{U})$. In contrast, if $\alpha_* < g < 1 + \alpha_*$ then $d_2(\widehat{\mathbf{U}}_g, \mathbf{U})$ converges to 0 at the slower rates of $n^{-(g-\alpha_*)/2}$. Convergence of $d_2(\widehat{\mathbf{U}}_g, \mathbf{U})$ to 0 is not guaranteed when $g \leq \alpha_*$. Finally, under the *weak signal regime* $n\rho_n \gtrsim \log n$, we can similarly show that $d_2(\widehat{\mathbf{U}}_g, \mathbf{U})$ is asymptotically equivalent to $d_2(\widehat{\mathbf{U}}, \mathbf{U})$ when $g \geq 1 + \frac{(1+o(1))\log(n/\tilde{k})}{\log n\rho_n}$, while convergence of $d_2(\widehat{\mathbf{U}}_g, \mathbf{U})$ to 0 is not guaranteed when $g \leq \frac{(1-o(1))\log(n/\tilde{k})}{\log n\rho_n}$.

We now discuss the behavior of $d_{2,\infty}(\widehat{\mathbf{U}}_g, \mathbf{U})$. For random graphs satisfying the assumptions in this section, the sharpest known upper bound for $d_{2,\infty}(\widehat{\mathbf{U}}, \mathbf{U})$ is

$$d_{2,\infty}(\widehat{\mathbf{U}}, \mathbf{U}) = O\left((\log n)^{1/2} \frac{E_n}{\sigma_{k_0}} \|\mathbf{U}\|_{2,\infty}\right) = O\left(\frac{(\log n)^{1/2}}{n\rho_n^{1/2}}\right)$$

with high probability; see e.g., [Cape et al. \(2019a\)](#); [Rubin-Delanchy et al. \(2022\)](#); [Abbe et al.](#)

(2020); Mao et al. (2021); Xie (2024) for more details. Define

$$g_* = \max \left\{ 1 + \frac{(1 + o(1))(\log(n/\tilde{k}) + \log \log n)}{\log n \rho_n}, \frac{1}{3} + \frac{(1 + o(1))(\log(n^3/\tilde{k}^2) + \log \log n)}{3 \log n \rho_n} \right\}.$$

where the hidden factor in $o(1)$ does not depend on n, \tilde{k} and ρ_n . Then by Corollary 3, for $g \geq g_*$ we have

$$d_{2,\infty}(\hat{\mathbf{U}}_g, \mathbf{U}) = O\left(\frac{(\log n)^{1/2}}{n \rho_n^{1/2}}\right) \quad (3.3)$$

with probability at least $1 - 6n^{-3}$. Furthermore, under the strong signal regime $n \rho_n = \Omega(n^\beta)$, a careful investigation of the proof of Corollary 3 can strengthen Eq. (3.3) to yield

$$d_{2,\infty}(\hat{\mathbf{U}}_g, \mathbf{U}) = \begin{cases} O\left(\frac{(\log n)^{1/2}}{n \rho_n^{1/2}}\right) & \text{if } g \geq \max\{1 + \alpha_*^{(1)}, 1/3 + \alpha_*^{(2)}\} \\ O\left(\frac{(\log n)^{1/2}}{n^{1/2}(n \rho_n)^{\xi_g}}\right) & \text{if } \max\{\alpha_*^{(1)}, \alpha_*^{(2)}\} < g < \max\{1 + \alpha_*^{(1)}, 1/3 + \alpha_*^{(2)}\} \end{cases} \quad (3.4)$$

where $\alpha_*^{(1)} = \frac{\log(n/\tilde{k})}{\log n \rho_n} \leq \beta^{-1}$, $\alpha_*^{(2)} = \frac{\log(n^3/\tilde{k}^2)}{3 \log n \rho_n} \leq \beta^{-1}$, and $\xi_g = \frac{1}{2} \min\{g - \alpha_*^{(1)}, 3(g - \alpha_*^{(2)})\} \leq \frac{1}{2}$. Eq. (3.3) and Eq. (3.4) also imply a phase transition for $d_{2,\infty}(\hat{\mathbf{U}}_g, \mathbf{U})$ as g increases, e.g., if $g \geq \max\{1 + \alpha_*^{(1)}, 1/3 + \alpha_*^{(2)}\}$ then $d_{2,\infty}(\hat{\mathbf{U}}_g, \mathbf{U})$ converges to 0 at the same rate as $d_{2,\infty}(\hat{\mathbf{U}}, \mathbf{U})$, while if $\max\{\alpha_*^{(1)}, \alpha_*^{(2)}\} < g < \max\{1 + \alpha_*^{(1)}, 1/3 + \alpha_*^{(2)}\}$ then $d_{2,\infty}(\hat{\mathbf{U}}_g, \mathbf{U})$ converges to 0 at a slower (degenerate) rate of $n^{-1/2}(n \rho_n)^{-\xi_g}$; convergences of $d_{2,\infty}(\hat{\mathbf{U}}_g, \mathbf{U})$ is not guaranteed when $g \leq \max\{\alpha_*^{(1)}, \alpha_*^{(2)}\}$.

To further illustrate our results, we focus on a practical and computationally efficient scenario where the RSVD sketching dimension is $\tilde{k} \asymp \log n$ under the strong signal regime $n \rho_n \asymp n^\beta$. Eq. (3.2) and Eq. (3.4) then become

$$d_2(\hat{\mathbf{U}}_g, \mathbf{U}) = \begin{cases} O(n^{-\beta/2}) & \text{if } g \geq 1 + \beta^{-1} \\ O(n^{(-\beta g + 1)/2}) & \text{if } \beta^{-1} \leq g \leq 1 + \beta^{-1} \end{cases}, \quad (3.5)$$

$$d_{2,\infty}(\hat{\mathbf{U}}_g, \mathbf{U}) = (\log n)^{1/2} \begin{cases} n^{-\beta/2-1/2} & \text{if } g \geq 1 + \beta^{-1} \\ n^{(-\beta g + 1)/2-1/2} & \text{if } \beta^{-1} \leq g \leq 1 + \beta^{-1} \end{cases}. \quad (3.6)$$

Similar to our previous discussions, the above rates are optimal when $g \geq 1 + \beta^{-1}$, degenerate when $\beta^{-1} \leq g \leq 1 + \beta^{-1}$, and no convergence can be guaranteed when $g \leq \beta^{-1}$. See Section 3.2 for matching lower bounds (up to logarithmic factors), Section 4.1 for further numerical evidence, and Figure 1 for a summary of these phase transitions. In summary the convergence rates in

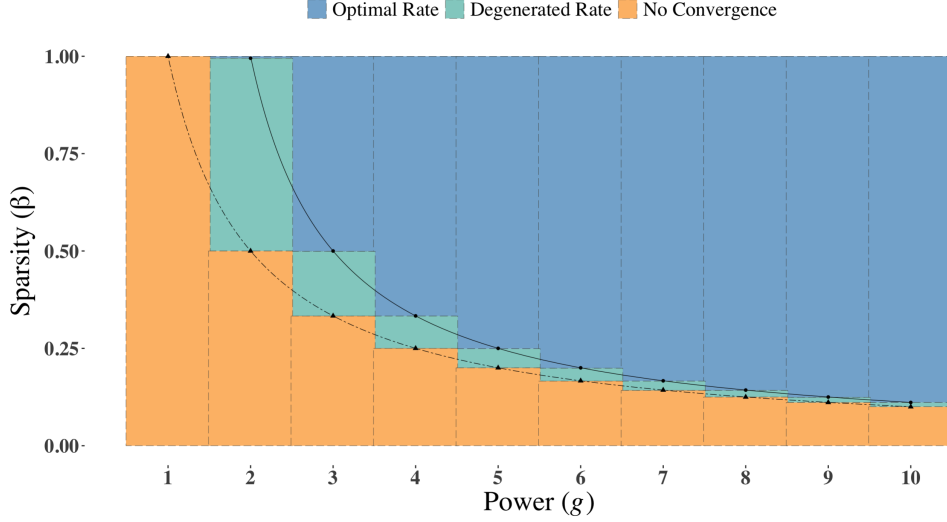


Figure 1: Phase transition diagram of error rates under the random graph setting with $\tilde{k} \asymp \log n$ and $n\rho_n \asymp n^\beta$. Different regions correspond to different convergence rates of $d_2(\hat{\mathbf{U}}_g, \mathbf{U})$ or $d_{2 \rightarrow \infty}(\hat{\mathbf{U}}_g, \mathbf{U})$; see Eq. (3.5) for details. The X- and Y-axes represent g and β , respectively, and dashed and solid lines represent the thresholds $g = \beta^{-1}$ and $g = 1 + \beta^{-1}$.

Eq. (3.5) and Eq. (3.6) support the well-known recommendation that selecting \tilde{k} slightly larger than k_0 and increasing g is crucial for the practical success of RSVD (Martinsson and Tropp, 2020).

3.2 Lower bound and phase transition sharpness

We now study the sharpness of the phase transition thresholds described in Section 3.1. More specifically, we derive lower bounds for $d_2(\hat{\mathbf{U}}_g, \mathbf{U})$ and $d_{2,\infty}(\hat{\mathbf{U}}_g, \mathbf{U})$ under the same regime as the upper bounds in Eq. (3.5), namely with $n\rho_n \asymp n^\beta$ and $\tilde{k} \asymp \log n$. Our lower bounds depend on the following assumption for the growth rate of $\text{tr } \hat{\mathbf{M}}^{2g}$.

Assumption 1. For any $g \geq 1$ there exists a constant $c_g > 0$ depending on g such that

$$\mathbb{E}(\text{tr } \hat{\mathbf{M}}^{2g}) \geq c_g \{n^{g+1} \rho_n^g + (n\rho_n)^{2g}\}. \quad (3.7)$$

Assumption 1 is satisfied by any edge-independent random graphs with homogeneous variances including stochastic blockmodel graphs, their degrees-corrected and mixed membership variants (Karrer and Newman, 2011; Airolidi et al., 2008), and (generalized) random dot product graphs (Rubin-Delanchy et al., 2022). More specifically, let \mathbf{M} be such that $m_{ij} \asymp \rho_n$ for all i, j .

Then by Theorem 1 and Lemma S.7 in [Maugis et al. \(2017\)](#), we have

$$\mathbb{E}(\text{tr } \widehat{\mathbf{M}}^{2g}) \asymp_g (n\rho_n)^{2g} + n^{g+1} \mathbb{P}(\{v_1, v_2, \dots, v_{g+1}\} \text{ forms a tree}) \asymp_g n^{g+1} \rho_n^g + (n\rho_n)^{2g}$$

where $\{v_1, \dots, v_{g+1}\}$ is any collection of $g+1$ distinct indices in $\widehat{\mathbf{M}}$.

Theorem 3. *Assume the setting of Corollary 2 where k_0 is bounded by a finite constant not depending on n . Furthermore suppose that (i) $\sigma_1 \asymp n\rho_n \asymp n^\beta$ and $\sigma_{k_0}/E_n \gtrsim n^{\beta/2}$ for some constant $\beta > 0$ and (ii) $\widehat{\mathbf{M}}$ satisfies Assumption 1. Choose $\tilde{k} = 2c_{\text{gap}} \log n$ and let $p_0 \in (0, 1)$ be fixed but arbitrary. Then there exists a constant $C_{p_0} > 0$ depending only on p_0 such that for all $g < \beta^{-1}$ we have with probability at least $1 - 2p_0$,*

$$d_2(\widehat{\mathbf{U}}_g, \mathbf{U}) \geq C_{p_0} c_g, \quad d_{2,\infty}(\widehat{\mathbf{U}}_g, \mathbf{U}) \geq C_{p_0} c_g \cdot n^{-1/2},$$

and for all $\beta^{-1} \leq g < 1 + \beta$, we have with probability at least $1 - 2p_0$,

$$d_2(\widehat{\mathbf{U}}_g, \mathbf{U}) \geq C_{LB} c_g \cdot (\log n)^{-1/2} n^{(-g\beta+1)/2}, \quad d_{2,\infty}(\widehat{\mathbf{U}}_g, \mathbf{U}) \geq C_{LB} c_g \cdot (\log n)^{-1/2} n^{(-g\beta+1)/2-1/2}.$$

Theorem 3 implies that if $g < \beta^{-1}$ then $\widehat{\mathbf{U}}_g$ is not a consistent estimator for \mathbf{U} . In contrast, if $g \geq 1 + \beta^{-1}$ then $d_2(\widehat{\mathbf{U}}_g, \mathbf{U})$ and $d_{2,\infty}(\widehat{\mathbf{U}}_g, \mathbf{U})$ attain the same convergence rates as $d_2(\widehat{\mathbf{U}}, \mathbf{U})$ and $d_{2,\infty}(\widehat{\mathbf{U}}, \mathbf{U})$ (see Eq. (3.5) and Eq. (3.6)), so that $\widehat{\mathbf{U}}_g$ is rate-optimal.

3.3 Exact recovery for stochastic blockmodels

We first recall the notion of stochastic blockmodel graphs ([Holland et al., 1983](#)), one of the most widely used generative model for networks with an intrinsic community structure.

Definition 1 (SBM). Let $K \geq 1$ be a positive integer and let $\boldsymbol{\pi} \in \mathbb{R}^K$ be a probability vector. Let \mathbf{B} be a symmetric $K \times K$ matrix whose entries are in $[0, 1]$. We say that $(\mathbf{A}, \boldsymbol{\tau}) \sim \text{SBM}(\mathbf{B}, \boldsymbol{\pi})$ is a K -blocks stochastic blockmodel (SBM) graph with parameters \mathbf{B} and $\boldsymbol{\pi}$, and sparsity factor ρ_n , if the following holds. First, sample $\boldsymbol{\tau} = (\tau_1, \dots, \tau_n)$ where the τ_i are iid with $\mathbb{P}(\tau_i = \ell) = \pi_\ell$ for all $\ell \in [K]$. Then sample \mathbf{A} as a $n \times n$ symmetric binary matrix whose upper triangular entries $\{A_{ij}\}_{i \leq j}$ are independent Bernoulli random variables with $\mathbb{P}(A_{ij} = 1) = \rho_n B_{\tau_i, \tau_j}$.

Community detection is a well-known problem with many available techniques; see [Abbe \(2017\)](#) for a survey. We focus on spectral clustering, a simple and popular algorithm wherein,

given \mathbf{A} , we first choose an embedding dimension d and compute the matrix $\hat{\mathbf{U}}$ of eigenvectors corresponding to the d largest (in modulus) eigenvalues of \mathbf{A} . Next we cluster the rows of $\hat{\mathbf{U}}$ into K cluster using either the K -means or K -medians algorithms and let $\hat{\tau}_i$ be the resulting cluster membership for the i th row of $\hat{\mathbf{U}}$. Statistical properties of spectral clustering had been widely studied in recent years. See e.g., [Rohe et al. \(2011\)](#); [Lei and Rinaldo \(2015\)](#); [Abbe et al. \(2020\)](#) for an incomplete list of references.

In real-world applications like social or biological networks, the number of nodes can be on the order of 10^6 ([Gopalan and Blei, 2013](#)). As a result, obtaining $\hat{\mathbf{U}}$ using standard SVD algorithms can be prohibitively demanding in terms of both the computational time and memory requirement. We thus consider a RSVD-based spectral clustering procedure that replaces $\hat{\mathbf{U}}$ by its approximation $\hat{\mathbf{U}}_g$, which results in a procedure with running time $O(g\tilde{k} \times \text{nnz}(\mathbf{A}))$ and memory consumption $O(\text{nnz}(\mathbf{A}))$ where $\text{nnz}(\mathbf{A})$ denote the number of non-zero entries of \mathbf{A} . We leverage our bounds for $d_{2,\infty}(\hat{\mathbf{U}}_g, \mathbf{U})$ to show that K -means clustering over $\hat{\mathbf{U}}_g$ yields an exact recovery of $\boldsymbol{\tau}$ with high probability, i.e., it yields a $\hat{\boldsymbol{\tau}}$ such that there exists a permutation ς of $\{1, \dots, K\}$ for which $\hat{\tau}_i = \varsigma(\tau_i)$ for all $i \in \{1, \dots, n\}$.

Theorem 4. *Let $(\mathbf{A}, \boldsymbol{\tau}) \sim \text{SBM}(\mathbf{B}, \boldsymbol{\pi})$ be a K -blocks SBM with sparse parameter ρ_n where $\pi_\ell > 0$ for all $\ell \in [K]$ and $n\rho_n = \omega(\log n)$. Let $d = \text{rk}(\mathbf{B})$ and suppose that $\hat{\boldsymbol{\tau}}$ is the K -means clustering of the rows of $\hat{\mathbf{U}}_g$ where $\tilde{k} \asymp \log n$ and $g \geq \frac{2\log n}{\log n\rho_n}$. Then for sufficiently large n , $\hat{\boldsymbol{\tau}}$ exactly recovers $\boldsymbol{\tau}$ with probability at least $1 - 2n^{-3}$. If $n\rho_n \gtrsim n^\beta$ for any fixed but arbitrary $\beta > 0$ then the threshold for exact recovery of $\hat{\boldsymbol{\tau}}$ can be sharpened to $g \geq 1 + \beta^{-1}$.*

Remark 7. Community detection using RSVD was also studied in [Zhang et al. \(2022\)](#). In particular, Theorem 1 in [Zhang et al. \(2022\)](#) shows that if $n\rho_n = \omega(\log n)$ then weak recovery is possible using $\hat{\mathbf{U}}_g$, provided that one choose $\tilde{k} \geq k + 4$ and $g = \Omega(n^\delta)$ for any fixed but arbitrary $\delta > 0$. Recall that weak recovery only requires the *proportion* of mis-clustered vertices to converge to 0. Comparing the results in [Zhang et al. \(2022\)](#) to Theorem 4, we see that while they have the same sparsity requirement, the exact recovery in Theorem 4 is a much stronger guarantee than the weak recovery in [Zhang et al. \(2022\)](#). Furthermore Theorem 4 only requires at most $g = O(\log n)$ power iterations (which can be reduced further to $O(1)$ iterations whenever $n\rho_n = \Omega(n^\beta)$ for some $\beta > 0$) while [Zhang et al. \(2022\)](#) require $g = \Omega(n^\delta)$ power iterations for some fixed but arbitrary $\delta > 0$.

3.4 Row-wise normal approximation

We now consider the row-wise fluctuations of $\hat{\mathbf{U}}_g$. For random graphs satisfying the assumptions at the beginning of this section, there exists a sequence of orthogonal matrices \mathbf{W}_n such that for any index $i \in [n]$ we have

$$\mathbf{\Gamma}_i^{-1/2}(\mathbf{W}_n[\hat{\mathbf{U}}]_i - [\mathbf{U}]_i) \xrightarrow{d} \mathcal{N}(0, \mathbf{I}) \quad (3.8)$$

as $n \rightarrow \infty$. Here $[\hat{\mathbf{U}}]_i$ (resp. $[\mathbf{U}]_i$) denote the i th row of $\hat{\mathbf{U}}$ (resp. \mathbf{U}) and $\mathbf{\Gamma}_i$ is defined as

$$\mathbf{\Gamma}_i = \mathbf{\Lambda}^{-1} \left(\sum_j m_{ij}(1 - m_{ij})[\mathbf{U}]_j([\mathbf{U}]_j)^\top \right) \mathbf{\Lambda}^{-1} \quad (3.9)$$

where $\{m_{ij}\}$ are the entries of \mathbf{M} and $\mathbf{\Lambda}$ are the non-zero eigenvalues of \mathbf{M} ; we note that $\|\mathbf{\Gamma}_i^{-1/2}\| \asymp n\rho_n^{1/2}$ for all i . Eq. (3.8) provides normal approximations for the rows of $\hat{\mathbf{U}}$ when centered around the corresponding rows of \mathbf{U} ; see e.g., [Rubin-Delanchy et al. \(2022\)](#); [Cape et al. \(2019a\)](#); [Xie \(2024\)](#) for more details. By Corollary 3 there exists a choice of $g = O(\log n)$ and orthogonal \mathbf{W}_g depending on g and n such that for any $i \in [n]$ we have

$$\begin{aligned} \mathbf{W}_n \mathbf{W}_g [\hat{\mathbf{U}}_g]_i - [\mathbf{U}]_i &= \mathbf{W}_n (\mathbf{W}_g [\hat{\mathbf{U}}_g]_i - [\hat{\mathbf{U}}]_i) + \mathbf{W}_n [\hat{\mathbf{U}}]_i - [\mathbf{U}]_i \\ &= \mathbf{W}_n [\hat{\mathbf{U}}]_i - [\mathbf{U}]_i + o(n^{-1} \rho_n^{-1/2}) \end{aligned}$$

with probability at least $1 - 5n^{-3}$. Combining Eq. (3.8) with the above bound we obtain the following normal approximations for the rows of $\hat{\mathbf{U}}_g$.

Theorem 5. *Let $\hat{\mathbf{M}}$ be the adjacency matrix for a random graph with edge probabilities matrix \mathbf{M} where \mathbf{M} satisfies the assumption at the beginning of this section. Let $\hat{\mathbf{U}}_g$ be generated via Algorithm 1 with $\tilde{k} \asymp \log n$ and $g \geq \frac{2 \log n}{\log n \rho_n}$. Suppose $n\rho_n = \omega(\log n)$. Then there exist a sequence of orthogonal matrices \mathbf{W}_n^* such that for any $i \in [n]$ we have*

$$\mathbf{\Gamma}_i^{-1/2}(\mathbf{W}_n^*[\hat{\mathbf{U}}_g]_i - [\mathbf{U}]_i) \xrightarrow{d} \mathcal{N}(\mathbf{0}, \mathbf{I}). \quad (3.10)$$

Moreover, if $n\rho_n \gtrsim n^\beta$ for some $\beta > 0$ then Eq. (3.10) holds for all $g \geq 2 + \beta^{-1}$.

Under the strong signal regime $n\rho_n \gtrsim n^\beta$, the condition $g \geq 2 + \beta^{-1}$ in Theorem 5 is slightly more stringent than $g \geq 1 + \beta^{-1}$ in Eq. (3.4), and the reason for this discrepancy is that while $g \geq 1 + \beta^{-1}$ is sufficient for $d_{2 \rightarrow \infty}(\hat{\mathbf{U}}_g, \mathbf{U})$ to achieve the optimal error rate, it does not guarantee

that the fluctuations of $\mathbf{W}_n^*[\hat{\mathbf{U}}_g]_i - [\mathbf{U}]_i$ is asymptotically equivalent to that of $\mathbf{W}_n[\hat{\mathbf{U}}]_i - [\mathbf{U}]_i$. See Section 4.2 for a numerical experiment supporting this claim.

4 Numerical studies

We conduct simulations to support our theoretical results for RSVD-based random graph inference, and present a real-data analysis using RSVD-based PCA. Section 4.1 illustrates the subspace perturbation error rates from Section 3.1, and Section 4.2 illustrate the Gaussian approximation from Section 3.4. Section 4.3 analyzes an scRNA-seq data using the RSVD-based PCA in Section S3.1. Additional numerical results, including simulations for missing-data PCA, exact recovery in SBM, and a real-data analysis for distance matrix completion, are further provided in the Supplementary File.

For the general simulation setting, we consider two-blocks SBM graphs with equal sized blocks and block probabilities matrix $\mathbf{B}_0 = \rho_n \begin{pmatrix} 0.8 & 0.3 \\ 0.3 & 0.8 \end{pmatrix}$. Recall that ρ_n is the sparsity scaling parameter. We consider three different regimes for ρ_n , namely $\rho_n = 1$ (dense setting), $\rho_n = 3n^{-1/3}$ (semi-sparse setting I), $\rho_n = 4n^{-1/2}$ (semi-sparse setting II). As $\text{rk}(\mathbf{B}_0) = 2$, we also set $k = 2$.

4.1 Phase transition

We first verify the convergence rate for $d_2(\hat{\mathbf{U}}_g, \mathbf{U})$ and $d_{2 \rightarrow \infty}(\hat{\mathbf{U}}_g, \mathbf{U})$ as we vary g and ρ_n . For simplicity we only consider $\rho_n = 1$ and $\rho_n = 3n^{-1/3}$, and we ignore any potential logarithmic factors in the convergence rate for $d_2(\hat{\mathbf{U}}_g, \mathbf{U})$ and $d_{2,\infty}(\hat{\mathbf{U}}_g, \mathbf{U})$ as n increases. For each choice of ρ_n we numerically estimate the convergence rates of $d_2(\hat{\mathbf{U}}_g, \mathbf{U})$ and $d_{2,\infty}(\hat{\mathbf{U}}_g, \mathbf{U})$ as follows. We first generate a realization of \mathbf{A} with $n \in \{2000, 3000, \dots, 7000\}$ vertices from \mathbf{B}_0 with equal block sizes, and then compute $\hat{\mathbf{U}}_g$ via Algorithm 1 with $\tilde{k} = 5 \log n$ and $1 \leq g \leq 5$. We then evaluate $d_2(\hat{\mathbf{U}}_g, \mathbf{U})$ and $d_{2 \rightarrow \infty}(\hat{\mathbf{U}}_g, \mathbf{U})$ and compare it against the theoretical error rate given in Section 3.1 by running a simple linear regression between the (negative logarithm) of the empirical error as the response variable against $\log n$ as the predictor variable. The estimated coefficient $\hat{\beta}$ are then recorded. We repeat the above steps for 500 Monte Carlo (MC) iterations to get an empirical distribution for $\hat{\beta}$ as g varies, and present their box-plots in Figure 2. For comparison we had also included the (estimated) convergence rate for $d_2(\hat{\mathbf{U}}, \mathbf{U})$ and $d_{2 \rightarrow \infty}(\hat{\mathbf{U}}, \mathbf{U})$ (these are labeled as “true SVD”). The empirical results in Figure 2 match the theoretical rates presented

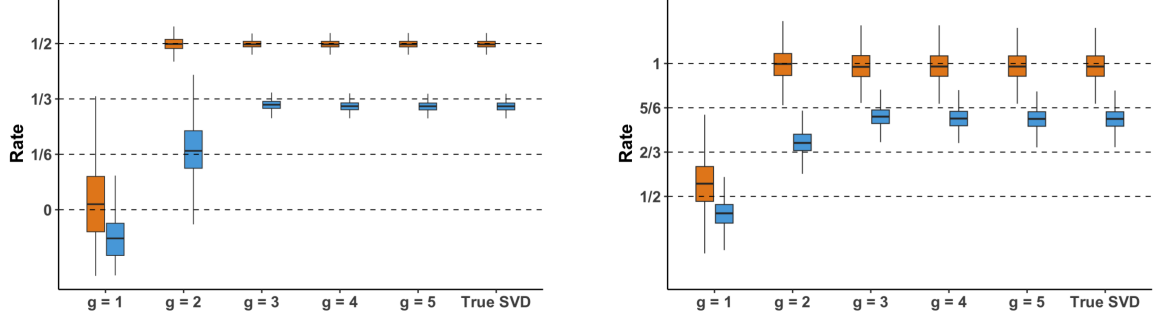


Figure 2: Box plots of error rate for $d_2(\hat{\mathbf{U}}_g, \mathbf{U})$ (top panel) and $d_{2,\infty}(\hat{\mathbf{U}}_g, \mathbf{U})$ (bottom panel), where $\tilde{k} = 5 \log n$ and $1 \leq g \leq 5$. The colors denote different sparsity level, with $\rho_n = 1$ being blue and $\rho_n = 3n^{-1/3}$ being yellow.

in Theorem 3 and Eq.(3.4) exactly (see Section S1.1): in particular we see no convergence when $g = 1$ and $\rho_n = 1$, slow or no convergence when $g \leq 2$ and $\rho_n = 3n^{-1/3}$, and asymptotically optimal convergence when $g \geq 2$ and $\rho_n = 1$, or $g \geq 3$ and $\rho_n = 3n^{-1/3}$.

4.2 Limiting distribution

We now illustrate the normal approximations for the row-wise fluctuations of $\hat{\mathbf{U}}_g$ as implied by Theorem 5. For brevity we set $\tilde{k} = \log n$. We generate a single realization of \mathbf{A} on $n = 2000$ vertices and ρ_n follows either the dense setting ($\rho_n = 1$) or the semi-sparse setting II ($\rho_n = 4n^{-1/2}$), with equal sized blocks and block probabilities \mathbf{B}_0 . Scatter plots of the rows of $\hat{\mathbf{U}}_g$ for $g \in \{1, 2, \dots, 5\}$ as well as the rows of $\hat{\mathbf{U}}$ are presented in Figure 3. The top panels of Figure 3 show that under the dense regime $\rho_n \asymp 1$, $g \geq 2$ suffices for the rows of $\hat{\mathbf{U}}_g$ to form two clusters, while $g \geq 3$ is required for the empirical 95% confidence ellipses to align with the theoretical ellipses from Theorem 5. The bottom panels show that under the semi-sparse regime $\rho_n \asymp n^{-1/2}$, $g \geq 3$ suffices for exact recovery, and $g \geq 4$ is necessary for confidence ellipse alignment. Moreover, for $g \geq 4$, the scatter plots are nearly indistinguishable from those of $\hat{\mathbf{U}}$. These observations confirm that the threshold $g \geq 2 + \beta^{-1}$ in Theorem 5 is both necessary and sufficient for the normal approximation of $\hat{\mathbf{U}}_g$; note that $\beta^{-1} = 1$ for $\rho_n \asymp 1$ and $\beta^{-1} = 2$ for $\rho_n \asymp n^{-1/2}$.

4.3 Subpopulation discovery of large immune population

We evaluate the performance of RSVD-based PCA with missing data (cf. Section S3) on a widely used single-cell RNA-seq dataset introduced by Zheng et al. (2017), which includes the gene expressions of approximately 6.8×10^4 peripheral blood mononuclear cells (PBMCs) from

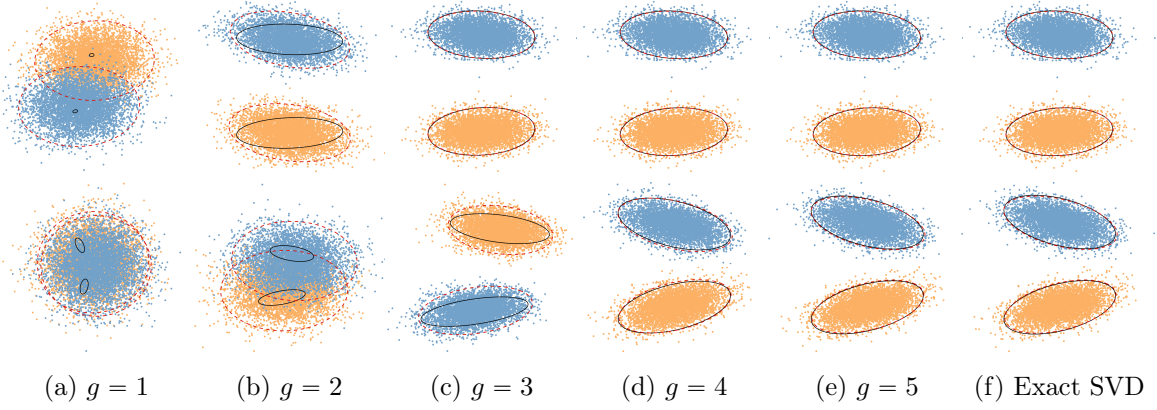


Figure 3: Row-wise fluctuations of $\hat{\mathbf{U}}_g$ and $\hat{\mathbf{U}}$ for the two-block SBM with $n = 2000$ and either $\rho_n \asymp 1$ (top panels) or $\rho_n \asymp n^{-1/2}$ (bottom panels). From left to right, scatter plots show the row vectors of $\hat{\mathbf{U}}_g$ for $g = 1, \dots, 5$ and $\hat{\mathbf{U}}$. Points are colored according to true community memberships. Red dashed curves represent the 95% empirical confidence ellipses; solid black curves represent the 95% theoretical confidence ellipses.

a single donor.¹ Each cell contains expression measurements for $\approx 2 \times 10^4$ genes, resulting in a data matrix of size $\approx (6.8 \times 10^4) \times (2 \times 10^4)$. The analysis in Zheng et al. (2017) first filtered the data by selecting the top 1,000 genes ranked by normalized dispersion (Macosko et al., 2015), producing a matrix of size $\approx (6.8 \times 10^4) \times 10^3$. PCA was then applied to this filtered and thinned matrix to obtain projections of the cell expressions data onto the top 50 principal components (PCs). A two-dimensional t -distributed stochastic neighbor embedding (t -SNE) of the projected data, colored by inferred cell types based on the reference profiles from 11 purified PBMC subpopulations (Zheng et al., 2017, Supplementary Figure 7), is shown in the top-right panel of Figure 4.

As the original dataset is quite large of size $\approx (6.8 \times 10^4) \times (2 \times 10^4)$, direct computation of its SVD (as required by traditional PCA or missing-data PCA of Cai et al. (2021)) is infeasible using the memory capacity of a standard laptop (e.g., a MacBook with 36GB of RAM). The filtering step in Zheng et al. (2017) directly reduces the data dimension by dropping a large amount of the gene expression measurements, thereby easing the memory and computational burden for PCA. As an alternative, we apply our RSVD-based PCA with missing data (Algorithm S2) to the *whole* data matrix, enabling efficient and scalable approximations to the top PCs. More specifically we project the whole data onto the leading $k = 50$ approximated PCs (computed for various choices of \tilde{k} and g) and visualize the resulting low-dimensional embeddings via t -SNE. The results are presented in Figure 4 and Figure S9, where cell types are labeled using the same classification scheme as that in Zheng et al. (2017). We observe that if \tilde{k} and g are both small then the t -SNE

¹The dataset is available at <https://github.com/10XGenomics/single-cell-3prime-paper>.

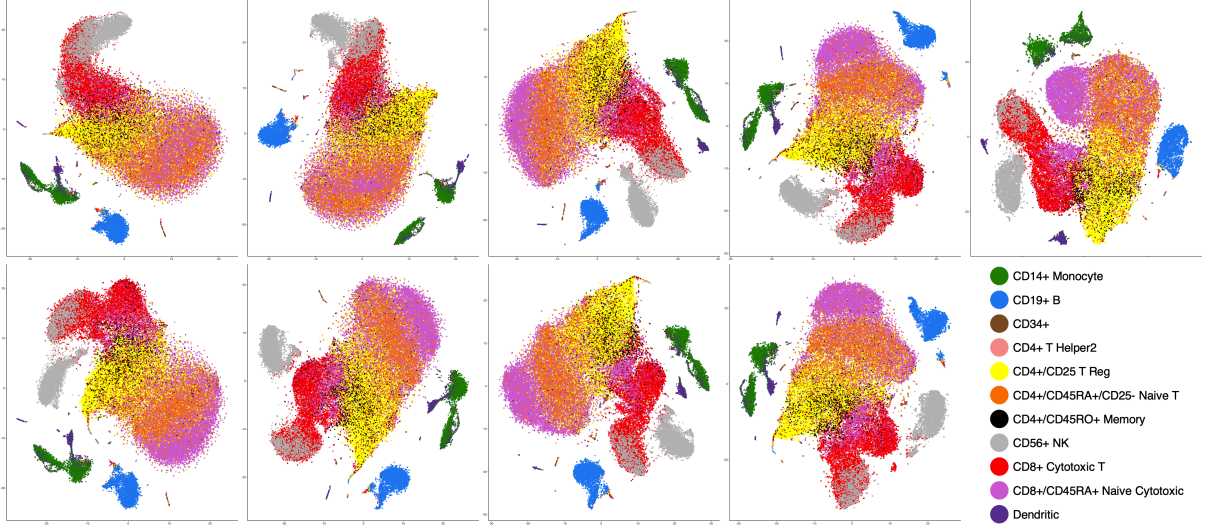


Figure 4: The t -SNE embeddings of the 68k PBMC gene expressions, projected on the top 50 PCs obtained via RSVD-based PCA (Algorithm S2). Top row (left to right): results for $g = 1$ with $\tilde{k} = 55, 100, 300, 1000$, and the reference embeddings from Zheng et al. (2017). Bottom row (left to right): results for $g = 2$ with the same sequence of \tilde{k} values.

embeddings exhibit weaker separation among subpopulations. For instance, when $g = 1$ and $\tilde{k} = 55$, CD56⁺ NK cells (grey) are not well-separated from CD8⁺ cytotoxic T cells (red). When $g = 1$ and $\tilde{k} = 55$ or 100, CD8⁺/CD45RA⁺ T cells (light purple) are indistinguishable from CD4⁺/CD45RA⁺/CD25⁻ T cells (orange). In contrast, as \tilde{k} and g increase, the RSVD-based PCA closely resembles the original analysis from Zheng et al. (2017), recovering meaningful cell subpopulations. Figure S9 shows that while the embeddings do vary for different values of g and \tilde{k} when $g \geq 3$, the overall subpopulation clustering patterns remain consistent. These findings align with our theoretical insights, and demonstrate the computational and statistical efficiency of RSVD for large-scale scRNA-seq analysis.

References

- Abbe, E. (2017). Community detection and stochastic block models: recent developments. *JMLR* 18, 6446–6531.
- Abbe, E., J. Fan, K. Wang, and Y. Zhong (2020). Entrywise eigenvector analysis of random matrices with low expected rank. *Annals of Statistics* 48, 1452–1474.
- Achlioptas, D. and F. McSherry (2007). Fast computation of low-rank matrix approximations. *Journal of the ACM* 54, 9.
- Agterberg, J., Z. Lubberts, and C. E. Priebe (2022). Entrywise estimation of singular vectors of

- low-rank matrices with heteroskedasticity and dependence. *IEEE Transactions on Information Theory* 68, 4618–4650.
- Airoldi, E. M., D. M. Blei, S. E. Fienberg, and E. P. Xing (2008). Mixed membership stochastic blockmodels. *JMLR* 9, 1981–2014.
- Bandeira, A. S. and R. Van Handel (2016). Sharp nonasymptotic bounds on the norm of random matrices with independent entries. *Annals of Probability* 44, 2479–2506.
- Baumer, B. S., D. T. Kaplan, and N. J. Horton (2017). *Modern Data Science with R*. Chapman and Hall/CRC.
- Belkin, M. and P. Niyogi (2003). Laplacian eigenmaps for dimensionality reduction and data representation. *Neural Computation* 15, 1373–1396.
- Cai, C., G. Li, Y. Chi, H. V. Poor, and Y. Chen (2021). Subspace estimation from unbalanced and incomplete data matrices: $\ell_{2,\infty}$ statistical guarantees. *Annals of Statistics* 49, 944–967.
- Cai, T. T. and A. Zhang (2018). Rate-optimal perturbation bounds for singular subspaces with applications to high-dimensional statistics. *Annals of Statistics* 46, 60–89.
- Cape, J., M. Tang, and C. E. Priebe (2019a). Signal-plus-noise matrix models: eigenvector deviations and fluctuations. *Biometrika* 106, 243–250.
- Cape, J., M. Tang, and C. E. Priebe (2019b). The two-to-infinity norm and singular subspace geometry with applications to high-dimensional statistics. *Annals of Statistics* 47, 2405–2439.
- Cape, J., X. Yu, and J. Z. Liao (2024). Robust spectral clustering with rank statistics. *Journal of Machine Learning Research* 25(398), 1–81.
- Charisopoulos, V., A. R. Benson, and A. Damle (2020). Entrywise convergence of iterative methods for eigenproblems. In *NIPS*, Volume 34, pp. 5644–5655.
- Chatterjee, S. (2015). Matrix estimation by universal singular value thresholding. *Annals of Statistics* 43, 177–214.
- Chen, S., S. Liu, and Z. Ma (2022). Global and individualized community detection in inhomogeneous multilayer networks. *Annals of Statistics* 50, 2664–2693.

- Chen, X., J. D. Lee, H. Li, and Y. Yang (2022). Distributed estimation for principal component analysis: An enlarged eigenspace analysis. *Journal of the American Statistical Association* 117, 1775–1786.
- Chen, Y., Y. Chi, J. Fan, and C. Ma (2021). Spectral methods for data science: A statistical perspective. *Foundations and Trends® in Machine Learning* 14, 566–806.
- Chen, Y., J. Fan, C. Ma, and K. Wang (2019). Spectral method and regularized MLE are both optimal for top- k ranking. *Annals of Statistics* 47, 2204–2235.
- Cheng, J., Q. Ye, H. Jiang, D. Wang, and C. Wang (2012). Stcdg: An efficient data gathering algorithm based on matrix completion for wireless sensor networks. *IEEE Transactions on Wireless Communications* 12, 850–861.
- Cormode, G., M. Garofalakis, P. J. Haas, and C. Jermaine (2011). Synopses for massive data: samples, histogram, wavelets, sketches. *Foundations and Trends in Databases* 4, 1–294.
- Crainiceanu, C. M., B. S. Caffo, S. Luo, and N. M. Punjabi (2011). Population value decomposition, a framework for the analysis of image populations. *Journal of the American Statistical Association* 106, 775–790.
- Damle, A. and Y. Sun (2020). Uniform bounds for invariant subspace perturbations. *SIAM Journal on Matrix Analysis and Applications* 41, 1208–1236.
- Davenport, M. A. and J. Romberg (2016). An overview of low-rank matrix recovery from incomplete observations. *IEEE Journal of Selected Topics in Signal Processing* 10, 608–622.
- Davidson, K. R. and S. J. Szarek (2001). *Handbook of the geometry of Banach spaces, Vol. I*, Chapter Local operator theory, random matrices and Banach spaces, pp. 317–366. North-Holland.
- Davis, C. and W. M. Kahan (1970). The rotation of eigenvectors by a perturbation. III. *SIAM Journal on Numerical Analysis* 7, 1–46.
- De Lathauwer, L., B. De Moor, and J. Vandewalle (2000). On the best rank-1 and rank- (r_1, r_2, \dots, r_n) approximation of higher-order tensors. *SIAM Journal on Matrix Analysis and Applications* 21, 1324–1342.

- Dobriban, E. and Y. Sheng (2020). Wonder: Weighted one-shot distributed ridge regression in high dimensions. *JMLR* 21, 2483–2534.
- Drineas, P., R. Kannan, and M. W. Mahoney (2006). Fast Monte Carlo algorithms for matrices ii: Computing a low-rank approximation to a matrix. *SIAM Journal on Computing* 36, 158–183.
- Edelman, A. (1991). The distribution and moments of the smallest eigenvalue of a random matrix of Wishart type. *Linear Algebra and its Applications* 159, 55–80.
- Eldridge, J., M. Belkin, and Y. Wang (2018). Unperturbed: spectral analysis beyond Davis-Kahan. In *Proceedings of Algorithmic Learning Theory*, pp. 321–358.
- Fan, J., D. Wang, K. Wang, and Z. Zhu (2019). Distributed estimation of principal eigenspaces. *Annals of Statistics* 47, 3009–3031.
- Fan, J., W. Wang, and Y. Zhong (2018). An ℓ_∞ eigenvector perturbation bound and its application to robust covariance estimation. *JMLR* 18, 1–42.
- Golub, G. H. and C. F. Van Loan (2013). *Matrix Computations* (3rd ed.). JHU press.
- Gopalan, P. K. and D. M. Blei (2013). Efficient discovery of overlapping communities in massive networks. *Proceedings of the National Academy of Sciences* 110, 14534–14539.
- Halko, N., P.-G. Martinsson, and J. A. Tropp (2011). Finding structure with randomness: Probabilistic algorithms for constructing approximate matrix decompositions. *SIAM Review* 53, 217–288.
- Hanson, D. L. and E. T. Wright (1971). A bound on tail probabilities for quadratic forms in independent random variables. *Annals of Mathematical Statistics* 42, 1079–1083.
- Hie, B., B. Bryson, and B. Berger (2019). Efficient integration of heterogeneous single-cell transcriptomes using scanorama. *Nature Biotechnology* 37, 685–691.
- Holland, P. W., K. B. Laskey, and S. Leinhardt (1983). Stochastic blockmodels: First steps. *Social Networks* 5, 109–137.
- Huo, X. and S. Cao (2019). Aggregated inference. *WIREs Computational Statistics* 11, e1451.
- Javanmard, A. and A. Montanari (2013, Jun). Localization from incomplete noisy distance measurements. *Foundations of Computational Mathematics* 13, 297–345.

- Jing, B.-Y., T. Li, Z. Lyu, and D. Xia (2021). Community detection on mixture multilayer networks via regularized tensor decomposition. *Annals of Statistics* 49, 3181–3205.
- Kannan, R. and S. Vempala (2017). Randomized algorithms in numerical linear algebra. *Acta Numerica* 26, 95–135.
- Karrer, B. and M. E. Newman (2011). Stochastic blockmodels and community structure in networks. *Physical Review E* 83, 016107.
- Ke, Z. T. and J. Wang (2024). Optimal network membership estimation under severe degree heterogeneity. *Journal of the American Statistical Association*, 1–15.
- Keshavan, R. H., A. Montanari, and S. Oh (2010). Matrix completion from noisy entries. *JMLR* 11, 2057–2078.
- Kumar, R., M. Graff, I. Vasconcelos, and F. J. Herrmann (2019). Target-oriented imaging using extended image volumes: a low-rank factorization approach. *Geophysical Prospecting* 67, 1312–1328.
- Lei, J. and K. Z. Lin (2024). Bias-adjusted spectral clustering in multi-layer stochastic block models. *Journal of the American Statistical Association* 118, 2433–2445.
- Lei, J. and A. Rinaldo (2015). Consistency of spectral clustering in stochastic block models. *Annals of Statistics* 43, 215–237.
- Lei, L. (2019). Unified $\ell_{2 \rightarrow \infty}$ eigenspace perturbation theory for symmetric random matrices. arXiv preprint #1909.04798.
- Li, G., C. Cai, H. V. Poor, and Y. Chen (2024). Minimax estimation of linear functions of eigenvectors in the face of small eigen-gaps. *IEEE Transactions on Information Theory* 71, 1200–1247.
- Lock, E. F., K. A. Hoadley, J. S. Marron, and A. B. Nobel (2013). Joint and individual variation explained (JIVE) for integrated analysis of multiple data types. *Annals of Applied Statistics* 7, 523–542.
- Lopes, M., N. B. Erichson, and M. Mahoney (2020). Error estimation for sketched SVD via the bootstrap. In *Proceedings of the 37th ICML*, pp. 6382–6392.

- Macosko, E. Z., A. Basu, R. Satija, J. Nemesh, K. Shekhar, M. Goldman, I. Tirosh, A. R. Bialas, N. Kamitaki, E. M. Martersteck, et al. (2015). Highly parallel genome-wide expression profiling of individual cells using nanoliter droplets. *Cell* *161*, 1202–1214.
- Mahoney, M. W. (2011). Randomized algorithms for matrices and data. *Foundations and Trends in Machine Learning* *3*, 123–224.
- Mao, X., P. Sarkar, and D. Chakrabarti (2021). Estimating mixed memberships with sharp eigenvector deviations. *Journal of the American Statistical Association* *116*, 1928–1940.
- Martinsson, P.-G. and J. A. Tropp (2020). Randomized numerical linear algebra: Foundations and algorithms. *Acta Numerica* *29*, 403–572.
- Maugis, P.-A. G., S. C. Ohlede, and P. J. Wolfe (2017). Topology reveals universal features for network comparison. arXiv preprint [#1705.05677](#).
- Musco, C. and C. Musco (2015). Randomized block Krylov methods for stronger and faster approximate singular value decomposition. In *NIPS*, Volume 28, pp. 1396–1404.
- Oliveira, R. I. (2010). Sum of random Hermitean matrices and an inequality by Rudelson. *Electronic Communications in Probability* *15*, 203–212.
- Paul, S. and Y. Chen (2020). Spectral and matrix factorization methods for consistent community detection in multi-layer networks. *Annals of Statistics* *48*, 230–250.
- Rohe, K., S. Chatterjee, and B. Yu (2011). Spectral clustering and the high-dimensional stochastic blockmodel. *Annals of Statistics* *39*, 1878–1915.
- Rokhlin, V., A. Szlam, and M. Tygert (2010). A randomized algorithm for principal component analysis. *SIAM Journal on Matrix Analysis and Applications* *31*, 1100–1124.
- Rubin-Delanchy, P., J. Cape, M. Tang, and C. E. Priebe (2022). A statistical interpretation of spectral embedding: the generalised random dot product graph. *Journal of the Royal Statistical Society, Series B* *84*, 1446–1473.
- Saibaba, A. K. (2019). Randomized subspace iterations: Analysis of canonical angles and unitarily invariant norms. *SIAM Journal on Matrix Analysis and Applications* *40*, 23–38.
- Stewart, G. W. and J.-G. Sun (1990). *Matrix Perturbation Theory*. Academic Press.

- Tang, T. M. and G. I. Allen (2021). Integrated principal components analysis. *JMLR* 22, 8953–9023.
- Tropp, J. A. (2012). User-friendly tail bounds for sums of random matrices. *Foundations of Computational Mathematics* 12, 389–434.
- Tropp, J. A., A. Yurtsever, M. Udell, and V. Cevher (2019). Streaming low-rank matrix approximation with an application to scientific simulation. *SIAM Journal on Scientific Computing* 41, A2430–A2463.
- Tsiligkaridis, T. and A. O. Hero (2013). Covariance estimation in high dimensions via Kronecker product expansions. *IEEE Transactions on Signal Processing* 61, 5347–5360.
- Tsuyuzaki, K., H. Sato, K. Sato, and I. Nikaido (2020). Benchmarking principal component analysis for large-scale single-cell rna-sequencing. *Genome Biology* 21, 9.
- Vershynin, R. (2012). *Compressed Sensing: Theory and Applications*, Chapter Introduction to the non-asymptotic analysis of random matrices, pp. 210–268. Cambridge University Press.
- Vershynin, R. (2018). *High-dimensional probability: An introduction with applications in data science*. Cambridge University Press.
- Wedin, P.-Å. (1972). Perturbation bounds in connection with singular value decomposition. *BIT Numerical Mathematics* 12, 99–111.
- Woodruff, D. P. (2014). Sketching as a tool for numerical linear algebra. *Foundations and Trends in Theoretical Computer Science* 10, 1–157.
- Xie, F. (2024). Entrywise limit theorems for eigenvectors of signal-plus-noise matrix models with weak signals. *Bernoulli* 30, 388–418.
- Yan, Y., Y. Chen, and J. Fan (2024). Inference for heteroskedastic PCA with missing data. *Annals of Statistics* 52, 729–756.
- Yang, F., S. Liu, E. Dobriban, and D. P. Woodruff (2021). How to reduce dimension with PCA and random projections? *IEEE Transactions on Information Theory* 67, 8154–8189.
- Zhang, A. and D. Xia (2018). Tensor SVD: Statistical and computational limits. *IEEE Transactions on Information Theory* 64, 7311–7338.

- Zhang, A. R., T. T. Cai, and Y. Wu (2022). Heteroskedastic PCA: Algorithm, optimality, and applications. *Annals of Statistics* 50, 53–80.
- Zhang, C., Y. Xie, H. Bai, B. Yu, and W. L. Y. Gao (2021). A survey on federated learning. *Knowledge-based systems* 216, 106775.
- Zhang, H., X. Guo, and X. Change (2022). Randomized spectral clustering in large-scale stochastic blockmodels. *Journal of Computational and Graphical Statistics* 31, 887–906.
- Zhang, Z., P. Cui, H. Li, X. Wang, and W. Zhu (2018). Billion-scale network embedding with iterative random projection. In *Proceedings of the 2018 ICDM*, pp. 787–796.
- Zheng, G. X., J. M. Terry, P. Belgrader, P. Ryvkin, Z. W. Bent, R. Wilson, S. B. Ziraldo, T. D. Wheeler, G. P. McDermott, J. Zhu, et al. (2017). Massively parallel digital transcriptional profiling of single cells. *Nature Communications* 8, 14049.
- Zhou, Y. and Y. Chen (2025). Deflated HeteroPCA: Overcoming the curse of ill-conditioning in heteroskedastic pca. *Annals of Statistics* 53, 91–116.

Supplementary File for “Perturbation Analysis of Randomized SVD and its Applications to Statistics”

Section S1 complements Section 3 by providing additional discussion and numerical results for random graph inference. In Sections S2 and S3, we apply our general theoretical framework to two additional inference problems: matrix completion with noise and PCA with missing data, and present the corresponding theoretical results, computational refinement, and numerical experiments. Section S4 introduces the application of RSVD to distributed estimation in multi-layer networks, along with the associated theoretical guarantees. Section S5 discusses several directions for future research. Sections S6 and S7 contain all technical proofs.

S1 Additional results for random graph inference

S1.1 Examples of error rates under different parameter regimes

We provide a few additional examples of the error rates presented in Section 3.1 for random graph inference under different parameter regimes. These examples illustrate the impact of g , n , \tilde{k} , and $n\rho_n$ on the convergence rates for $d_2(\hat{\mathbf{U}}_g, \mathbf{U})$ and $d_{2,\infty}(\hat{\mathbf{U}}_g, \mathbf{U})$. see also the visual summary in Figure 1. For ease of exposition we will ignore all factors depending on $\log n$ when discussing the convergence rates for $d_2(\hat{\mathbf{U}}_g, \mathbf{U})$ and $d_{2,\infty}(\hat{\mathbf{U}}_g, \mathbf{U})$. We also assume, unless stated otherwise, that $n\rho_n \asymp n^\beta$ for some $\beta \in (0, 1]$. This corresponds to graphs where the average degree is of order $\Theta(n^\beta)$.

(i) Suppose $\tilde{k} \asymp \log n$. Then the threshold for convergence of $d_2(\hat{\mathbf{U}}_g, \mathbf{U})$ and $d_{2,\infty}(\hat{\mathbf{U}}_g, \mathbf{U})$ are the same, and are given by $\alpha_* = \frac{\log n}{\log(n\rho_n)}$. In particular:

- if $n\rho_n \asymp n^{1/2}$ then $g \geq 2$ is sufficient for $d_2(\hat{\mathbf{U}}_g, \mathbf{U})$ and $d_{2,\infty}(\hat{\mathbf{U}}_g, \mathbf{U})$ to attain the optimal rate of $n^{-1/2}$ and n^{-1} , respectively; no convergence is guaranteed when $g = 1$.
- if $n\rho_n \asymp n^{2/3}$ then for $d_2(\hat{\mathbf{U}}_g, \mathbf{U})$, the optimal rate $n^{-1/3}$ is attained when $g \geq 3$ and a sub-optimal rate $n^{-1/6}$ is attained when $g = 2$. For $d_{2,\infty}(\hat{\mathbf{U}}_g, \mathbf{U})$, the optimal rate $n^{-5/6}$ is attained when $g \geq 3$ and a sub-optimal rate $n^{-2/3}$ is attained when $g = 2$. No convergence is guaranteed when $g = 1$.

- If $n\rho_n \asymp n^{1/2}$ then for $d_2(\hat{\mathbf{U}}_g, \mathbf{U})$, the optimal rate $n^{-1/4}$ is attained when $g \geq 3$. For $d_{2,\infty}(\hat{\mathbf{U}}_g, \mathbf{U})$, the optimal rate $n^{-3/4}$ is attained when $g \geq 3$. No convergence is guaranteed when $g \leq 2$.

(ii) Next suppose $\tilde{k} = \Omega(n)$. Then $d_2(\hat{\mathbf{U}}_g, \mathbf{U})$ attains the optimal rate of $n^{-\beta/2}$ for all $g \geq 1$ and for any $\beta > 0$. In contrast, $d_{2,\infty}(\hat{\mathbf{U}}_g, \mathbf{U})$ attains the optimal rate of $n^{-(1+\beta)/2}$ for $g \geq 1$ and any $\beta \geq 1/2$, but a possibly slower rate when $g = 1$ and $\beta < 1/2$, i.e.,

- if $3a + 2 < \beta^{-1} < 3a + 3$ for some integer $a \geq 0$ then $d_{2,\infty}(\hat{\mathbf{U}}_g, \mathbf{U})$ attain the optimal rate of $n^{-(1+\beta)/2}$ when $g \geq a + 2$, a slower rate of $n^{-3(a+1)\beta/2}$ when $g = a + 1$, and might not converge when $g = a$.
- if $3a \leq \beta^{-1} \leq 3a + 2$ for some integer $a \geq 0$ then $d_{2,\infty}(\hat{\mathbf{U}}_g, \mathbf{U})$ attain the optimal rate of $n^{-(1+\beta)/2}$ when $g \geq a + 1$ but might not converge when $g \leq a$.

In summary, the above discussions provide further evidence to the well-known advice that choosing a slightly larger g and \tilde{k} are essential to the success of RSVD in practical applications (Martinsson and Tropp, 2020).

S1.2 Additional numerical results for exact recovery

We used the same simulation setting as that described in Section 4.1 in the main paper, with $n \in \{1000, \dots, 5000\}$ and $\rho_n \in \{1, 3n^{-1/3}, 4n^{-1/2}\}$. For each combination of n and ρ_n , we generate an adjacency matrix \mathbf{A} with equal sized blocks and block probabilities \mathbf{B}_0 . We then perform RSVD-based spectral clustering with $g \leq 3$, where we use the `Gmedian` library in `R` to perform fast (approximate) K -medians clustering on the rows of $\hat{\mathbf{U}}_g$. For comparison, we also use `Gmedian` to perform K -medians clustering on the rows of $\hat{\mathbf{U}}$. We repeat the above steps for 500 Monte Carlo replicates. The proportion of times (among these 500 replicates) in which the K -medians clustering of either $\hat{\mathbf{U}}_g$ or $\hat{\mathbf{U}}$ correctly recover the community memberships for *all* nodes are reported in Table S1.

From Table S1 we see that K -means clustering on $\hat{\mathbf{U}}_g$ exactly recover the underlying community assignment with probabilities converging to 1 as n increases, provided that $g \geq 2$ when

Table S1: Proportion of times that RSVD-based spectral clustering ($g = 1, 2, 3$) or the original spectral clustering (OSC) exactly recover the memberships of all nodes, among 500 MC rounds; here $\tilde{k} = 5 \log n$. Standard errors are reported in parentheses.

| Sparsity | n | $g = 1$ | $g = 2$ | $g = 3$ | OSC |
|--------------------------|------|---------------|---------------|---------------|---------------|
| $\rho_n \asymp 1$ | 1000 | 0.536 (0.022) | 0.384 (0.000) | 1.000 (0.000) | 1.000 (0.000) |
| | 2000 | 0.616 (0.022) | 1.000 (0.000) | 1.000 (0.000) | 1.000 (0.000) |
| | 3000 | 0.674 (0.021) | 1.000 (0.000) | 1.000 (0.000) | 1.000 (0.000) |
| | 4000 | 0.600 (0.022) | 1.000 (0.000) | 1.000 (0.000) | 1.000 (0.000) |
| | 5000 | 0.626 (0.022) | 1.000 (0.000) | 1.000 (0.000) | 1.000 (0.000) |
| $\rho_n \asymp n^{-1/3}$ | 1000 | 0.000 (0.000) | 0.982 (0.012) | 1.000 (0.000) | 1.000 (0.000) |
| | 2000 | 0.000 (0.000) | 0.996 (0.006) | 1.000 (0.000) | 1.000 (0.000) |
| | 3000 | 0.000 (0.000) | 1.000 (0.000) | 1.000 (0.000) | 1.000 (0.000) |
| | 4000 | 0.000 (0.000) | 1.000 (0.000) | 1.000 (0.000) | 1.000 (0.000) |
| | 5000 | 0.000 (0.000) | 1.000 (0.000) | 1.000 (0.000) | 1.000 (0.000) |
| $\rho_n \asymp n^{-1/2}$ | 1000 | 0.000 (0.000) | 0.000 (0.000) | 0.604 (0.022) | 0.914 (0.013) |
| | 2000 | 0.000 (0.000) | 0.000 (0.000) | 0.892 (0.014) | 1.000 (0.000) |
| | 3000 | 0.000 (0.000) | 0.000 (0.000) | 0.974 (0.007) | 1.000 (0.000) |
| | 4000 | 0.000 (0.000) | 0.000 (0.000) | 0.996 (0.003) | 1.000 (0.000) |
| | 5000 | 0.000 (0.000) | 0.000 (0.000) | 0.998 (0.002) | 1.000 (0.000) |

$\rho_n \in \{1, 3n^{-1/3}\}$ and $g \geq 3$ when $\rho_n = 4n^{-1/2}$. These empirical results are consistent with the theoretical results presented in Theorem 4, i.e., exact recover is guaranteed if and only if $g > \beta^{-1}$. Note that $\beta^{-1} = 1$ when $\rho_n = 1$, $\beta^{-1} = \frac{3}{2}$ when $\rho_n \asymp n^{-1/3}$, and $\beta^{-1} = 2$ when $\rho_n \asymp n^{-1/2}$. Finally we note that if $g = 1$ and $\rho_n = 1$ then RSVD-based spectral clustering occasionally recovers the community membership for all nodes. This is due to the fact that although $d_{2,\infty}(\hat{\mathbf{U}}_1, \mathbf{U}) = \Omega(n^{-1/2})$ with high probability, it is still possible that $d_{2,\infty}(\hat{\mathbf{U}}_1, \mathbf{U}) \leq \zeta_*$ where ζ_* is the minimum ℓ_2 distance between any two nodes i and j belonging to different communities; exact recovery is certainly expected if $d_2(\hat{\mathbf{U}}_1, \mathbf{U}) \leq \zeta_*$.

S2 Matrix completion with noises

S2.1 Theoretical results

Let $\mathbf{T} \in \mathbb{R}^{n \times n}$ be a matrix whose entries are only partially and noisily observed. Such matrix occurs in many real-world applications, including the well-known Netflix challenge. As another example, if \mathbf{T} is an Euclidean distance matrix (EDM) between n points in \mathbb{R}^d then $\text{rk}(\mathbf{T}) \leq d + 2$ and it is commonly the case that \mathbf{T} is noisily observed (Javanmard and Montanari, 2013); similarly, if \mathbf{T} is a signal correlation matrix between multiple remote sensors then \mathbf{T} is partially observed due to power constraints (Cheng et al., 2012). Assume, for the current discussion, that

\mathbf{T} is symmetric and we observed

$$\hat{\mathbf{T}} = \mathcal{P}_{\mathbf{\Omega}}(\mathbf{T} + \mathbf{N}) := \mathbf{\Omega} \circ (\mathbf{T} + \mathbf{N}), \quad (\text{S2.1})$$

where \mathbf{N} denote an unobserved symmetric $n \times n$ noise matrix, $\mathbf{\Omega}$ is a symmetric matrix with $\{0, 1\}$ entries, and \circ denote the Hadamard product. We shall assume, for ease of exposition, that the (upper triangle) entries of \mathbf{N} are iid $\mathcal{N}(0, \sigma^2)$ random variables while the (upper triangular) entries of $\mathbf{\Omega}$ are iid Bernoulli random variables with success probability p . As $\mathbb{E}[p^{-1}\hat{\mathbf{T}}] = \mathbf{T}$, one simple and widely used estimate for \mathbf{T} is given by $p^{-1}\hat{\mathbf{T}}^{(k)}$ where $\hat{\mathbf{T}}^{(k)}$ is the truncated rank- k SVD of $\hat{\mathbf{T}}$ for some choice of k ; see [Abbe et al. \(2020\)](#); [Chen et al. \(2021\)](#); [Chatterjee \(2015\)](#) and the references therein.

In many real-world applications, the dimensions of $\hat{\mathbf{T}}$ can be rather large and yet $\hat{\mathbf{T}}$ can be quite sparse compared to \mathbf{T} , i.e., the number of non-zero entries of $\hat{\mathbf{T}}$ is much smaller than n^2 . It is thus computationally attractive to approximate the left singular vectors of $\hat{\mathbf{T}}$ using randomized SVD. More specifically, let $\hat{\mathbf{U}}_g$ be the output of Algorithm 1 with $\hat{\mathbf{M}} = \hat{\mathbf{T}}$ for some choices of k, \tilde{k} and g . Given $\hat{\mathbf{U}}_g$ we compute a rank- k approximation for $\hat{\mathbf{T}}$ via $\hat{\mathbf{U}}_g \hat{\mathbf{U}}_g^\top \hat{\mathbf{T}}$. We can then take $\hat{\mathbf{T}}_g := p^{-1} \hat{\mathbf{U}}_g \hat{\mathbf{U}}_g^\top \hat{\mathbf{T}}$ or $2^{-1}(\hat{\mathbf{T}}_g + \hat{\mathbf{T}}_g^\top)$ as an estimate for \mathbf{T} .

We now combine the $\ell_{2,\infty}$ perturbation and entrywise concentration bounds in Corollary 3 of our paper with Theorem 3.4 of [Abbe et al. \(2020\)](#) to obtain error bounds for $\hat{\mathbf{U}}_g$ and $\hat{\mathbf{T}}_g$ as estimates for \mathbf{U} and \mathbf{M} , respectively. For ease of exposition we shall assume that p is known. If p is unknown then, as the entries of \mathbf{T} are assumed to be missing completely at random, it can be consistently estimated from the proportion of observed entries in $\hat{\mathbf{T}}$. The resulting \hat{p} converges to p at rate $n^{-1}p^{-1/2}$ and has no effect on the theoretical results.

Theorem S6. *Let \mathbf{T} be a symmetric $n \times n$ matrix and denote $k_0 := \text{rk}(\mathbf{T})$. Let $\hat{\mathbf{T}}$ be a noisily observed version of \mathbf{T} sampled according to Eq. (S2.1) for some known value of $p \in (0, 1)$. Let $\lambda_i(\mathbf{T})$ denote the i th largest eigenvalue (in modulus) of \mathbf{T} . Define $E_n = (n/p)^{1/2} \{\|\mathbf{T}\|_{\max} + \sigma\}$ and suppose that*

$$np \gtrsim \log n, \quad \text{and} \quad |\lambda_{k_0}(\mathbf{T})|/E_n \gtrsim \kappa(\log n)^{1/2}, \quad (\text{S2.2})$$

where $\kappa = |\lambda_1(\mathbf{T})/\lambda_{k_0}(\mathbf{T})|$ is the condition number for \mathbf{T} . Let $\hat{\mathbf{U}}_g$ be obtained from Algorithm 1 with $\tilde{k} = (1 - c_{\text{gap}})^{-2}\{k_0 + \sqrt{12k_0 \log n} + 6 \log n\}$ and $g \geq g_* := \frac{\log(n/\tilde{k})}{\log(|\lambda_{k_0}(\mathbf{T})|/E_n)}$. We then have, with probability at least $1 - 2n^{-3}$, that

$$d_2(\hat{\mathbf{U}}_g, \mathbf{U}) \lesssim \frac{(n/p)^{1/2}\{\|\mathbf{T}\|_{\max} + \sigma\}}{|\lambda_{k_0}(\mathbf{T})|}, \quad (\text{S2.3})$$

$$d_{2,\infty}(\hat{\mathbf{U}}_g, \mathbf{U}) \lesssim \frac{\kappa^2(n/p)^{1/2}(\log n)^{1/2}\{\|\mathbf{T}\|_{\max} + \sigma\}\|\mathbf{U}\|_{2,\infty}}{|\lambda_{k_0}(\mathbf{T})|}, \quad (\text{S2.4})$$

$$\|\hat{\mathbf{T}}_g - \mathbf{T}\|_{\max} \lesssim \kappa^4(n/p)^{1/2}(\log n)^{1/2}\{\|\mathbf{T}\|_{\max} + \sigma\}\|\mathbf{U}\|_{2,\infty}^2 \quad (\text{S2.5})$$

simultaneously. If $|\lambda_{k_0}(\mathbf{T})|/E_n \gtrsim n^\epsilon$ for a fixed but arbitrary $\epsilon > 0$ then Eq. (S2.3) through Eq. (S2.5) holds for all $g \geq 1 + (2\epsilon)^{-1}$.

The uniform entrywise bound for $\hat{\mathbf{T}}_g - \mathbf{T}$ in Eq. (S2.5) can be further refined to yield entrywise limiting distributions. For ease of exposition we only consider the case where \mathbf{T} is homogeneous, has finite rank, and bounded condition number, as these assumptions lead to results that are simple to state while containing all key features of more general results.

Corollary S4. Consider the setting in Theorem S6 with \mathbf{T} satisfying following assumptions

- C1. $\min_{k\ell} |T_{k\ell}| \asymp \|\mathbf{T}\|_{\max}$ and $\text{rk}(\mathbf{T}) = k_0$ for some finite constant k_0 .
- C2. $\kappa := |\lambda_1(\mathbf{T})/\lambda_{k_0}(\mathbf{T})| \leq C_\kappa$ for some finite constant C_κ not depending on n .
- C3. $np \gtrsim \log^6 n$ and $p \leq 1 - \delta$ for some constant δ not depending on n .
- C4. $\lambda_{k_0}(\mathbf{T}) \gtrsim (n/p)^{1/2}\sigma \log^3 n$.

Let $\zeta_{k\ell} = [\mathbf{U}\mathbf{U}^\top]_{k\ell}$ and denote the variance of $[\mathbf{U}\mathbf{U}^\top \mathbf{E}]_{ij} + [\mathbf{E}\mathbf{U}\mathbf{U}^\top]_{ij}$ by

$$v_{ij}^* := \frac{1}{p} \sum_{\ell \neq j} \{(1-p)T_{i\ell}^2 + \sigma^2\} \zeta_{\ell j}^2 + \frac{1}{p} \sum_{\ell \neq i} \{(1-p)T_{\ell j}^2 + \sigma^2\} \zeta_{i\ell}^2 \quad (\text{S2.6})$$

Then for \tilde{k} and $g \geq g_*$ as specified in Theorem S6, and for any indices pair (i, j) , we have

$$(v_{ij}^*)^{-1/2}[\hat{\mathbf{T}}_g - \mathbf{T}]_{ij} \rightsquigarrow \mathcal{N}(0, 1) \quad \text{as } n \rightarrow \infty. \quad (\text{S2.7})$$

(*Entrywise confidence interval*) Let $\hat{\zeta}_{k\ell} = [\hat{\mathbf{U}}_g \hat{\mathbf{U}}_g^\top]_{k\ell}$ and define

$$\hat{v}_{ij} := \sum_{\ell \neq j} [\hat{\mathbf{E}}]_{i\ell}^2 \hat{\zeta}_{\ell j}^2 + \sum_{\ell \neq i} [\hat{\mathbf{E}}]_{\ell j}^2 \hat{\zeta}_{i\ell}^2 + [\hat{\mathbf{E}}]_{ij}^2 \{\hat{\zeta}_{ii} + \hat{\zeta}_{jj}\}^2 \quad (\text{S2.8})$$

where $\hat{\mathbf{E}} := \hat{\mathbf{T}}_g - p^{-1}\hat{\mathbf{T}}$. Then for any indices pair (i, j) , we have

$$(\hat{v}_{ij})^{-1/2} [\hat{\mathbf{T}}_g - \mathbf{T}]_{ij} \rightsquigarrow \mathcal{N}(0, 1), \quad \text{as } n \rightarrow \infty. \quad (\text{S2.9})$$

If $|\lambda_{k_0}(\mathbf{T})|/E_n \gtrsim n^\epsilon$ for any fixed $\epsilon > 0$ then Eqs. (S2.7) and (S2.9) holds for $g \geq 2 + (2\epsilon)^{-1}$.

Corollary S4 provides more precise control of the entrywise fluctuations for $\hat{\mathbf{T}}_g - \mathbf{T}$ compared to Theorem S6 and thus require slightly stronger conditions for np and $\lambda_{k_0}(\mathbf{T})$ compared to that in Eq. (S2.2). These same conditions for np and $\lambda_{k_0}(\mathbf{T})$ as well as the assumption that \mathbf{T} is homogeneous were also used in the proof of Theorem 4.12 of Chen et al. (2021) for the estimator $p^{-1}\hat{\mathbf{T}}^{(k)}$; homogeneity of \mathbf{T} guarantees that the entrywise noise levels for $\hat{\mathbf{T}}$ are roughly on the same order and leads to a convenient lower bound for v_{ij}^* . The assumption that p is bounded away from 1 is a mild assumption (it is used implicitly in the proof of Theorem 4.12 in Chen et al. (2021)) as the typical setting for matrix completion is that $p = o(1)$ as n increases. The assumptions of finite rank and bounded condition numbers are also commonly seen in the literature. These assumptions can be relaxed with substantially more involved book-keeping; see Eqs. (4.80) and (4.169) of Chen et al. (2021) for examples of conditions where κ and k_0 are allowed to vary with n . Finally, \hat{v}_{ij} in Eq. (S2.8) is computable using only the RSVD output $\hat{\mathbf{U}}_g$.

S2.2 Real data application: Distance matrix completion

For this section we apply Algorithm 1 to recover the missing entries of a partially observed Euclidean distance matrix. In particular we use the `world_cities` dataset containing the locations of the 4428 most populous cities around the world; this dataset is part of the `mdsr` library in R

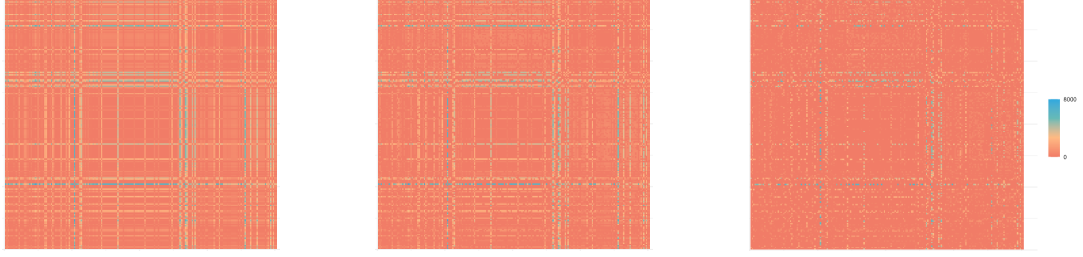


Figure S5: Matrix plots for the true \mathbf{D} (Left), partially observed $\mathbf{D}_{0.8}$ (Middle), and partially observed $\mathbf{D}_{0.4}$ (Right).

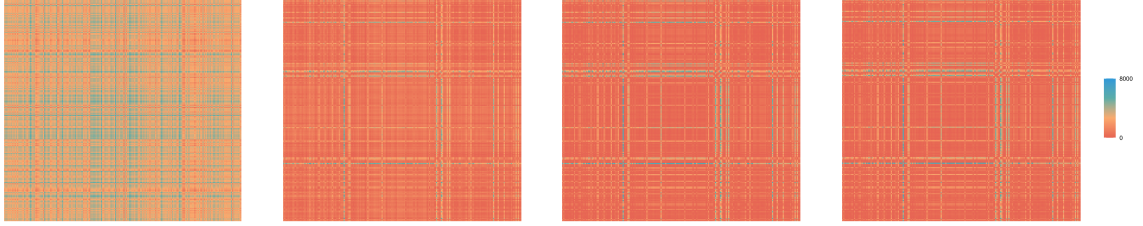


Figure S6: From left to right: matrix plots of RSVD-based estimates $\hat{\mathbf{D}}_{0.8}^{(1)}$, $\hat{\mathbf{D}}_{0.8}^{(2)}$, $\hat{\mathbf{D}}_{0.8}^{(5)}$, and exact SVD estimate $\hat{\mathbf{D}}_{0.8}$

Table S2: The α th-quantiles for the relative entrywise errors of the RSVD-based estimates $\hat{\mathbf{D}}_p^{(g)}$ and truncated (exact) SVD estimate $\hat{\mathbf{D}}_p$.

| α | 0.05 | 0.15 | 0.35 | 0.5 | 0.65 | 0.85 | 0.95 |
|--------------------------------|--------|--------|--------|--------|--------|--------|---------|
| $\hat{\mathbf{D}}_{0.8}^{(1)}$ | 0.0169 | 0.0517 | 0.1320 | 0.2210 | 0.4199 | 2.4288 | 15.3182 |
| $\hat{\mathbf{D}}_{0.8}^{(2)}$ | 0.0038 | 0.0115 | 0.0298 | 0.0504 | 0.0899 | 0.3170 | 1.8230 |
| $\hat{\mathbf{D}}_{0.8}^{(5)}$ | 0.0024 | 0.0073 | 0.0182 | 0.0289 | 0.0465 | 0.1532 | 0.7829 |
| $\hat{\mathbf{D}}_{0.8}$ | 0.0024 | 0.0073 | 0.0182 | 0.0289 | 0.0464 | 0.1530 | 0.7816 |
| $\hat{\mathbf{D}}_{0.4}^{(1)}$ | 0.0381 | 0.1140 | 0.2701 | 0.4120 | 0.6794 | 3.9035 | 24.6562 |
| $\hat{\mathbf{D}}_{0.4}^{(2)}$ | 0.0106 | 0.0326 | 0.0858 | 0.1488 | 0.2750 | 1.3274 | 9.0400 |
| $\hat{\mathbf{D}}_{0.4}^{(5)}$ | 0.0073 | 0.0221 | 0.0558 | 0.0911 | 0.1570 | 0.5468 | 3.3533 |
| $\hat{\mathbf{D}}_{0.4}$ | 0.0064 | 0.0194 | 0.0484 | 0.0774 | 0.1269 | 0.4439 | 2.4614 |

(Baumer et al., 2017). We first construct the 4428×4428 matrix $\mathbf{D} = [D_{ij}]$ whose elements are

$$D_{ij} = (\text{Lon}_i - \text{Lon}_j)^2 + (\text{Lat}_i - \text{Lat}_j)^2.$$

Here Lon_i and Lat_i represent the longitude and latitude of the i th city, respectively. We then sample a matrix $\mathbf{D}_{0.8}$ (resp. $\mathbf{D}_{0.4}$) by keeping roughly 80% (resp. 40%) of the entries in \mathbf{D} , i.e., $\mathbf{D}_{0.8} = \mathbf{\Omega} \circ \mathbf{D}$ where $\mathbf{\Omega}$ is a symmetric matrix whose upper triangular entries are iid Bernoulli(0.8). We now recover \mathbf{D} from $\mathbf{D}_{0.8}$ (resp. $\mathbf{D}_{0.4}$) using Algorithm 1. As the entries of \mathbf{D} are Euclidean distances between points in \mathbb{R}^2 , we have $\text{rk}(\mathbf{D}) \leq 4$. We therefore choose $k = 4$, $\tilde{k} = 20$ and $g \in \{1, 2, 5\}$, and let $\hat{\mathbf{D}}_{0.8}^{(g)}$ (resp. $\hat{\mathbf{D}}_{0.4}^{(g)}$) be the resulting estimate of \mathbf{D} . For

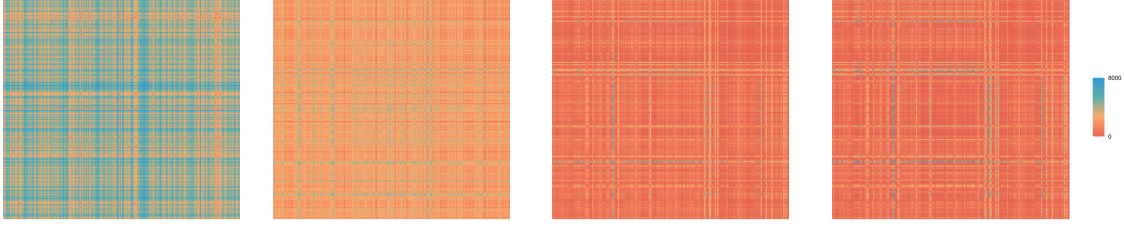


Figure S7: From left to right: matrix plots of RSVD-based estimates $\hat{\mathbf{D}}_{0.4}^{(1)}$, $\hat{\mathbf{D}}_{0.4}^{(2)}$, $\hat{\mathbf{D}}_{0.4}^{(5)}$, and truncated (exact) SVD estimate $\hat{\mathbf{D}}_{0.4}$

comparison we also consider the spectral estimate $\hat{\mathbf{D}}_{0.8}$ (resp. $\hat{\mathbf{D}}_{0.4}$) obtained by truncating the exact SVD of $\mathbf{D}_{0.8}$ (resp. $\mathbf{D}_{0.4}$); see [Keshavan et al. \(2010\)](#) for more details.

A plot of the true distance matrix \mathbf{D} and one random realization of the partially observed $\mathbf{D}_{0.8}$ and $\mathbf{D}_{0.4}$ are presented in Figure S5. The corresponding RSVD-based estimates and exact SVD based estimates of \mathbf{D} are then shown in Figure S6–S7. Figure S6 shows that $\hat{\mathbf{D}}_{0.8}^{(2)}$ and $\hat{\mathbf{D}}_{0.8}^{(5)}$ both have comparable accuracy to $\hat{\mathbf{D}}_{0.8}$ while Figure S7 shows that $\hat{\mathbf{D}}_{0.4}^{(2)}$ has much worse accuracy compared to $\hat{\mathbf{D}}_{0.4}^{(5)}$ and $\hat{\mathbf{D}}_{0.4}$.

We also record the entrywise relative errors between the RSVD-based estimates $\hat{\mathbf{D}}_p^{(g)}$ (resp. the exact SVD-based estimate $\hat{\mathbf{D}}_p$) against that of \mathbf{D} . A summary of the quantile levels for these relative errors are presented in Tables S2. The α th-quantile of the entrywise relative errors between an estimate \mathbf{Z} and the true distance \mathbf{D} is defined as the α th quantile of $\{||[\mathbf{Z}-\mathbf{D}]_{ij}|/[\mathbf{D}]_{ij}| : (i, j) \in [4428] \times [4428]\}$; for example the median relative error for $\hat{\mathbf{D}}_{0.8}^{(5)}$ and $\hat{\mathbf{D}}_{0.4}^{(5)}$ are ≈ 0.029 and ≈ 0.086 , respectively. Note that the numbers in Table S2 are averaged over 200 independent random samples of either $\mathbf{D}_{0.8}$ or $\mathbf{D}_{0.4}$. From Table S2 we see that the relative error decreases as g increases with p fixed; indeed, the relative errors of $\hat{\mathbf{D}}_{0.8}^{(5)}$ are nearly identical to those of $\hat{\mathbf{D}}_{0.8}$. Table S2 also indicates that as p decrease we need to increase g to achieve a recovery rate close to that of $\hat{\mathbf{D}}$. These observations are consistent with the theoretical results in Theorem S6.

S3 PCA with missing data

S3.1 Computational refinement and theoretical results

We now consider principal components estimation with missing data. In particular, we focus on the following factor model from [Cai et al. \(2021\)](#):

$$\mathbf{X} = \mathbf{B}\mathbf{F} + \mathbf{N}. \quad (\text{S3.1})$$

Here \mathbf{B} is a $d \times k_0$ matrix, $\mathbf{F} = [\mathbf{f}_1, \dots, \mathbf{f}_m] \in \mathbb{R}^{k_0 \times m}$ is a $k_0 \times m$ matrix whose entries are iid $\mathcal{N}(0, 1)$, and \mathbf{N} is a $d \times m$ matrix whose entries are iid $\mathcal{N}(0, \sigma^2)$; note that \mathbf{B} , \mathbf{N} and \mathbf{F} are assumed to be mutually independent. The columns of \mathbf{X} are then iid random vectors with mean $\mathbf{0}$ and covariance matrix $\mathbf{B}\mathbf{B}^\top + \sigma^2\mathbf{I}_d$. The columns of $\mathbf{B}\mathbf{F}$ are iid signal random vectors with mean $\mathbf{0}$ and a low-rank covariance matrix $\mathbf{B}\mathbf{B}^\top$. Denote eigendecomposition $\mathbf{B}\mathbf{B}^\top = \mathbf{U}\mathbf{\Lambda}\mathbf{U}^\top$ where $\mathbf{U} \in \mathbb{O}_{d \times k}$ and $\mathbf{\Lambda} = \text{diag}(\lambda_1, \dots, \lambda_k)$; the columns of \mathbf{U} are the leading principal components.

Due to sampling issues and/or privacy-preserving intention, it is often the case that only a partial subset of the entries in \mathbf{X} are observed. More specifically let $\mathbf{\Omega}$ be a $d \times m$ binary matrix whose entries are iid Bernoulli random variables with success probability p . Then, instead of observing \mathbf{X} , we only observe

$$\mathbf{Y} = \mathcal{P}_{\mathbf{\Omega}}(\mathbf{X}) = \mathbf{\Omega} \circ \mathbf{X} = \mathbf{\Omega} \circ (\mathbf{B}\mathbf{F} + \mathbf{N}),$$

where \circ denotes the Hadamard product between matrices. Given observed \mathbf{Y} , [Cai et al. \(2021\)](#) propose the following spectral procedure for recovering the principle components \mathbf{U} : form the matrix

$$\mathbf{Q} = \frac{1}{mp^2} \mathcal{P}_{\text{off-diag}}(\mathbf{Y}\mathbf{Y}^\top), \quad (\text{S3.2})$$

where $\mathcal{P}_{\text{off-diag}}(\cdot)$ sets diagonal entries of the corresponding matrix to zero, and compute the $d \times k_0$ matrix $\hat{\mathbf{U}}$ whose columns are the leading singular vectors of \mathbf{Q} . As the dimension d can be reasonably large compared to the number of samples m while the number of non-zero entries in \mathbf{Y} can be much smaller than md , we can replace the singular vectors $\hat{\mathbf{U}}$ of \mathbf{Q} by the

Algorithm S2: RSVD-based PCA with missing data

Input: $\mathbf{Y} \in \mathbb{R}^{d \times m}$, rank $k \geq 1$, sketching dimension $\tilde{k} \geq k$, power iterations $g \geq 1$.

- 1 Generate a $d \times k$ sketching matrix \mathbf{G} whose elements are iid standard normals;
- 2 Compute the diagonal entries of $\mathbf{Y}\mathbf{Y}^\top$ and obtain $\mathcal{P}_{\text{diag}}(\mathbf{Y}\mathbf{Y}^\top)$;
- 3 **for** $s = 1$ **to** g **do**
- 4 Compute:

$$\begin{aligned} \mathbf{Y}^\top \mathbf{Q}^{s-1} \mathbf{G} &\leftarrow \mathbf{Y}^\top (\mathbf{Q}^{s-1} \mathbf{G}); \\ \mathbf{Q}^s \mathbf{G} &\leftarrow \frac{1}{mp^2} \mathbf{Y} (\mathbf{Y}^\top \mathbf{Q}^{s-1} \mathbf{G}) - \frac{1}{mp^2} \mathcal{P}_{\text{diag}}(\mathbf{Y}\mathbf{Y}^\top) \mathbf{Q}^{s-1} \mathbf{G}; \end{aligned}$$
- 5 Obtain the *exact* SVD of $\mathbf{Q}^g \mathbf{G}$. Let $\hat{\mathbf{U}}_g$ be the $d \times k$ matrix whose columns are the k leading left singular vectors of $\mathbf{Q}^g \mathbf{G}$;
- 6 Compute the RSVD-based rank- k approximation of \mathbf{Q} . First, compute $\hat{\mathbf{U}}_g^\top \mathbf{Y}\mathbf{Y}^\top$ and $\hat{\mathbf{U}}_g^\top \mathcal{P}_{\text{diag}}(\mathbf{Y}\mathbf{Y}^\top)$ where the matrix multiplications are done from left to right. Then obtain

$$\hat{\mathbf{Q}}_g \leftarrow \frac{1}{mp^2} \hat{\mathbf{U}}_g \times (\hat{\mathbf{U}}_g^\top \mathbf{Y}\mathbf{Y}^\top) - \frac{1}{mp^2} \hat{\mathbf{U}}_g \times (\hat{\mathbf{U}}_g^\top \mathcal{P}_{\text{diag}}(\mathbf{Y}\mathbf{Y}^\top));$$

Output: Subspace estimate $\hat{\mathbf{U}}_g$ and covariance matrix estimate $\hat{\mathbf{Q}}_g$.

approximate singular vectors $\hat{\mathbf{U}}_g$ computed using RSVD.

Note that direct computation of \mathbf{Q} as the input to Algorithm 1 may involve large-scale matrix multiplications when d and m are large. In particular, we need to compute $\mathbf{Y}\mathbf{Y}^\top$, which incurs a cost of $O(md^2p)$ floating point operations (flops) and also require substantial memory storage. We address these computational challenges by refining the standard RSVD-based approach for missing-data PCA to avoid the need for explicit computation of $\mathbf{Y}\mathbf{Y}^\top$ as follows. First, for any $\mathbf{\Gamma} \in \mathbb{R}^{d \times \tilde{k}}$,

$$\begin{aligned} \mathbf{Q}\mathbf{\Gamma} &= \frac{1}{mp^2} \mathcal{P}_{\text{off-diag}}(\mathbf{Y}\mathbf{Y}^\top) \mathbf{\Gamma} \\ &= \frac{1}{mp^2} \{\mathbf{Y}\mathbf{Y}^\top - \mathcal{P}_{\text{diag}}(\mathbf{Y}\mathbf{Y}^\top)\} \mathbf{\Gamma} = \frac{1}{mp^2} \mathbf{Y} (\mathbf{Y}^\top \mathbf{\Gamma}) - \frac{1}{mp^2} \mathcal{P}_{\text{diag}}(\mathbf{Y}\mathbf{Y}^\top) \mathbf{\Gamma}, \end{aligned} \tag{S3.3}$$

where $\mathcal{P}_{\text{diag}}(\cdot)$ denotes the operator that preserves only the diagonal entries. Hence, instead of explicitly forming \mathbf{Q} and then computing the sketched matrix $\mathbf{Q}\mathbf{G}$ in Algorithm 1, we can set $\mathbf{\Gamma} = \mathbf{G}$ and compute

$$\frac{1}{mp^2} \mathbf{Y} (\mathbf{Y}^\top \mathbf{G}) - \frac{1}{mp^2} \mathcal{P}_{\text{diag}}(\mathbf{Y}\mathbf{Y}^\top) \mathbf{G}, \tag{S3.4}$$

which only requires access to \mathbf{Y} and the diagonal entries of $\mathbf{Y}\mathbf{Y}^\top$. In addition, the first term

in the right-hand side of Eq. (S3.4) involves matrix multiplication between smaller matrices and has a computational cost of $O(m\tilde{k}p)$ flops while the second term requires computing the diagonal entries of $\mathbf{Y}\mathbf{Y}^\top$ (which require $O(mdp)$ flops) followed by a matrix multiplication between $\mathcal{P}_{\text{diag}}(\mathbf{Y}\mathbf{Y}^\top)$ and \mathbf{G} (which costs $O(d\tilde{k})$ flops). Overall, Eq. (S3.4) reduces the cost for computing $\mathbf{Q}\mathbf{G}$ from $O(md^2p)$ to $O(m\tilde{k}p + d\tilde{k})$ flops (which is significant reduction when $\tilde{k} \ll d$). The same approach can also be used for computing $\mathbf{Q}(\mathbf{Q}\mathbf{G}), \mathbf{Q}(\mathbf{Q}^2\mathbf{G}), \dots, \mathbf{Q}(\mathbf{Q}^{g-1}\mathbf{G})$ by simply replacing $\mathbf{\Gamma} = \mathbf{G}$ with $\mathbf{\Gamma} = \mathbf{Q}\mathbf{G}, \mathbf{Q}^2\mathbf{G}, \dots, \mathbf{Q}^{g-1}\mathbf{G}$ in Eq. (S3.3). See Algorithm S2 for more details.

The following result combines Corollary 3 with error bounds given in Corollary 4.3 of Cai et al. (2021) to show that the $\hat{\mathbf{U}}_g$ achieves the same estimation rate as that for $\hat{\mathbf{U}}$ in approximating the principal subspace; note that the condition for m in Eq. (S3.5) below is identical to Eq. (4.14) of Cai et al. (2021).

Theorem S7. *Let \mathbf{X} be a $d \times m$ matrix sampled according to Eq. (S3.1). Let $\mu = dr^{-1}\|\mathbf{U}\|_{2,\infty}^2$ denote the coherence parameter for \mathbf{U} , $\kappa = \lambda_1/\lambda_{k_0}$ the condition number for $\mathbf{B}\mathbf{B}^\top$, and $s_* = \log(m+d)$. Suppose there exist constants $\tilde{c}_0 > 0$ and $\tilde{c}_1 > 0$ such that $k_0 \leq \frac{\tilde{c}_1 d}{\mu\kappa^2}$ and m satisfies the sample size condition*

$$m \geq \tilde{c}_0 \max\left\{\frac{\mu^2\kappa^6 k_0^2 s_*^6}{dp^2}, \frac{\mu\kappa^5 k_0 s_*^3}{p}, \frac{\sigma^4 \kappa^2 s_*^2}{\lambda_{k_0}^2 p^2}, \frac{\sigma^2 \kappa^3 ds_*}{\lambda_{k_0} p}\right\}. \quad (\text{S3.5})$$

Now define

$$\mathcal{E} := \frac{\mu\kappa^2 k_0 s_*^2}{(md)^{1/2}p} + \frac{(\mu\kappa^3 k_0)^{1/2} s_*}{(md)^{1/2}} + \frac{\sigma^2 d^{1/2} s_*}{\lambda_{k_0}^2 m^{1/2} p} + \frac{\sigma(\kappa ds_*)^{1/2}}{(\lambda_{k_0} mp)^{1/2}} + \frac{\mu\kappa k_0}{d}. \quad (\text{S3.6})$$

Let $\hat{\mathbf{U}}_g$ be generated via Algorithm S2 (or equivalently, generated from Algorithm 1 with $\hat{\mathbf{M}} = \mathbf{Q}$), $\tilde{k} \geq (1 - c_{\text{gap}})^{-2}\{k_0 + \sqrt{24k_0 \log d} + 6 \log d\}$ and $g \geq \frac{\log d}{\log(1/\mathcal{E})}$. Then with probability at least $1 - m^{-3}$, we have

$$d_2(\hat{\mathbf{U}}_g, \mathbf{U}) \lesssim \mathcal{E}, \quad \text{and} \quad d_{2,\infty}(\hat{\mathbf{U}}_g, \mathbf{U}) \lesssim \kappa^{3/2} \log^{1/2}(m+d) \mathcal{E} \|\mathbf{U}\|_{2,\infty}. \quad (\text{S3.7})$$

Finally, if $\mathcal{E} \lesssim d^{-\epsilon}$ for a fixed $\epsilon > 0$ then Eq. (S3.7) holds for all $g \geq 1 + (2\epsilon)^{-1}$.

S3.2 Extension: HeteroPCA with RSVD approximation

Recent work has studied heteroskedastic PCA (HeteroPCA) (Zhang et al., 2022; Agterberg et al., 2022; Yan et al., 2024; Zhou and Chen, 2025), a more elaborate PCA algorithm compared with the diagonal-deleted PCA in Section S3.1. It is designed to address bias arising from heteroskedastic noise in \mathbf{N} and to further enable efficient inference for the underlying principal subspace. Rather than directly using the leading singular vectors of the diagonal-deleted matrix \mathbf{Q} to estimate \mathbf{U} , HeteroPCA treats the top- k eigendecomposition of \mathbf{Q} as an initial spectral estimator of the underlying covariance matrix $\mathbf{B}\mathbf{B}^\top = \mathbf{U}\mathbf{\Lambda}\mathbf{U}^\top$. It then iteratively imputes the diagonal entries of $(mp^2)^{-1}\mathcal{P}_{\text{off-diag}}(\mathbf{Y}\mathbf{Y}^\top)$ with the diagonal entries of the current spectral estimate of $\mathbf{B}\mathbf{B}^\top$, followed by updating the spectral estimate of $\mathbf{B}\mathbf{B}^\top$ via the top- k eigendecomposition of the newly imputed matrix; see Algorithm 1 in Zhang et al. (2022) for details. As each iteration of HeteroPCA requires an SVD of a $d \times d$ matrix, we can replace the SVD step with RSVD to improve computational efficiency. See Algorithm S3 for more details. Note that Algorithm S3 also avoids direct computation of the matrix $\mathbf{Y}\mathbf{Y}^\top$.

Remark S8. The matrix \mathbf{Q}_t in Algorithm S3 denotes the RSVD-based approximation of the diagonal-imputed sample covariance matrix at the t -th iteration of HeteroPCA, i.e.,

$$\mathbf{Q}_t = \frac{1}{mp^2}\mathcal{P}_{\text{off-diag}}(\mathbf{Y}\mathbf{Y}^\top) + \mathcal{P}_{\text{diag}}(\hat{\mathbf{Q}}_g^{(t-1)}) = \frac{1}{mp^2}\mathbf{Y}\mathbf{Y}^\top - \frac{1}{mp^2}\mathcal{P}_{\text{diag}}(\mathbf{Y}\mathbf{Y}^\top) + \mathcal{P}_{\text{diag}}(\hat{\mathbf{Q}}_g^{(t-1)}),$$

where $\hat{\mathbf{Q}}_g^{(t-1)}$ is the RSVD-based rank- k approximation of \mathbf{Q}_{t-1} .

Similar to Theorem S7, we can apply Corollary 2 and Corollary 3 to show that, if \tilde{k} and g are both sufficient large in each step of Algorithm S3 then the RSVD-based subspace estimator $\hat{\mathbf{U}}_g^{(T)}$ will achieves the same ℓ_2 and $\ell_{2,\infty}$ error rates as HeteroPCA (with exact SVD) for recovering the true principal subspace \mathbf{U} ; see Zhang et al. (2022); Yan et al. (2024) for theoretical results on HeteroPCA with exact SVD. Correspondingly, we also expect that one can use RSVD-based HeteroPCA to construct confidence regions for the principal subspaces and entrywise confidence

Algorithm S3: RSVD-based HeteroPCA

Input: $\mathbf{Y} \in \mathbb{R}^{d \times m}$, rank $k \geq 1$, sketching dimension $\tilde{k} \geq k$, power iterations $g \geq 1$, number of HeteroPCA iterations $T \geq 1$.

- 1 Run Algorithm S2;
- 2 Obtain $\hat{\mathbf{Q}}_g^{(0)} \leftarrow \hat{\mathbf{Q}}_g$ and $\mathcal{P}_{\text{diag}}(\mathbf{Y}\mathbf{Y}^\top)$ from Algorithm S2;
- 3 **for** $t = 1$ **to** T **do**
- 4 Generate a $d \times k$ sketching matrix $\mathbf{G}^{(t)}$ whose elements are iid $\mathcal{N}(0, 1)$;
- 5 **for** $s = 1$ **to** g **do**
- 6 Compute:

$$\begin{aligned} \mathbf{Y}^\top \mathbf{Q}_t^{s-1} \mathbf{G}^{(t)} &\leftarrow \mathbf{Y}^\top \times \left(\mathbf{Q}_t^{s-1} \mathbf{G}^{(t)} \right); \\ \mathbf{Q}_t^s \mathbf{G}^{(t)} &\leftarrow \frac{1}{mp^2} \mathbf{Y} \times \left(\mathbf{Y}^\top \mathbf{Q}_t^{s-1} \mathbf{G}^{(t)} \right) - \frac{1}{mp^2} \mathcal{P}_{\text{diag}}(\mathbf{Y}\mathbf{Y}^\top) \times \mathbf{Q}_t^{s-1} \mathbf{G}^{(t)} \\ &\quad + \mathcal{P}_{\text{diag}}(\hat{\mathbf{Q}}_g^{(t-1)}) \times \mathbf{Q}_t^{s-1} \mathbf{G}^{(t)}; \end{aligned}$$
- 7 Obtain the *exact* SVD of $\mathbf{Q}_t^g \mathbf{G}^{(t)}$. Let $\hat{\mathbf{U}}_g^{(t)}$ be the $d \times k$ matrix whose columns are the k leading left singular vectors of $\mathbf{Q}_t^g \mathbf{G}^{(t)}$;
- 8 Compute the RSVD-based rank- k approximation of \mathbf{Q}_t . First, compute $(\hat{\mathbf{U}}_g^{(t)})^\top \mathbf{Y}\mathbf{Y}^\top$, $(\hat{\mathbf{U}}_g^{(t)})^\top \mathcal{P}_{\text{diag}}(\mathbf{Y}\mathbf{Y}^\top)$ and $(\hat{\mathbf{U}}_g^{(t)})^\top \mathcal{P}_{\text{diag}}(\hat{\mathbf{Q}}_g^{(t-1)})$ where the matrix multiplications are proceeded from left to right. Then compute

$$\begin{aligned} \hat{\mathbf{Q}}_g^{(t)} &\leftarrow \frac{1}{mp^2} \hat{\mathbf{U}}_g^{(t)} \times \left((\hat{\mathbf{U}}_g^{(t)})^\top \mathbf{Y}\mathbf{Y}^\top \right) - \frac{1}{mp^2} \hat{\mathbf{U}}_g^{(t)} \times \left((\hat{\mathbf{U}}_g^{(t)})^\top \mathcal{P}_{\text{diag}}(\mathbf{Y}\mathbf{Y}^\top) \right) \\ &\quad + \hat{\mathbf{U}}_g^{(t)} \times \left((\hat{\mathbf{U}}_g^{(t)})^\top \mathcal{P}_{\text{diag}}(\hat{\mathbf{Q}}_g^{(t-1)}) \right); \end{aligned}$$

Output: Subspace estimate $\hat{\mathbf{U}}_g^{(T)}$ and covariance matrix estimate $\hat{\mathbf{Q}}_g^{(T)}$.

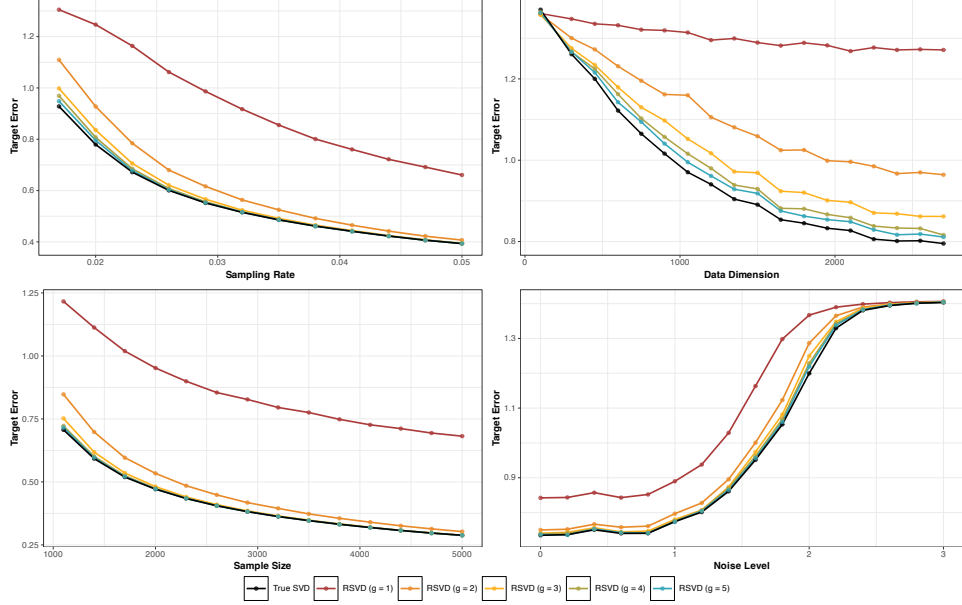


Figure S8: (Top Left) ℓ_2 recovery errors vs. p (here $d = 3000, n = 1000, \sigma = 1$); (Top Right) ℓ_2 recovery errors vs. d (here $n = 1000, p = 0.02, \sigma = 1$); (Bottom Left) ℓ_2 recovery errors vs. n (here $d = 3000, p = 0.02, \sigma = 1$); (Bottom Right) ℓ_2 recovery errors vs. σ (here $d = 3000, n = 1000, p = 0.02$).

intervals for the covariance matrix (as done in [Yan et al. \(2024\)](#) for HeteroPCA with exact SVD). Finally we note that there are two iterations loops in Algorithm S3: the outer loop for diagonal imputation and the inner loop for RSVD. An interesting open problem is how to choose the number of iterations (g and T) in each loop to achieve the optimal trade-off between estimation accuracy and computational cost. Addressing this requires delicate analysis of how g and T jointly affect the error rates of the RSVD-based HeteroPCA, and so we leave it for future work.

S3.3 Numerical experiments

For this simulation study we used the same data generation mechanism as that described in section 7 of [Cai et al. \(2021\)](#) but with larger values of d . More specifically we first sample a $d \times n$ matrix \mathbf{X}^* whose columns are iid multivariate normal random vectors with mean $\mathbf{0}$ and covariance matrix $\mathbf{U}^* \mathbf{U}^{*\top}$; here \mathbf{U}^* is a $d \times 4$ matrix whose entries are iid standard normals. We then generate $\mathcal{P}_{\Omega}(\mathbf{X}) = \Omega \circ (\mathbf{X}^* + \mathbf{E})$ where the entries of \mathbf{E} are iid $\mathcal{N}(0, \sigma^2)$, the entries of Ω are iid Bernoulli(p) and \circ denote the Hadamard product. The matrix $\mathcal{P}_{\Omega}(\mathbf{X})$ represent a noisily observed version of \mathbf{X}^* (with missing entries). The matrices \mathbf{U}^*, \mathbf{E} and Ω are resampled for each Monte Carlo replicate.

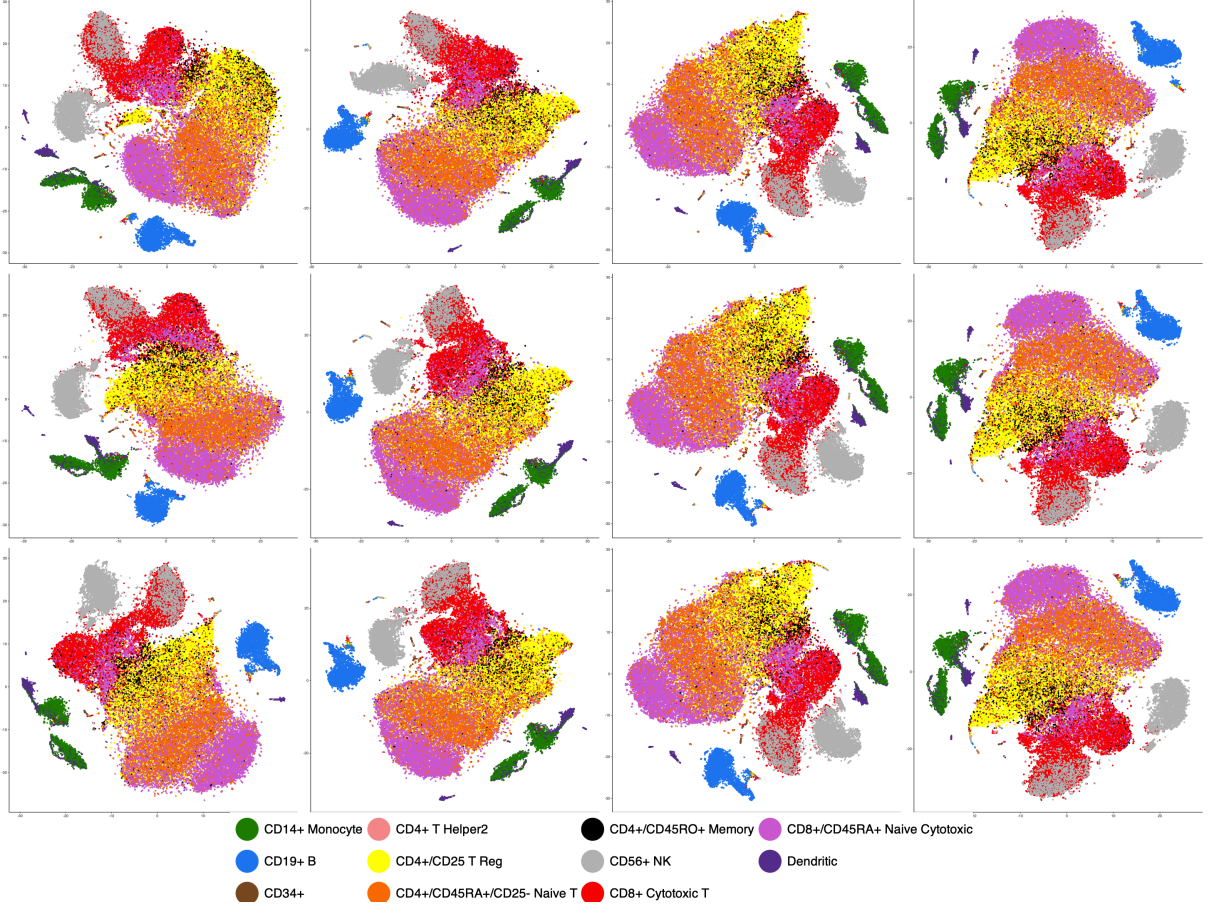


Figure S9: t -SNE embeddings of the 68k PBMC gene expressions, projected on the top 50 PCs obtained via RSVD-based PCA (Algorithm S2). Top row (left to right): results for $g = 3$ with $\tilde{k} = 55, 100, 300$, and 1000 . Middle and bottom rows (left to right): results for $g = 4$ and $g = 5$, respectively, using the same sequence of \tilde{k} values.

Given $\mathcal{P}_{\Omega}(\mathbf{X})$, we compute $\hat{\mathbf{U}}_g$ using Algorithm S2 with $k = 4$, $\tilde{k} = 45$ and $g \in \{1, 2, \dots, 5\}$. We then record $d_2(\hat{\mathbf{U}}_g, \mathbf{U})$; here \mathbf{U} denotes the $d \times 4$ matrix whose columns are the leading eigenvectors of $\mathbf{U}^* \mathbf{U}^{*\top}$. For comparison, we also record $d_2(\hat{\mathbf{U}}, \mathbf{U})$ where $\hat{\mathbf{U}}$ is the $d \times 4$ matrix of leading eigenvectors of \mathbf{Q} and \mathbf{Q} is as defined in Eq. (S3.2). Figure S8 reports sample means for $d_2(\hat{\mathbf{U}}_g, \mathbf{U})$ and $d_2(\hat{\mathbf{U}}, \mathbf{U})$ as we vary the sampling probability p , data dimension d , sample size n , and noise level σ ; these sample means are computed based on 500 Monte Carlo replicates where we resampled the matrices \mathbf{U}^* , \mathbf{E} and Ω in each replicate. Figure S8 shows that the RSVD estimate $\hat{\mathbf{U}}_g$ yields nearly-optimal performance (as compared to $\hat{\mathbf{U}}$) when $g \geq 3$ for most settings of p , d , σ and n . It is only when d is large with respect to n that $\hat{\mathbf{U}}_3$ have worse performance compared to $\hat{\mathbf{U}}_4$, $\hat{\mathbf{U}}_5$ and $\hat{\mathbf{U}}$. Finally, $\hat{\mathbf{U}}_1$ is always sub-optimal. These observations are consistent with the theoretical results presented in Section S3.1.

S3.4 Additional results for Section 4.3

Additional results for the 68k PBMC scRNA-seq data analysis are provided. We apply Algorithm S2 to the full data matrix with $g = 3, 4, 5$ and $\tilde{k} = 55, 100, 300, 1000$. The data are projected onto the top $k = 50$ estimated principal components obtained from Algorithm S2, and the resulting low-dimensional embeddings are visualized using t -SNE in Figure S9.

S4 Distributed estimation for multi-layer networks

Distributed estimation, also known as divide-and-conquer or aggregated inference, is used in numerous methodological applications including PCA Crainiceanu et al. (2011); Tang and Allen (2021); Fan et al. (2019); Chen et al. (2022), regression Huo and Cao (2019); Dobriban and Sheng (2020), integrative data analysis Lock et al. (2013), and is also a key component underlying federated learning Zhang et al. (2021). These types of procedures are particularly important for analyzing large-scale datasets that are scattered across multiple organizations or computing nodes, where both the computational complexities and communication costs (including possible privacy constraints) prevent the transfer of all the raw data to a single location.

We now describe how RSVD can be adapted to tackle estimation of \mathbf{U} in a distributed setting, thereby reducing the communication and computation costs. For conciseness we will only present, as a notional example, community detection on multi-layer networks. More specifically, let $\mathbf{A}_1, \mathbf{A}_2, \dots, \mathbf{A}_L$ be a collection of adjacency matrices for undirected graphs, where \mathbf{A}_ℓ is a stochastic blockmodel graph with edge probabilities $\mathbf{P}_\ell = \mathbf{Z}\mathbf{B}_\ell\mathbf{Z}^\top$; here \mathbf{Z} denote the community assignments and \mathbf{B}_ℓ denote the block connection probabilities. The form for \mathbf{P}_ℓ indicates that the community assignments \mathbf{Z} are shared between all L graphs but the connection probabilities \mathbf{B}_ℓ could be different between any pair of graphs. The main inference task is to recover, from the $\{\mathbf{A}_\ell\}_{\ell=1}^L$, the community assignments in \mathbf{Z} ; see e.g., Paul and Chen (2020); Jing et al. (2021); Chen et al. (2022) for a few recent references. In the event when each individual graph \mathbf{A}_ℓ is very sparse, e.g., the average degree of \mathbf{A}_ℓ is of order $O(1)$, consistent estimation of \mathbf{Z} is statistically infeasible using only a single graph \mathbf{A}_ℓ and thus it is necessary to aggregate the $\{\mathbf{A}_\ell\}$. One simple approach is based on first forming $\widehat{\mathbf{M}} = \sum_{\ell=1}^L (\mathbf{A}_\ell^2 - \mathbf{D}_\ell)$ where \mathbf{D}_ℓ is either the $n \times n$

Algorithm S4: Spectral clustering for multi-layer networks using distributed RSVD

- Input:** $\{\mathbf{A}_\ell\} \subset \mathbb{R}^{n \times n}$, rank $k \geq 1$, sketching dimension $\tilde{k} \geq k$, power $g \geq 1$.
- 1 A central server \mathcal{C} generates a seed s and send to each machine $\{\mathcal{M}_\ell\}$;
 - 2 The $\{\mathcal{M}_\ell\}$ uses s to generate the same random Gaussian matrix \mathbf{Y}_0 ;
 - 3 Each \mathcal{M}_ℓ computes $\mathbf{T}_{\ell,1} \leftarrow (\mathbf{A}_\ell^2 - \mathbf{D}_\ell)\mathbf{Y}_0$ and send it back to \mathcal{C} ;
 - 4 **for** $t \leftarrow 2$ **to** g **do**
 - 5 \mathcal{C} computes $\mathbf{Y}_t \leftarrow L^{-1} \sum_\ell \mathbf{T}_{\ell,t}$ and send it to each of the $\{\mathcal{M}_\ell\}$;
 - 6 Each \mathcal{M}_ℓ computes $\mathbf{T}_{\ell,t} \leftarrow (\mathbf{A}_\ell^2 - \mathbf{D}_\ell)\mathbf{Y}_{t-1}$ and send it back to \mathcal{C} ;
 - 7 \mathcal{C} computes $\hat{\mathbf{U}}_g$ as the k leading singular vectors of $\mathbf{Y}_g = L^{-1} \sum_\ell \mathbf{X}_{\ell,g}$;
 - 8 Cluster the rows of $\hat{\mathbf{U}}_g$ using K -means clustering for some choice of K ;
- Output:** Estimated singular vectors $\hat{\mathbf{U}}_g^{(k)}$
-

diagonal matrix whose diagonal entries are the vertices degrees in \mathbf{A}_ℓ or the diagonal matrix containing the diagonal entries of \mathbf{A}_ℓ^2 , then extract $\hat{\mathbf{U}}$ as the leading singular vectors of $\hat{\mathbf{M}}$, and finally recover \mathbf{Z} by clustering the rows of $\hat{\mathbf{U}}$ using K -means or K -median clustering; see [Lei and Lin \(2024\)](#); [Cai et al. \(2021\)](#) for more details. In particular the subtraction of $\{\mathbf{D}_\ell\}$ corresponds to a bias-removal step and is essential when the $\{\mathbf{A}_\ell\}$ are extremely sparse as then the diagonal entries of $\sum_{i=1}^m \mathbf{A}_\ell^2$ are much larger in magnitudes compared to the non-diagonal entries.

If each \mathbf{A}_ℓ is of dimensions $n \times n$, and the collection $\{\mathbf{A}_\ell\}$ is stored on multiple different machines, then calculating $\hat{\mathbf{M}}$ requires sending up to $O(Ln^2)$ bits to a central machine for aggregation, which can be prohibitive when n is large and/or infeasible due to privacy constraints. These issues can be readily addressed by the RSVD estimate $\hat{\mathbf{U}}_g$ as the use of sketching matrices \mathbf{G} when constructing $\hat{\mathbf{M}}^g \mathbf{G}$ alleviate the need for transmitting the \mathbf{A}_ℓ directly; see [Algorithm S4](#) for more details. Let $\text{nnz}(\mathbf{A}_\ell)$ denote the number of non-zero entries in \mathbf{A}_ℓ and $N = \sum_\ell \text{nnz}(\mathbf{A}_\ell)$ be the total number of non-zero entries among all $\{\mathbf{A}_\ell\}$. In [Algorithm S4](#), each iteration of step 5 involves $O(Ln\tilde{k})$ flops and transfers of $O(Ln\tilde{k})$ bits, each iteration of step 6 as well as step 3 involves $O(N\tilde{k})$ flops and transfers of $O(Ln\tilde{k})$ bits, Step 7 involves $O(Ln\tilde{k} + n\tilde{k}^2)$ flops, and thus [Algorithm S4](#) requires a total of $O(g(Ln + N)\tilde{k} + n\tilde{k}^2)$ flops and transfer of $O(gLn\tilde{k})$ bits. If $g = O(\log n)$ and $\tilde{k} \ll n$ then the computational complexity of [Algorithm S4](#) is considerably smaller than computing the spectral clustering of $\hat{\mathbf{M}}$ directly, and require transfer of at most $O(gLn\tilde{k})$ bits between the individual machines $\{\mathcal{M}_\ell\}$ and the central server \mathcal{C} . Finally, we note that [Algorithm S4](#) can also be used for distributed PCA [Chen et al. \(2022\)](#); [Fan et al.](#)

(2019) by simply removing step 8 and changing the updates $\mathbf{T}_{\ell,t} \leftarrow (\mathbf{A}_\ell^2 - \mathbf{D}_\ell)\mathbf{Y}_t$ in step 3 to $\mathbf{T}_{\ell,t} \leftarrow \mathbf{X}_\ell \mathbf{X}_\ell^\top \mathbf{Y}_{t-1}$ where \mathbf{X}_ℓ is the $n_\ell \times p$ data matrices whose rows represent observations stored on the ℓ th machine and whose columns are the feature vectors for these observations.

Let $\mathbf{M} = \sum_\ell \mathbf{P}_\ell^2$ and suppose that $\text{rk}(\mathbf{M}) = k_0$ for some finite constant k_0 not depending on L and n . Suppose also that the average degrees of each \mathbf{A}_ℓ is of order $\Theta(n\rho_n)$ for some $\rho_n \in [0, 1]$ satisfying $n\rho_n = O(1)$. If $L^{1/2}n\rho_n \gtrsim \log^{1/2}(L+n)$, then from the proof of Theorem 1 in [Lei and Lin \(2024\)](#), we have

$$d_2(\hat{\mathbf{U}}, \mathbf{U}) \lesssim L^{-1/2}(n\rho_n)^{-1} \log^{1/2}(L+n) + n^{-1} \quad (\text{S4.1})$$

with high probability, where \mathbf{U} contains the eigenvectors corresponding to the non-zero eigenvalues of $\hat{\mathbf{M}}$. Furthermore, under the stronger condition that $L^{1/2}n\rho_n \gtrsim \log(L+n)$, we have by Theorem 1 in [Cai et al. \(2021\)](#) that

$$d_{2,\infty}(\hat{\mathbf{U}}, \mathbf{U}) \lesssim k_0^{1/2} n^{-1/2} (L^{-1/2}(n\rho_n)^{-1} \log(m+n) + n^{-1}) \quad (\text{S4.2})$$

with high probability. By Corollary 2 of our paper, $d_2(\hat{\mathbf{U}}_g, \mathbf{U})$ and $d_{2,\infty}(\hat{\mathbf{U}}_g, \mathbf{U})$ achieve the same upper bounds as that for $d_2(\hat{\mathbf{U}}, \mathbf{U})$ and $d_{2,\infty}(\hat{\mathbf{U}}, \mathbf{U})$ in Eq. (S4.1) and Eq. (S4.2), respectively, whenever $\hat{\mathbf{U}}_g$ is computed using Algorithm S4 with $\tilde{k} \asymp \log n$ and

$$g \geq \frac{2 \log(n/\tilde{k})}{\log(1/(n^{-1} + L^{-1/2}(n\rho_n)^{-1} \log^{1/2}(L+n)))}. \quad (\text{S4.3})$$

S5 Future directions

We discuss several directions for future work in this section. Firstly, as we shown in Section 3.2, our d_2 and $d_{2,\infty}$ bounds and the corresponding phase transition are sharp whenever $\hat{\mathbf{M}}$ satisfies the trace growth condition in Eq. (3.7). This condition holds for edge-indepdent random graphs with homogeneous edge probabilities and it is of interest to find other inference problem where this condition is also satisfied. Secondly, our discussions in Section 3 and Section S2 through Section S4 focus exclusively on the case where $\text{rk}(\mathbf{M}) = k_0 < n$, and this is because sharp upper bounds for $d_{2,\infty}(\hat{\mathbf{U}}^{(k)}, \mathbf{U}^{(k)})$ are available mainly when $k \leq k_0 \ll n$. Extending the bounds for

$d_{2,\infty}(\hat{\mathbf{U}}^{(k)}, \mathbf{U}^{(k)})$ to the case where $k_0 = n$ or $k_0 \asymp n$ is an important question and furthermore, when combined with the results in this paper, also leads directly to bounds for $d_{2,\infty}(\hat{\mathbf{U}}_g^{(k)}, \mathbf{U}^{(k)})$. Thirdly, while randomized subspace iterations (as considered in this paper) is one of the most popular approach for RSVD, there are other approaches such as those based on Krylov subspaces (Musco and Musco, 2015); deriving $2 \rightarrow \infty$ norm bounds for RSVD using Krylov subspaces may require different techniques than those presented here. Fourthly, many modern dataset are represented as tensors and are analyzed using higher-order SVD by flattening the tensor into matrices across different dimensions and then computing the truncated SVD of the resulting matrices (De Lathauwer et al., 2000; Zhang and Xia, 2018). Perturbation analysis of RSVD for noisy tensor data is thus of some theoretical and practical interest.

Finally, for some random graph models, the degree heterogeneity of the nodes can cause the ℓ_2 norms of the rows of $\mathbf{U}^{(k)}$ or $\hat{\mathbf{U}}^{(k)}$ to vary significantly (unlike the delocalized setting in Section 3 for which these row-wise ℓ_2 norms are of order $O(n^{-1/2})$); see e.g., Ke and Wang (2024) and Cape et al. (2024). Under such scenario, we may be interested in row-specific entry-wise bounds as they will aid further theoretical analysis for RSVD-based spectral methods. We thus devote the remainder of this section to a discussion on row-specific perturbation analysis for $\hat{\mathbf{U}}_g^{(k)}$.

Firstly, if g is sufficiently large then we can show that, under *minimal* assumptions, the RSVD-based singular vectors $\hat{\mathbf{U}}_g^{(k)}$ achieve the same row-specific entrywise error rates in recovering $\mathbf{U}^{(k)}$ as the exact singular vectors $\hat{\mathbf{U}}^{(k)}$. Indeed, Theorem 2 requires only a lower bound on the sketching dimension \tilde{k} and make no assumptions on the structure of $\widehat{\mathbf{M}}$, while still guaranteeing that if $\hat{\zeta}_k < 1$ then $d_{2 \rightarrow \infty}(\hat{\mathbf{U}}_g^{(k)}, \hat{\mathbf{U}}^{(k)})$ decays *exponentially fast* as g increases. More specifically, for any $L > 0$, we have

$$d_{2 \rightarrow \infty}(\hat{\mathbf{U}}_g^{(k)}, \hat{\mathbf{U}}^{(k)}) = O(n^{-L}) \quad (\text{S5.1})$$

with high probability, provided that $g \geq CL(\log n)/(\log \hat{\zeta}_k^{-1})$ for a sufficiently large constant C and $\tilde{k} \gtrsim \log n$. Thus we can decompose the error between $\hat{\mathbf{U}}_g^{(k)}$ and $\mathbf{U}^{(k)}$ into two parts: one between $\hat{\mathbf{U}}_g^{(k)}$ and $\hat{\mathbf{U}}^{(k)}$ (which holds under minimal assumptions on $\widehat{\mathbf{M}}$) and the other between

$\hat{\mathbf{U}}^{(k)}$ and $\mathbf{U}^{(k)}$ (which depends on the probabilistic model for $\hat{\mathbf{M}}$ as a noisy realization of \mathbf{M}).

This decomposition naturally extends our results to the case of row-specific entrywise bound.

In particular, suppose we have a row-specific bound between $\hat{\mathbf{U}}^{(k)}$ and $\mathbf{U}^{(k)}$, that is, for some orthogonal matrix $\mathbf{Q}_n \in \mathbb{O}_k$ and for any $i \in [n]$ we have $\|\mathbf{U}^{(k)} - \hat{\mathbf{U}}^{(k)}\mathbf{Q}_n\|_{i,\ell_2} \leq \vartheta_i$ where $\|\mathbf{M}\|_{i,\ell_2}$ denotes the ℓ_2 norm of the i th row of a matrix \mathbf{M} and ϑ_i is a quantity depending possibly on the row index i . Then, by choosing $g \geq CL(\log n)/(\log \hat{\zeta}_k^{-1})$ and $\tilde{k} \gtrsim \log n$, we also have for any $i \in [n]$ that

$$\begin{aligned} \|\hat{\mathbf{U}}_g^{(k)} - \mathbf{U}^{(k)}\mathbf{Q}'_n\|_{i,\ell_2} &\leq \|\hat{\mathbf{U}}_g^{(k)} - \hat{\mathbf{U}}^{(k)}\mathbf{Q}_n\mathbf{Q}'_n\|_{i,\ell_2} + \|\hat{\mathbf{U}}^{(k)}\mathbf{Q}_n\mathbf{Q}'_n - \mathbf{U}^{(k)}\mathbf{Q}'_n\|_{i,\ell_2} \\ &= \|\hat{\mathbf{U}}_g^{(k)} - \hat{\mathbf{U}}^{(k)}\mathbf{Q}_n\mathbf{Q}'_n\|_{i,\ell_2} + \|\mathbf{U}^{(k)} - \hat{\mathbf{U}}^{(k)}\mathbf{Q}_n\|_{i,\ell_2} \\ &= O(n^{-L}) + \vartheta_i \end{aligned} \tag{S5.2}$$

with high probability, where \mathbf{Q}'_n is a $k \times k$ orthogonal matrix for aligning $\hat{\mathbf{U}}_g^{(k)}$ and $\hat{\mathbf{U}}^{(k)}$ to achieve the rate in Eq. (S5.1). Hence, if g is *sufficiently large* then, with high probability, the row-specific error between $\hat{\mathbf{U}}_g^{(k)}$ and $\mathbf{U}^{(k)}$ is the same (up to an additional negligible term of order $O(n^{-L})$) as that between $\hat{\mathbf{U}}^{(k)}$ and $\mathbf{U}^{(k)}$.

Secondly, if $g \geq 1$ is arbitrary then, by a more careful inspection of the proof of Theorem 2 we can also obtain the following row-specific bound between $\hat{\mathbf{U}}_g^{(k)}$ and $\mathbf{U}^{(k)}$; note that this new bound holds under the same set of *minimal assumptions* as that for Theorem 2.

Theorem S8. *Consider the setting in Theorem 1. Define $\|\mathbf{M}\|_{i,\ell_2}$ as the ℓ_2 norm of the i th row of any matrix \mathbf{M} , and for an arbitrary $\delta > 0$, define*

$$r_{i,2} = \frac{\sqrt{128}e(k \log \delta^{-1})^{1/2}\hat{\zeta}_k^{\tilde{g}}}{c_{\text{gap}}^2 \tilde{k}^{1/2}} + \frac{18n\|\hat{\mathbf{U}}^{(k)}\|_{i,\ell_2}\hat{\zeta}_k^{2\tilde{g}}}{c_{\text{gap}}^2 \tilde{k}} + \frac{36n(\log \delta^{-1})^{1/2}\hat{\zeta}_k^{3\tilde{g}}}{c_{\text{gap}}^3 \tilde{k}}.$$

Then there exists some $\mathbf{Q} \in \mathbb{O}_k$ such that uniformly for all $i \in [n]$,

$$\|\hat{\mathbf{U}}_g^{(k)} - \hat{\mathbf{U}}^{(k)}\mathbf{Q}\|_{i,\ell_2} \leq r_{i,2},$$

with probability at least $1 - 4m\tilde{k}\delta - \vartheta - 2e^{-n/2}$.

Compared with the $\ell_{2,\infty}$ perturbation bound

$$r_{2,\infty} = \frac{\sqrt{128}e(k \log \delta^{-1})^{1/2} \hat{\zeta}_k^{\tilde{g}}}{c_{\text{gap}}^2 \tilde{k}^{1/2}} + \frac{18n \|\hat{\mathbf{U}}^{(k)}\|_{2,\infty} \hat{\zeta}_k^{2\tilde{g}}}{c_{\text{gap}}^2 \tilde{k}} + \frac{36n(\log \delta^{-1})^{1/2} \hat{\zeta}_k^{3\tilde{g}}}{c_{\text{gap}}^3 \tilde{k}},$$

we see that the only difference between $r_{i,2}$ and $r_{2,\infty}$ is the second term in $r_{i,2}$ which uses $\|\hat{\mathbf{U}}^{(k)}\|_{i,\ell_2}$ instead of $\|\hat{\mathbf{U}}^{(k)}\|_{2,\infty}$. As a result, following a similar argument as in Remark 3, $r_{i,2}$ can be sharper than $r_{2,\infty}$ when $\|\hat{\mathbf{U}}^{(k)}\|_{i,\ell_2} \ll \|\hat{\mathbf{U}}^{(k)}\|_{2,\infty}$, especially in the regimes where g is moderately large and \tilde{k} grows slowly with n .

The proof of Theorem S8 is straightforward. In particular from the proof of Theorem 2 we have the decomposition

$$\hat{\mathbf{U}}_g^{(k)} - \hat{\mathbf{U}}^{(k)} \mathbf{Q}_{\check{\mathbf{U}}_g} = \mathbf{T}_1 + \mathbf{T}_2 + \mathbf{T}_3,$$

for some $\mathbf{Q}_{\check{\mathbf{U}}_g} \in \mathbb{O}_k$, where $\mathbf{T}_3 = \check{\mathbf{U}}_g^{(k)} ((\check{\mathbf{U}}_g^{(k)})^\top \hat{\mathbf{U}}_g^{(k)} - \mathbf{Q}_{\check{\mathbf{U}}_g})$, and $\check{\mathbf{U}}_g^{(k)} = \hat{\mathbf{U}}^{(k)} \check{\mathbf{Q}}_g$ for some $\check{\mathbf{Q}}_g \in \mathbb{O}_k$. Then for Theorem S8 we bound \mathbf{T}_3 as

$$\|\mathbf{T}_3\|_{i,\ell_2} \leq \|\hat{\mathbf{U}}^{(k)} \check{\mathbf{Q}}_g\|_{i,\ell_2} \times \|(\check{\mathbf{U}}_g^{(k)})^\top \hat{\mathbf{U}}_g^{(k)} - \mathbf{Q}_{\check{\mathbf{U}}_g}\|,$$

while \mathbf{T}_1 and \mathbf{T}_2 are bounded using their $\ell_{2 \rightarrow \infty}$ norms as in the proof of Theorem 2.

Finally, while it is certainly possible that one can derive row-specific bounds for RSVD sharper than those in Theorem S8, we expect that these bounds also require substantially stronger assumptions on $\widehat{\mathbf{M}}$. Recall that row-specific bounds for $\hat{\mathbf{U}}^{(k)}$ (such as those for random graphs) typically rely on probabilistic assumptions on $\widehat{\mathbf{M}}$, for example that the entries of $\widehat{\mathbf{M}}$ are independent or that $\widehat{\mathbf{M}}$ is a transformation of such a random matrix; see, e.g., Li et al. (2024); Ke and Wang (2024) and Cape et al. (2024). This indicates that, to obtain sharper row-specific bounds between $\hat{\mathbf{U}}_g^{(k)}$ and $\hat{\mathbf{U}}^{(k)}$, one need to impose additional structural or distribution assumptions on $\widehat{\mathbf{M}}$, and the theoretical analysis also has to be tailored to the inference problems of interests; e.g., sharp row-specific bounds for random graphs may require techniques that are different from those for matrix completion. As the primary theoretical goal of our work is to develop a *general* framework for RSVD perturbation under *minimal* assumptions, we leave the

more refined row-specific (and problem-centric) analysis for future work.

S6 Proofs for Section 2

S6.1 Primary

We first recall and introduce a few notations that will be used throughout this section. Let $\widehat{\mathbf{M}}$ be a $m \times n$ rectangular or asymmetric matrix and write the SVD of $\widehat{\mathbf{M}}$ as

$$\widehat{\mathbf{M}} = \widehat{\mathbf{U}}^\top \widehat{\mathbf{\Sigma}} \widehat{\mathbf{V}}^\top + \widehat{\mathbf{U}}_\perp^\top \widehat{\mathbf{\Sigma}}_\perp \widehat{\mathbf{V}}_\perp^\top$$

where $\widehat{\mathbf{U}}$ and $\widehat{\mathbf{V}}$ are $m \times k$ and $n \times k$ matrices containing the leading k left and right singular vectors, respectively, and $\widehat{\mathbf{\Sigma}}$ are the corresponding singular values; the remaining singular vectors and singular values are denoted by $\widehat{\mathbf{U}}_\perp$, $\widehat{\mathbf{V}}_\perp$ and $\widehat{\mathbf{\Sigma}}_\perp$. Note that, for ease of notations, we have omitted the dependency on k from all of these matrices. Next let \mathbf{G} be a $n \times \tilde{k}$ random Gaussian matrix. Then Algorithm 1 computes $\widehat{\mathbf{U}}_g$ as the leading k left singular vectors of

$$\widehat{\mathbf{M}}(\widehat{\mathbf{M}}^\top \mathbf{M})^g \mathbf{G} = \widehat{\mathbf{U}} \widehat{\mathbf{\Sigma}}^{2g+1} \widehat{\mathbf{V}}^\top \mathbf{G} + \widehat{\mathbf{U}}_\perp \widehat{\mathbf{\Sigma}}_\perp^{2g+1} \widehat{\mathbf{V}}_\perp^\top \mathbf{G}.$$

Similarly, if $\widehat{\mathbf{M}}$ is a $n \times n$ symmetric matrix with eigendecomposition

$$\widehat{\mathbf{M}} = \widehat{\mathbf{U}} \widehat{\mathbf{\Lambda}} \widehat{\mathbf{U}}^\top + \widehat{\mathbf{U}}_\perp \widehat{\mathbf{\Lambda}}_\perp \widehat{\mathbf{U}}_\perp^\top,$$

where $\widehat{\mathbf{\Lambda}}$ contains the top- k eigenvalues in magnitude while $\widehat{\mathbf{\Lambda}}_\perp$ contains the rest of the eigenvalues. Then Algorithm 1 computes $\widehat{\mathbf{U}}_g$ as the leading k left singular vectors of

$$\widehat{\mathbf{M}}^g \mathbf{G} = \widehat{\mathbf{U}} \widehat{\mathbf{\Lambda}}^g \widehat{\mathbf{U}}^\top \mathbf{G} + \widehat{\mathbf{U}}_\perp \widehat{\mathbf{\Lambda}}_\perp^g \widehat{\mathbf{U}}_\perp^\top \mathbf{G} = \widehat{\mathbf{U}} \widehat{\mathbf{\Sigma}}^g \widehat{\mathbf{V}}^\top \mathbf{G} + \widehat{\mathbf{U}}_\perp \widehat{\mathbf{\Sigma}}_\perp^g \widehat{\mathbf{V}}_\perp^\top \mathbf{G},$$

where $\widehat{\mathbf{\Sigma}} = |\widehat{\mathbf{\Lambda}}|$ and the columns of $\widehat{\mathbf{V}}$ are the same as those for $\widehat{\mathbf{U}}$, but with their signs flipped whenever the corresponding eigenvalues in $\widehat{\mathbf{\Lambda}}^g$ are negative. Consolidating both of the above

cases, we can define \mathbf{Y}_g as the matrix

$$\mathbf{Y}_g = \widehat{\mathbf{U}} \widehat{\boldsymbol{\Sigma}}^{\tilde{g}} \widehat{\mathbf{V}}^\top \mathbf{G} + \widehat{\mathbf{U}}_\perp \widehat{\boldsymbol{\Sigma}}_\perp^{\tilde{g}} \widehat{\mathbf{V}}_\perp^\top \mathbf{G} = \begin{cases} \widehat{\mathbf{M}}(\widehat{\mathbf{M}}^\top \widehat{\mathbf{M}})^{\tilde{g}} \mathbf{G} & \widehat{\mathbf{M}} \text{ is symmetric} \\ \widehat{\mathbf{M}}^{\tilde{g}} \mathbf{G} & \text{otherwise} \end{cases}, \quad (\text{S6.1})$$

where $\tilde{g} = g$ if $\widehat{\mathbf{M}}$ is symmetric and $\tilde{g} = 2g + 1$ otherwise. Then $\widehat{\mathbf{U}}_g$ is the leading left singular vectors of \mathbf{Y}_g . More specifically, we have the following SVD

$$\mathbf{Y}_g = \widehat{\mathbf{U}}_g \widehat{\boldsymbol{\Sigma}}_g \widehat{\mathbf{W}}_g^\top + \widehat{\mathbf{U}}_{g,\perp} \widehat{\boldsymbol{\Sigma}}_{g,\perp} \widehat{\mathbf{W}}_{g,\perp}^\top.$$

where $\widehat{\mathbf{U}}_g$ and $\widehat{\mathbf{W}}_g^\top$ are $m \times k$ and $n \times k$ matrices with orthonormal columns. We emphasize that $\widehat{\boldsymbol{\Sigma}}^g$ and $\widehat{\boldsymbol{\Sigma}}_g$ denote different quantities, i.e., $\widehat{\boldsymbol{\Sigma}}^g$ contains the g th powers of the leading k singular values of $\widehat{\mathbf{M}}$ while $\widehat{\boldsymbol{\Sigma}}_g$ contains the k leading singular values of \mathbf{Y}_g . Finally, our subsequent analysis of $\widehat{\mathbf{U}}_g$ is based on viewing \mathbf{Y}_g as an additive perturbation of $\widehat{\mathbf{U}} \widehat{\boldsymbol{\Sigma}}^{\tilde{g}} \widehat{\mathbf{V}}^\top \mathbf{G}$, and thus we also consider the SVD

$$\widehat{\mathbf{U}} \widehat{\boldsymbol{\Sigma}}^{\tilde{g}} \widehat{\mathbf{V}}^\top \mathbf{G} = \check{\mathbf{U}}_g \check{\boldsymbol{\Sigma}}_g \check{\mathbf{W}}_g^\top$$

where $\check{\mathbf{U}}_g$ and $\check{\mathbf{W}}_g$ are $m \times k$ and $n \times k$ matrices with orthonormal columns.

S6.2 Technical lemmas

Before commencing with the proofs of the main results, we first state some technical lemmas that will be used throughout this paper. We start by listing some basic properties of the $\ell_{2,\infty}$ norm.

Lemma S1. *For any $\mathbf{M}_1 \in \mathbb{R}^{d_1 \times d_2}$, $\mathbf{M}_2 \in \mathbb{R}^{d_2 \times d_3}$ and $\mathbf{M}_3 \in \mathbb{R}^{d_4 \times d_1}$, we have*

$$\|\mathbf{M}_1 \mathbf{M}_2\|_{2,\infty} \leq \|\mathbf{M}_1\|_{2,\infty} \|\mathbf{M}_2\|;$$

$$\|\mathbf{M}_3 \mathbf{M}_1\|_{2,\infty} \leq \|\mathbf{M}_3\|_\infty \|\mathbf{M}_1\|_{2,\infty};$$

$$\|\mathbf{M}_1\|_\infty \leq \sqrt{d_2} \|\mathbf{M}_1\|_{2,\infty}.$$

For $\mathbf{U}_1, \mathbf{U}_2 \in \mathbb{O}_{d \times d'}$, let $\mathbf{W}_* := \operatorname{argmin}_{\mathbf{W} \in \mathbb{O}_{d'}}$ $\|\mathbf{U}_1 - \mathbf{U}_2 \mathbf{W}\|_F$. Then

$$\|\mathbf{U}_1^\top \mathbf{U}_2 - \mathbf{W}_*\| \leq d_2^2(\mathbf{U}_1, \mathbf{U}_2).$$

For a proof of Lemma S1, see e.g., Cai and Zhang (2018) and Cape et al. (2019b). The following Lemma S2 and Lemma S3 provide a collection of bounds for the quantities depending on the Gaussian sketching matrix \mathbf{G} in the proofs of Theorem 1 and Theorem 2. For ease of notations, we will fix k and thus omit the index k from our matrices, e.g., we write $\hat{\mathbf{U}}$ and $\hat{\mathbf{U}}_\perp$ in place of $\hat{\mathbf{U}}^{(k)}$ and $\hat{\mathbf{U}}_\perp^{(k)}$.

Lemma S2. *Consider the setting in Theorem 1 and let \mathbf{G} be a random Gaussian sketching matrix of dimension $n \times \tilde{k}$. We then have $\|\mathbf{G}\| \leq 3\sqrt{n}$ with probability at least $1 - 2e^{-n/2}$. Furthermore, we also have*

$$\|\hat{\mathbf{U}}_\perp \hat{\Sigma}_\perp^\ell \hat{\mathbf{V}}_\perp^\top \mathbf{G}\|_{2,\infty} \leq \hat{\sigma}_{k+1}^\ell (2\tilde{k} \log(1/\delta))^{1/2}$$

with probability at least $1 - 2m\tilde{k}\delta$, where ℓ is any arbitrary and given positive integer.

Proof of Lemma S2. We first bound $\|\mathbf{G}\|$. Recall the non-asymptotic bound for the spectral norm of a Gaussian random matrix (see e.g. Corollary 5.35 in Vershynin (2012)). We then have

$$\|\mathbf{G}\| \leq n^{1/2} + \tilde{k}^{1/2} + t, \tag{S6.2}$$

with probability at least $1 - 2\exp(-t^2/2)$, and hence we can take $t = n^{1/2}$ in Eq. (S6.2) to obtain $\|\mathbf{G}\| \leq 3\sqrt{n}$ with probability at least $1 - 2\exp(-n/2)$.

We now bound $\|\hat{\mathbf{U}}_\perp \hat{\Sigma}_\perp^\ell \hat{\mathbf{V}}_\perp^\top \mathbf{G}\|_{2,\infty}$. First, we have

$$\|\hat{\mathbf{U}}_\perp \hat{\Sigma}_\perp^\ell \hat{\mathbf{V}}_\perp^\top \mathbf{G}\|_{2,\infty} \leq \tilde{k}^{1/2} \max_{j \in [\tilde{k}]} \|\hat{\mathbf{U}}_\perp \hat{\Sigma}_\perp^\ell \hat{\mathbf{V}}_\perp^\top \mathbf{g}_j\|_{\max}, \tag{S6.3}$$

where \mathbf{g}_j denote the j th column of \mathbf{G} . Next we note that

$$\hat{\mathbf{U}}_\perp \hat{\Sigma}_\perp^\ell \hat{\mathbf{V}}_\perp^\top \mathbf{g}_j \sim \mathcal{N}(\mathbf{0}, \hat{\mathbf{U}}_\perp \hat{\Sigma}_\perp^{2\ell} \hat{\mathbf{U}}_\perp^\top), \quad \text{and} \quad \|\hat{\mathbf{U}}_\perp \hat{\Sigma}_\perp^{2\ell} \hat{\mathbf{U}}_\perp^\top\|_{\max} \leq \|\hat{\Sigma}_\perp\|^{2\ell} \leq \hat{\sigma}_{k+1}^{2\ell}.$$

Now for any Gaussian random variable ξ with $\text{Var}(\xi) \leq c$ we have

$$\mathbb{P}(|\xi| < t) \geq 1 - 2 \exp(-t^2/(2c)), \quad (\text{S6.4})$$

for all $t > 0$; see e.g Section 2.5.1 of [Vershynin \(2018\)](#). Therefore, by taking a union over all m elements of $\widehat{\mathbf{U}}_{\perp} \widehat{\boldsymbol{\Sigma}}_{\perp}^{\ell} \widehat{\mathbf{V}}_{\perp}^{\top} \mathbf{g}_j$ and then over all $j \leq \tilde{k}$, we have

$$\mathbb{P}\left(\max_{j \in [\tilde{k}]} \|\widehat{\mathbf{U}}_{\perp} \widehat{\boldsymbol{\Sigma}}_{\perp}^{\ell} \widehat{\mathbf{V}}_{\perp}^{\top} \mathbf{g}_j\|_{\max} < \widehat{\sigma}_{k+1}^{\ell} \sqrt{2 \log(1/\delta)}\right) \geq 1 - 2m\tilde{k}\delta. \quad (\text{S6.5})$$

Combining Eq. (S6.5) and Eq. (S6.3) we obtain

$$\|\widehat{\mathbf{U}}_{\perp} \widehat{\boldsymbol{\Sigma}}_{\perp}^{\ell} \widehat{\mathbf{V}}_{\perp}^{\top} \mathbf{G}\|_{2,\infty} < \widehat{\sigma}_{k+1}^{\ell} (2\tilde{k} \log(1/\delta))^{1/2}$$

with probability at least $1 - 2m\tilde{k}\delta$. □

Lemma S3. *Consider the setting in Theorem 1 where \mathbf{G} is a random $n \times \tilde{k}$ Gaussian matrix with*

$$\tilde{k} \geq (1 - c_{\text{gap}})^{-2} \left\{ k + (8k \log(1/\vartheta))^{1/2} + 2 \log(1/\vartheta) \right\}$$

for some arbitrary $c_{\text{gap}} \in (0, 1)$ and some arbitrary $\vartheta > 0$. Let g be an arbitrary positive integer and define \mathbf{Y}_g as in Eq. (S6.1) with $\tilde{g} = g$ if $\widehat{\mathbf{M}}$ is symmetric and $\tilde{g} = 2g + 1$ otherwise. Then

$$\sigma_k^2(\widehat{\mathbf{V}}^{\top} \mathbf{G}) \geq c_{\text{gap}}^2 \tilde{k} \quad \text{and} \quad \sigma_k^2(\mathbf{Y}_g) \geq \sigma_k^2(\widehat{\boldsymbol{\Sigma}}^{\tilde{g}} \widehat{\mathbf{V}}^{\top} \mathbf{G}) = \sigma_k^2(\check{\boldsymbol{\Sigma}}_g) \geq c_{\text{gap}}^2 \tilde{k} \widehat{\sigma}_k^{2\tilde{g}}.$$

with probability at least $1 - \vartheta$.

Proof. We first bound $\sigma_k^2(\widehat{\mathbf{V}}^{\top} \mathbf{G})$. As \mathbf{G} is a $n \times \tilde{k}$ matrix whose entries are independent standard normals, $\widehat{\mathbf{V}}^{\top} \mathbf{G}$ is a $k \times \tilde{k}$ matrix whose entries are also independent standard normals. By Theorem II.13 in [Davidson and Szarek \(2001\)](#) we have

$$\mathbb{P}\left(\sigma_k(\widehat{\mathbf{V}}^{\top} \mathbf{G}) \leq \tilde{k}^{1/2} - k^{1/2} - t\right) \leq e^{-t^2/2}. \quad (\text{S6.6})$$

Now choose an arbitrary $c_{\text{gap}} \in (0, 1)$. Then

$$\tilde{k}^{1/2} - k^{1/2} - t \geq c_{\text{gap}} \tilde{k}^{1/2} \iff \tilde{k} \geq (1 - c_{\text{gap}})^{-2} (k^{1/2} + t)^2.$$

Letting $t = (2 \log(1/\vartheta))^{1/2}$ yields

$$\mathbb{P} \left(\sigma_k(\hat{\mathbf{V}}^\top \mathbf{G}) \geq c_{\text{gap}} \tilde{k}^{1/2} \right) \geq 1 - \vartheta$$

for $\tilde{k} \geq (1 - c_{\text{gap}})^{-2} \{k + (8k \log(1/\vartheta))^{1/2} + 2 \log(1/\vartheta)\}$. Next, for $\hat{\Sigma}^{\tilde{g}} \hat{\mathbf{V}}^\top \mathbf{G}$ we have

$$\sigma_k^2(\hat{\Sigma}^{\tilde{g}} \hat{\mathbf{V}}^\top \mathbf{G}) = \lambda_k(\mathbf{G}^\top \hat{\mathbf{V}} \hat{\Sigma}^{2\tilde{g}} \hat{\mathbf{V}}^\top \mathbf{G}) \geq \lambda_k(\mathbf{G}^\top \hat{\mathbf{V}} \hat{\mathbf{V}}^\top \mathbf{G}) \times \hat{\sigma}_k^{2\tilde{g}} \quad (\text{S6.7})$$

Substituting the above bound for $\sigma_k(\hat{\mathbf{V}}^\top \mathbf{G})$ into Eq. (S6.7) we obtain

$$\sigma_k^2(\hat{\Sigma}^{\tilde{g}} \hat{\mathbf{V}}^\top \mathbf{G}) \geq c_{\text{gap}}^2 \tilde{k} \hat{\sigma}_k^{2\tilde{g}} \quad (\text{S6.8})$$

with probability at least $1 - \vartheta$. Finally,

$$\sigma_k^2(\mathbf{Y}_g) = \lambda_k(\mathbf{Y}_g^\top \mathbf{Y}_g) = \lambda_k(\mathbf{G}^\top (\hat{\mathbf{V}}^\top \hat{\Sigma}^{2\ell} \hat{\mathbf{V}} + \hat{\mathbf{V}}_\perp \hat{\Sigma}_\perp^{2\tilde{g}} \hat{\mathbf{V}}_\perp^\top) \mathbf{G}) \geq \lambda_k(\mathbf{G}^\top \hat{\mathbf{V}} \hat{\Sigma}^{2\tilde{g}} \hat{\mathbf{V}}^\top \mathbf{G}) = \sigma_k^2(\hat{\Sigma}^{\tilde{g}} \hat{\mathbf{V}}^\top \mathbf{G})$$

and hence $\sigma_k^2(\mathbf{Y}_g) \geq c_{\text{gap}}^2 \tilde{k} \hat{\sigma}_k^{2\tilde{g}}$ with probability at least $1 - \vartheta$. \square

S6.3 Proof of Theorem 1

For simplicity of notations, we will fix a value of k and thus omit it from our notations, e.g., we use $\hat{\mathbf{U}}_g$ and $\hat{\mathbf{U}}$ in place of $\hat{\mathbf{U}}_g^{(k)}$ and $\hat{\mathbf{U}}^{(k)}$, respectively. Furthermore let $\hat{\sigma}_i$ denote the i th largest singular value of $\hat{\mathbf{M}}$. Now recall the definition of \mathbf{Y}_g from Eq. (S6.1). As $\hat{\mathbf{V}}^\top \mathbf{G}$ is a $k \times \tilde{k}$ matrix whose entries are iid $\mathcal{N}(0, 1)$ with $\tilde{k} \geq k$, we have $\text{rk}(\hat{\mathbf{V}}^\top \mathbf{G}) = k$ almost surely; see e.g. [Edelman \(1991\)](#) for a justification of this claim. We thus have

$$\text{rk}(\hat{\mathbf{U}} \hat{\Sigma}^{\tilde{g}} \hat{\mathbf{V}}^\top \mathbf{G}) = \text{rk}(\hat{\mathbf{U}} \hat{\Sigma}^{\tilde{g}}) = \text{rk}(\hat{\mathbf{U}})$$

almost surely. Let $\check{\mathbf{U}}_g$ be the left singular vectors of $\hat{\mathbf{U}}\hat{\Sigma}^{\tilde{g}}\hat{\mathbf{V}}^\top \mathbf{G}$. As $\check{\mathbf{U}}_g$ and $\hat{\mathbf{U}}$ are both $m \times k$ matrices with orthonormal columns, $\text{rk}(\check{\mathbf{U}}_g) = \text{rk}(\hat{\mathbf{U}})$, and $\mathcal{C}(\check{\mathbf{U}}_g) \subset \mathcal{C}(\hat{\mathbf{U}})$, we conclude that

$$\check{\mathbf{U}}_g = \hat{\mathbf{U}}\check{\mathbf{Q}}_g \quad (\text{S6.9})$$

for some $\check{\mathbf{Q}}_g \in \mathbb{O}_k$. We can now view \mathbf{Y}_g as the perturbed version of $\hat{\mathbf{U}}\hat{\Sigma}^{\tilde{g}}\hat{\mathbf{U}}^\top \mathbf{G}$. Then by the Wedin $\sin\Theta$ theorem (see pages 262 and 267 of [Stewart and Sun \(1990\)](#)), we have

$$\|\sin\Theta(\hat{\mathbf{U}}_g, \check{\mathbf{U}}_g)\| \leq \frac{\|\hat{\mathbf{U}}_\perp \hat{\Sigma}_\perp^{\tilde{g}} \hat{\mathbf{V}}_\perp^\top \mathbf{G}\|}{\sigma_k(\mathbf{Y}_g)} \leq \frac{\|\hat{\Sigma}_\perp^{\tilde{g}}\| \cdot \|\mathbf{G}\|}{\sigma_k(\mathbf{Y}_g)} \leq \frac{3n^{1/2} \|\hat{\Sigma}_\perp^{\tilde{g}}\|}{c_{\text{gap}} \tilde{k}^{1/2} \hat{\sigma}_k^{\tilde{g}}} \quad (\text{S6.10})$$

with probability at least $1 - \vartheta - 2e^{-n/2}$, where the last inequality follows from Lemma [S2](#) and Lemma [S3](#). \square

S6.4 Proof of Theorem 2

For simplicity of notations, we will fix a value of k and thus omit it from our notations. Recall the definition of \mathbf{Y}_g in Eq. [\(S6.1\)](#). Next recall the SVD of \mathbf{Y}_g and $\hat{\mathbf{U}}\hat{\Sigma}^{\tilde{g}}\hat{\mathbf{V}}^\top \mathbf{G}$,

$$\begin{aligned} \mathbf{Y}_g &= \hat{\mathbf{U}}_g \hat{\Sigma}_g \hat{\mathbf{W}}_g^\top + \hat{\mathbf{U}}_{g,\perp} \hat{\Sigma}_{g,\perp} \hat{\mathbf{W}}_{g,\perp}^\top, \\ \hat{\mathbf{U}}\hat{\Sigma}^{\tilde{g}}\hat{\mathbf{V}}^\top \mathbf{G} &= \check{\mathbf{U}}_g \check{\Sigma}_g \check{\mathbf{W}}_g^\top, \end{aligned} \quad (\text{S6.11})$$

where $\hat{\mathbf{U}}_g$ and $\hat{\mathbf{W}}_g$ are $m \times k$ and $\tilde{k} \times k$ matrices whose columns are the k leading left and right singular vectors of \mathbf{Y}_g , respectively. Now define

$$\mathbf{Q}_{\check{\mathbf{U}}_g} = \underset{\mathbf{Q} \in \mathbb{O}_k}{\text{argmin}} \|\hat{\mathbf{U}}_g - \check{\mathbf{U}}_g \mathbf{Q}\|_{\text{F}} \quad \text{and} \quad \mathbf{Q}_{\check{\mathbf{W}}_g} = \underset{\mathbf{Q} \in \mathbb{O}_k}{\text{argmin}} \|\hat{\mathbf{W}}_g - \check{\mathbf{W}}_g \mathbf{Q}\|_{\text{F}}.$$

We derive the following decomposition:

$$\begin{aligned}
\hat{\mathbf{U}}_g - \check{\mathbf{U}}_g \mathbf{Q}_{\check{\mathbf{U}}_g} &= (\mathbf{I}_m - \check{\mathbf{U}}_g \check{\mathbf{U}}_g^\top) \hat{\mathbf{U}}_g + \check{\mathbf{U}}_g (\check{\mathbf{U}}_g^\top \hat{\mathbf{U}}_g - \mathbf{Q}_{\check{\mathbf{U}}_g}) \\
&= (\mathbf{I}_m - \check{\mathbf{U}}_g \check{\mathbf{U}}_g^\top) \mathbf{Y}_g \widehat{\mathbf{W}}_g \hat{\Sigma}_g^{-1} + \check{\mathbf{U}}_g (\check{\mathbf{U}}_g^\top \hat{\mathbf{U}}_g - \mathbf{Q}_{\check{\mathbf{U}}_g}) \\
&= (\mathbf{I}_m - \hat{\mathbf{U}} \hat{\mathbf{U}}^\top) \mathbf{Y}_g \widehat{\mathbf{W}}_g \hat{\Sigma}_g^{-1} + \check{\mathbf{U}}_g (\check{\mathbf{U}}_g^\top \hat{\mathbf{U}}_g - \mathbf{Q}_{\check{\mathbf{U}}_g}) \\
&= \hat{\mathbf{U}}_\perp \hat{\Sigma}_\perp^{\tilde{g}} \hat{\mathbf{V}}_\perp^\top \mathbf{G} \widehat{\mathbf{W}}_g \hat{\Sigma}_g^{-1} + \check{\mathbf{U}}_g (\check{\mathbf{U}}_g^\top \hat{\mathbf{U}}_g - \mathbf{Q}_{\check{\mathbf{U}}_g}) \\
&= \underbrace{\hat{\mathbf{U}}_\perp \hat{\Sigma}_\perp^{\tilde{g}} \hat{\mathbf{V}}_\perp^\top \mathbf{G} \widetilde{\mathbf{W}}_g \mathbf{Q}_{\widetilde{\mathbf{W}}_g} \hat{\Sigma}_g^{-1}}_{\mathbf{T}_1} \\
&\quad + \underbrace{\hat{\mathbf{U}}_\perp \hat{\Sigma}_\perp^{\tilde{g}} \hat{\mathbf{V}}_\perp^\top \mathbf{G} (\widehat{\mathbf{W}}_g - \widetilde{\mathbf{W}}_g \mathbf{Q}_{\widetilde{\mathbf{W}}_g}) \hat{\Sigma}_g^{-1}}_{\mathbf{T}_2} \\
&\quad + \underbrace{\check{\mathbf{U}}_g (\check{\mathbf{U}}_g^\top \hat{\mathbf{U}}_g - \mathbf{Q}_{\check{\mathbf{U}}_g})}_{\mathbf{T}_3}.
\end{aligned} \tag{S6.12}$$

where \mathbf{I}_m denotes the $m \times m$ identity matrix. Recall that $\hat{\Sigma}^{\tilde{g}}$ and $\hat{\Sigma}_g$ represent different quantities, i.e., $\hat{\Sigma}^{\tilde{g}}$ is the \tilde{g} -th power of $\hat{\Sigma}$, the leading k singular values of $\widehat{\mathbf{M}}$, while $\hat{\Sigma}_g$ are the leading singular values of either $\mathbf{Y}_g = \widehat{\mathbf{M}}^g \mathbf{G}$ or $\mathbf{Y}_g = \widehat{\mathbf{M}} (\widehat{\mathbf{M}}^\top \widehat{\mathbf{M}})^g \mathbf{G}$; see the discussion at the beginning of Section S6. We now bound the $2 \rightarrow \infty$ norms of \mathbf{T}_1 , \mathbf{T}_2 , and \mathbf{T}_3 .

S6.4.1 Bounding $\|\mathbf{T}_1\|_{2,\infty}$

Let $\hat{\mathbf{L}}_G \hat{\mathbf{D}}_G \hat{\mathbf{R}}_G^\top$ be the SVD of $\hat{\mathbf{G}}^\top \hat{\mathbf{V}}$ where the columns of $\hat{\mathbf{L}}_G \in \mathbb{O}_{\tilde{k} \times k}$ and $\hat{\mathbf{R}}_G \in \mathbb{O}_{k \times k}$ are the left and right singular vectors, respectively and the diagonal of $\hat{\mathbf{D}}_G \in \mathbb{R}^{k \times k}$ contains the singular values of $\hat{\mathbf{G}}^\top \hat{\mathbf{V}}$. Recalling Eq. (S6.11), we have $\widetilde{\mathbf{W}}_g = \mathbf{G}^\top \hat{\mathbf{V}} \hat{\Sigma}^{\tilde{g}} \hat{\mathbf{U}}^\top \check{\mathbf{U}}_g \check{\Sigma}_g^{-1}$ where $\hat{\Sigma}^{\tilde{g}} \hat{\mathbf{U}}^\top \check{\mathbf{U}}_g \check{\Sigma}_g^{-1}$ is invertible; see Eq. (S6.9). Therefore $\widetilde{\mathbf{W}}_g$ and $\mathbf{G}^\top \hat{\mathbf{V}}$ share the same column space and hence

$$\widetilde{\mathbf{W}}_g = \hat{\mathbf{L}}_G \mathbf{Q}_G = \mathbf{G}^\top \hat{\mathbf{V}} \hat{\mathbf{R}}_G \hat{\mathbf{D}}_G^{-1} \mathbf{Q}_G,$$

for some $\mathbf{Q}_G \in \mathbb{O}_k$. Using the above form for $\widetilde{\mathbf{W}}_g$, we can rewrite \mathbf{T}_1 as

$$\begin{aligned}
\mathbf{T}_1 &= \hat{\mathbf{U}}_\perp \hat{\Sigma}_\perp^{\tilde{g}} \hat{\mathbf{V}}_\perp^\top \mathbf{G} \mathbf{G}^\top \hat{\mathbf{V}} \hat{\mathbf{R}}_G \hat{\mathbf{D}}_G^{-1} \mathbf{Q}_G \mathbf{Q}_{\check{\mathbf{V}}_g} \hat{\Sigma}_g^{-1} \\
&= \hat{\sigma}_{k+1}^{\tilde{g}} \cdot \Xi \cdot \hat{\mathbf{R}}_G \hat{\mathbf{D}}_G^{-1} \mathbf{Q}_G \mathbf{Q}_{\check{\mathbf{V}}_g} \hat{\Sigma}_g^{-1},
\end{aligned} \tag{S6.13}$$

where $\hat{\sigma}_{k+1}$ is the $k + 1$ largest singular value of $\widehat{\mathbf{M}}$ and

$$\Xi = \widehat{\mathbf{U}}_{\perp}(\widehat{\Sigma}_{\perp}/\hat{\sigma}_{k+1})^{\tilde{g}}\widehat{\mathbf{V}}_{\perp}^{\top}\mathbf{G}\mathbf{G}^{\top}\widehat{\mathbf{V}}.$$

Let $\widehat{\mathbf{m}}_i$ and $\widehat{\mathbf{v}}_j$ denote the i th row of $\widehat{\mathbf{U}}_{\perp}(\widehat{\Sigma}_{\perp}/\hat{\sigma}_{k+1})^{\tilde{g}}\widehat{\mathbf{V}}_{\perp}^{\top}$ and j th column of $\widehat{\mathbf{V}}$, respectively.

Then the ij th element of Ξ is of the form

$$\Xi_{ij} = \sum_{\ell=1}^{\tilde{k}} \widehat{\mathbf{m}}_i^{\top} \mathbf{g}_{\ell} \mathbf{g}_{\ell}^{\top} \widehat{\mathbf{v}}_j \quad (\text{S6.14})$$

where \mathbf{g}_{ℓ} is the ℓ th column of \mathbf{G} . We further denote $\Xi_{ij\ell} = \widehat{\mathbf{m}}_i^{\top} \mathbf{g}_{\ell} \mathbf{g}_{\ell}^{\top} \widehat{\mathbf{v}}_j$. Now note that $\widehat{\mathbf{U}}_{\perp}(\widehat{\Sigma}_{\perp}/\hat{\sigma}_{k+1})^{\tilde{g}}\widehat{\mathbf{V}}_{\perp}^{\top}\widehat{\mathbf{V}} = \mathbf{0}_{n \times k}$ and thus $\widehat{\mathbf{m}}_i^{\top} \widehat{\mathbf{v}}_j = 0$ for any $(i, j) \in [n - k] \times [k]$. As the columns of \mathbf{G} are independent of $\widehat{\mathbf{M}}$, for any $\ell \in [\tilde{k}]$ and any $(i, j) \in [n - k] \times [k]$ we have

$$\mathbb{E}[\Xi_{ij\ell}] = \mathbb{E}[\widehat{\mathbf{m}}_i^{\top} \mathbf{g}_{\ell} \mathbf{g}_{\ell}^{\top} \widehat{\mathbf{v}}_j] = \widehat{\mathbf{m}}_i^{\top} \mathbb{E}[\mathbf{g}_{\ell} \mathbf{g}_{\ell}^{\top}] \widehat{\mathbf{v}}_j = \widehat{\mathbf{m}}_i^{\top} \widehat{\mathbf{v}}_j = 0.$$

Furthermore, $\|\widehat{\mathbf{m}}_i\| \leq \|\widehat{\mathbf{v}}_j\| = 1$ for all $(i, j) \in [n - k] \times [k]$, which implies that $\widehat{\mathbf{m}}_i^{\top} \mathbf{g}_{\ell}$ and $\widehat{\mathbf{v}}_j^{\top} \mathbf{g}_{\ell}$ are two independent Gaussian random variables with variances bounded by 1.

Denote $\|\cdot\|_{\psi_1}$ and $\|\cdot\|_{\psi_2}$ as the sub-exponential and sub-Gaussian norms of a random variable. Then $\|\widehat{\mathbf{m}}_i^{\top} \mathbf{g}_{\ell}\|_{\psi_2} \leq 2$, $\|\widehat{\mathbf{v}}_j^{\top} \mathbf{g}_{\ell}\|_{\psi_2} \leq 2$ and by Lemma 2.7.7 in [Vershynin \(2018\)](#),

$$\|\Xi_{ij\ell}\|_{\psi_1} = \|\widehat{\mathbf{m}}_i^{\top} \mathbf{g}_{\ell} \mathbf{g}_{\ell}^{\top} \widehat{\mathbf{v}}_j\|_{\psi_1} \leq \|\widehat{\mathbf{m}}_i^{\top} \mathbf{g}_{\ell}\|_{\psi_2} \|\widehat{\mathbf{v}}_j^{\top} \mathbf{g}_{\ell}\|_{\psi_2} \leq 4$$

Therefore, given $\widehat{\mathbf{M}}$, Ξ_{ij} in Eq. (S6.14) is a sum of *independent* random variables with sub-exponential norms bounded by 4. Then by a standard application of Bernstein's inequality (see, e.g., Theorem 2.8.1 of [Vershynin \(2018\)](#)), we have

$$\mathbb{P}\left(\max_{i,j} |\Xi_{ij}| \geq t\right) \leq 2m\tilde{k} \exp\left[-\min\left\{\frac{t^2}{128e^2\tilde{k}}, \frac{t}{16e}\right\}\right]$$

Taking $t = (128\tilde{k} \log(1/\delta))^{1/2}e$ and noting that, from our condition on \tilde{k} in Theorem 2, we have

$\tilde{k} \geq 2 \log(1/\delta)$ and hence $t/(16e) \geq \log(1/\delta)$. This then implies

$$\mathbb{P}\left(\max_{i,j} |\Xi_{ij}| \geq (128\tilde{k} \log(1/\delta))^{1/2} e\right) \leq 2m\tilde{k}\delta$$

We therefore have

$$\hat{\sigma}_{k+1}^{\tilde{g}} \|\Xi\|_{2,\infty} \leq \hat{\sigma}_{k+1}^{\tilde{g}} k^{1/2} \max_{i,j} |\Xi_{ij}| \leq \sqrt{128e} \hat{\sigma}_{k+1}^{\tilde{g}} (k\tilde{k} \log(1/\delta))^{1/2},$$

with probability at least $1 - 2m\tilde{k}\delta$. Finally, by Lemma S3, we have $\|\hat{\mathbf{D}}_{\mathbf{G}}^{-1}\| \leq c_{\text{gap}}^{-1} \tilde{k}^{-1/2}$ and $\|\hat{\Sigma}_g^{-1}\| \leq c_{\text{gap}}^{-1} \tilde{k}^{-1/2} \hat{\sigma}_k^{\tilde{g}}$ with probability at least $1 - \vartheta$. Lemma S1 then implies

$$\|\mathbf{T}_1\|_{2,\infty} \leq \hat{\sigma}_{k+1}^{\tilde{g}} \times \|\Xi\|_{2,\infty} \times \|\hat{\mathbf{D}}_{\mathbf{G}}^{-1}\| \times \|\hat{\Sigma}_g^{-1}\| \leq \frac{\sqrt{128e} (k \log(1/\delta))^{1/2} \hat{\sigma}_{k+1}^{\tilde{g}}}{c_{\text{gap}}^2 \tilde{k}^{1/2} \hat{\sigma}_k^{\tilde{g}}} \quad (\text{S6.15})$$

with probability at least $1 - 2m\tilde{k}\delta - \vartheta$.

S6.4.2 Bounding $\|\mathbf{T}_2\|_{2,\infty}$

We first observe that, by Lemma S1, Lemma S2 and Lemma S3, we have

$$\begin{aligned} \|\mathbf{T}_2\|_{2,\infty} &\leq \|\hat{\mathbf{U}}_{\perp} \hat{\Sigma}_{\perp}^{\tilde{g}} \hat{\mathbf{V}}_{\perp}^{\top} \mathbf{G}\|_{2,\infty} \|\widehat{\mathbf{W}}_g - \widetilde{\mathbf{W}}_g \mathbf{Q}_{\widetilde{\mathbf{W}}_g}\| \|\hat{\Sigma}_g^{-1}\| \\ &\leq c_{\text{gap}}^{-1} \hat{\zeta}_k^{\tilde{g}} (2 \log(1/\delta))^{1/2} \|\widehat{\mathbf{W}}_g - \widetilde{\mathbf{W}}_g \mathbf{Q}_{\widetilde{\mathbf{W}}_g}\| \end{aligned} \quad (\text{S6.16})$$

with probability at least $1 - 2m\tilde{k}\delta - \vartheta$, where $\hat{\zeta}_k = \hat{\sigma}_{k+1}/\hat{\sigma}_k$.

We first bound $\|\widehat{\mathbf{W}}_g - \widetilde{\mathbf{W}}_g \mathbf{Q}_{\widetilde{\mathbf{W}}_g}\|$ using the rate-optimal bound in Cai and Zhang (2018) which carefully analyzes the perturbation of asymmetric matrices. Let

$$\mathbf{X} = \hat{\mathbf{U}} \hat{\Sigma}^{\tilde{g}} \hat{\mathbf{V}}^{\top} \mathbf{G}, \quad \mathbf{Z} = \hat{\mathbf{U}}_{\perp} \hat{\Sigma}_{\perp}^{\tilde{g}} \hat{\mathbf{V}}_{\perp}^{\top} \mathbf{G}, \quad \widehat{\mathbf{X}} = \mathbf{X} + \mathbf{Z} = \mathbf{Y}_g$$

Recall that the columns of $\widetilde{\mathbf{W}}_g$ and $\widehat{\mathbf{W}}_g$ are the leading right singular vectors of \mathbf{X} and $\widehat{\mathbf{X}}$, respectively, while the columns of $\hat{\mathbf{U}}_g$ are the leading left singular vectors of $\widehat{\mathbf{X}}$. Eq. (S6.9) then

implies

$$\begin{aligned}\mathbf{Z}_{12} &:= \check{\mathbf{U}}_g \check{\mathbf{U}}_g^\top \mathbf{Z} (\mathbf{I} - \check{\mathbf{W}}_g \check{\mathbf{W}}_g^\top) = \mathbf{0}, \quad \mathbf{Z}_{21} := (\mathbf{I} - \check{\mathbf{U}}_g \check{\mathbf{U}}_g^\top) \mathbf{Z} \check{\mathbf{W}}_g \check{\mathbf{W}}_g^\top = \mathbf{Z} \check{\mathbf{W}}_g \check{\mathbf{W}}_g^\top \\ \check{\mathbf{U}}_g^\top \widehat{\mathbf{X}} \check{\mathbf{W}}_g &= \check{\mathbf{U}}_g^\top \mathbf{X} \check{\mathbf{W}}_g = \check{\boldsymbol{\Sigma}}_g, \quad \check{\mathbf{U}}_{g,\perp}^\top \widehat{\mathbf{X}} \check{\mathbf{W}}_{g,\perp} = \check{\mathbf{U}}_{g,\perp}^\top \mathbf{Z} \check{\mathbf{W}}_{g,\perp}\end{aligned}$$

where $\check{\mathbf{U}}_{g,\perp}^\top$ and $\check{\mathbf{W}}_{g,\perp}$ are matrices with orthonormal columns for the basis of $\mathbf{I} - \check{\mathbf{U}}_g \check{\mathbf{U}}_g^\top$ and $\mathbf{I} - \check{\mathbf{W}}_g \check{\mathbf{W}}_g^\top$, respectively. Let $\alpha = \sigma_k(\check{\boldsymbol{\Sigma}}_g)$ and $\beta = \|\check{\mathbf{U}}_{g,\perp}^\top \widehat{\mathbf{X}} \check{\mathbf{W}}_{g,\perp}\| \leq \|\mathbf{Z}\|$. We then have

$$\|\widehat{\mathbf{W}}_g - \check{\mathbf{W}}_g \mathbf{Q}_{\check{\mathbf{W}}_g}\| \leq \frac{2\sqrt{2}\|\mathbf{Z}\|^2}{\alpha^2}. \quad (\text{S6.17})$$

Indeed, if $\alpha^2 \geq 2\|\mathbf{Z}\|^2$ then Eq. (S6.17) follows from Theorem 1 in [Cai and Zhang \(2018\)](#), namely

$$\begin{aligned}\|\sin \Theta(\widehat{\mathbf{W}}_g, \check{\mathbf{W}}_g)\| &\leq \frac{\alpha\|\mathbf{Z}_{12}\| + \beta\|\mathbf{Z}_{21}\|}{\alpha^2 - \beta^2 - \min\{\|\mathbf{Z}_{12}\|^2, \|\mathbf{Z}_{21}\|^2\}} \\ &= \frac{\beta\|\mathbf{Z}_{21}\|}{\alpha^2 - \beta^2} \leq \frac{\|\mathbf{Z}\|^2}{\alpha^2 - \beta^2} \leq \frac{\|\mathbf{Z}\|^2}{\alpha^2 - \|\mathbf{Z}\|^2} \leq \frac{2\|\mathbf{Z}\|^2}{\alpha^2}.\end{aligned}$$

If $\alpha^2 \leq 2\|\mathbf{Z}\|^2$ then Eq. (S6.17) follows from the trivial bound $\|\sin \Theta(\widehat{\mathbf{W}}_g, \check{\mathbf{W}}_g)\| \leq 1$. We therefore have, by Lemma S2 and Lemma S3, that

$$\|\widehat{\mathbf{W}}_g - \check{\mathbf{W}}_g \mathbf{Q}_{\check{\mathbf{W}}_g}\| \leq \frac{2\sqrt{2}\|\widehat{\boldsymbol{\Sigma}}_\perp\|^{2\tilde{g}} \cdot \|\mathbf{G}\|^2}{\sigma_k^2(\check{\boldsymbol{\Sigma}}_g)} \leq \frac{2\sqrt{2}\widehat{\sigma}_{k+1}^{2\tilde{g}} \times 9n}{c_{\text{gap}}^2 \tilde{k} \widehat{\sigma}_k^{2\tilde{g}}} \leq \frac{18\sqrt{2}n \widehat{\zeta}_k^{2\tilde{g}}}{c_{\text{gap}}^2 \tilde{k}} \quad (\text{S6.18})$$

with probability at least $1 - \vartheta - 2e^{-n/2}$.

Combining Eq. (S6.16) and Eq. (S6.18), we obtain

$$\|\mathbf{T}_2\|_{2 \rightarrow \infty} \leq \frac{36n(\log(1/\delta))^{1/2} \widehat{\zeta}_k^{3\tilde{g}}}{c_{\text{gap}}^3 \tilde{k}}$$

with probability at least $1 - 2m\tilde{k}\delta - \vartheta - 2e^{-n/2}$.

S6.4.3 Bounding $\|\mathbf{T}_3\|_{2,\infty}$

First recall Eq. (S6.9). Then by Lemma S1 and Eq. (S6.10) we have

$$\begin{aligned}\|\mathbf{T}_3\|_{2,\infty} &\leq \|\check{\mathbf{U}}_g\|_{2,\infty} \|\check{\mathbf{U}}_g^\top \hat{\mathbf{U}}_g - \mathbf{Q}_{\check{\mathbf{U}}_g}\| \\ &\leq \|\check{\mathbf{U}}_g\|_{2,\infty} d_2^2(\hat{\mathbf{U}}_g, \check{\mathbf{U}}_g) \leq \|\hat{\mathbf{U}}\|_{2,\infty} \frac{18n\hat{\zeta}_k^{2\tilde{g}}}{c_{\text{gap}}^2 \tilde{k}}\end{aligned}$$

with probability at least $1 - \vartheta - 2e^{-n/2}$.

S6.4.4 Putting all pieces together

Combining the bounds for $\|\mathbf{T}_1\|_{2,\infty}$ through $\|\mathbf{T}_3\|_{2,\infty}$ we obtain

$$\begin{aligned}d_{2,\infty}(\hat{\mathbf{U}}_g, \hat{\mathbf{U}}) &= d_{2,\infty}(\hat{\mathbf{U}}_g, \check{\mathbf{U}}_g) \\ &\leq \|\hat{\mathbf{U}}_g - \check{\mathbf{U}}_g \mathbf{Q}_{\check{\mathbf{U}}_g}\|_{2,\infty} \\ &\leq \frac{\sqrt{128}e(k \log(1/\delta))^{1/2} \hat{\zeta}_k^{\tilde{g}}}{c_{\text{gap}}^2 \tilde{k}^{1/2}} + \frac{36n(\log(1/\delta))^{1/2} \hat{\zeta}_k^{3\tilde{g}}}{c_{\text{gap}}^3 \tilde{k}} + \|\hat{\mathbf{U}}\|_{2 \rightarrow \infty} \frac{18n\hat{\zeta}_k^{2\tilde{g}}}{c_{\text{gap}}^2 \tilde{k}}\end{aligned} \tag{S6.19}$$

with probability at least $1 - 4m\tilde{k}\delta - \vartheta - 2e^{-n/2}$. □

S6.4.5 Bounding $\|(\hat{\mathbf{U}}_g \hat{\mathbf{U}}_g^\top - \hat{\mathbf{U}} \hat{\mathbf{U}}^\top) \hat{\mathbf{M}}\|_{\max}$

Let $\mathbf{R}_g = \hat{\mathbf{U}}_g - \check{\mathbf{U}}_g \mathbf{Q}_{\check{\mathbf{U}}_g} = \hat{\mathbf{U}}_g - \hat{\mathbf{U}} \check{\mathbf{Q}}_g \mathbf{Q}_{\check{\mathbf{U}}_g}$. As $\check{\mathbf{U}}_g \mathbf{Q}_{\check{\mathbf{U}}_g} (\check{\mathbf{U}}_g \mathbf{Q}_{\check{\mathbf{U}}_g})^\top = \hat{\mathbf{U}} \hat{\mathbf{U}}^\top$, we have

$$(\hat{\mathbf{U}}_g \hat{\mathbf{U}}_g^\top - \hat{\mathbf{U}} \hat{\mathbf{U}}^\top) \hat{\mathbf{M}} = \mathbf{R}_g \mathbf{R}_g^\top \hat{\mathbf{M}} + \mathbf{R}_g (\check{\mathbf{Q}}_g \mathbf{Q}_{\check{\mathbf{U}}_g})^\top \hat{\mathbf{U}}^\top \hat{\mathbf{M}} + \hat{\mathbf{U}} \check{\mathbf{Q}}_g \mathbf{Q}_{\check{\mathbf{U}}_g} \mathbf{R}_g^\top \hat{\mathbf{M}}.$$

We therefore have

$$\begin{aligned}\|(\hat{\mathbf{U}}_g \hat{\mathbf{U}}_g^\top - \hat{\mathbf{U}} \hat{\mathbf{U}}^\top) \hat{\mathbf{M}}\|_{\max} &\leq \|\mathbf{R}_g\|_{2,\infty} (\|\hat{\mathbf{M}}^\top \mathbf{R}_g\|_{2,\infty} + \|\hat{\mathbf{M}}^\top \hat{\mathbf{U}}\|_{2,\infty}) + \|\hat{\mathbf{U}}\|_{2,\infty} \times \|\hat{\mathbf{M}} \mathbf{R}_g\|_{2,\infty} \\ &\leq \|\mathbf{R}_g\|_{2,\infty} (\|\hat{\mathbf{M}}^\top \mathbf{R}_g\|_{2,\infty} + \|\hat{\mathbf{V}}\|_{2,\infty} \times \|\hat{\Sigma}\|) + \|\hat{\mathbf{U}}\|_{2,\infty} \times \|\hat{\mathbf{M}}^\top \mathbf{R}_g\|_{2,\infty}.\end{aligned}$$

where we have used the fact that for any matrices \mathbf{A} and \mathbf{B} for which \mathbf{AB} is well defined,

$\|\mathbf{AB}\|_{\max} \leq \|\mathbf{A}\|_{2,\infty} \times \|\mathbf{B}^\top\|_{2,\infty}$. By Eq. (S6.19), we have $\|\hat{\mathbf{R}}_g\|_{2,\infty} \leq r_{2,\infty}$ with probability at least $1 - 4m\tilde{k}\delta - \vartheta - 2e^{-n/2}$. We now bound $\|\hat{\mathbf{M}}^\top \mathbf{R}_g\|_{2,\infty}$. Recalling Eq. (S6.12) and that

$\check{\mathbf{U}}_g \check{\mathbf{U}}_g^\top = \hat{\mathbf{U}} \hat{\mathbf{U}}^\top$, we have

$$\begin{aligned}
\widehat{\mathbf{M}}^\top \mathbf{R}_g &= \widehat{\mathbf{M}}^\top (\mathbf{I} - \hat{\mathbf{U}} \hat{\mathbf{U}}^\top) \widehat{\mathbf{R}}_g + \widehat{\mathbf{M}}^\top \hat{\mathbf{U}} \hat{\mathbf{U}}^\top \widehat{\mathbf{R}}_g \\
&= \widehat{\mathbf{M}}^\top (\mathbf{I} - \hat{\mathbf{U}} \hat{\mathbf{U}}^\top) \widehat{\mathbf{U}}_g + \widehat{\mathbf{V}} \widehat{\Sigma} \check{\mathbf{Q}}_g^\top (\check{\mathbf{U}}_g^\top \widehat{\mathbf{U}}_g - \mathbf{Q}_{\check{\mathbf{U}}_g}) \\
&= \widehat{\mathbf{V}}_\perp \widehat{\Sigma}_\perp \widehat{\mathbf{U}}_\perp^\top \mathbf{Y}_g \widehat{\mathbf{W}}_g \widehat{\Sigma}_g^{-1} + \widehat{\mathbf{V}} \widehat{\Sigma} \check{\mathbf{Q}}_g^\top (\check{\mathbf{U}}_g^\top \widehat{\mathbf{U}}_g - \mathbf{Q}_{\check{\mathbf{U}}_g}) \\
&= \underbrace{\widehat{\mathbf{V}}_\perp \widehat{\Sigma}_\perp^{\tilde{g}+1} \widehat{\mathbf{V}}_\perp^\top \mathbf{G} \widetilde{\mathbf{W}}_g \mathbf{Q}_{\widetilde{\mathbf{W}}_g} \widehat{\Sigma}_g^{-1}}_{\mathbf{T}'_1} + \underbrace{\widehat{\mathbf{V}}_\perp \widehat{\Sigma}_\perp^{\tilde{g}+1} \widehat{\mathbf{V}}_\perp^\top \mathbf{G} (\widehat{\mathbf{W}}_g - \widetilde{\mathbf{W}}_g \mathbf{Q}_{\widetilde{\mathbf{W}}_g}) \widehat{\Sigma}_g^{-1}}_{\mathbf{T}'_2} \\
&\quad + \underbrace{\widehat{\mathbf{V}} \widehat{\Sigma} \check{\mathbf{Q}}_g^\top (\check{\mathbf{U}}_g^\top \widehat{\mathbf{U}}_g - \mathbf{Q}_{\check{\mathbf{U}}_g})}_{\mathbf{T}'_3}
\end{aligned}$$

Following the same derivations as that for $\mathbf{T}_1, \mathbf{T}_2$ and \mathbf{T}_3 in the proof of Theorem 2, we have

$$\begin{aligned}
\|\mathbf{T}'_1\|_{2,\infty} &\leq \frac{\sqrt{128}e(k \log(1/\gamma))^{1/2} \widehat{\sigma}_{k+1} \widehat{\zeta}_k^{\tilde{g}}}{c_{\text{gap}}^2 \tilde{k}^{1/2}}, \quad \|\mathbf{T}'_2\|_{2,\infty} \leq \frac{36n(\log(1/\gamma))^{1/2} \widehat{\sigma}_{k+1} \widehat{\zeta}_k^{3\tilde{g}}}{c_{\text{gap}}^3 \tilde{k}}, \\
\|\mathbf{T}'_3\|_{2,\infty} &\leq \frac{18n\widehat{\sigma}_1 \widehat{\zeta}_k^{2g}}{c_{\text{gap}}^2 \tilde{k}} \|\widehat{\mathbf{V}}\|_{2,\infty},
\end{aligned}$$

with probability at least $1 - 4n\tilde{k}\gamma - \vartheta - 2e^{-n/2}$. We therefore have

$$\|\widehat{\mathbf{M}} \mathbf{R}_g\|_{2,\infty} \leq \|\mathbf{T}'_1\|_{2,\infty} + \|\mathbf{T}'_2\|_{2,\infty} + \|\mathbf{T}'_3\|_{2,\infty} \leq \widehat{\sigma}_1 \tilde{r}_{2,\infty}$$

with probability at least $1 - 4n\tilde{k}\gamma - \vartheta - 2e^{-n/2}$. In summary we have

$$\begin{aligned}
\|(\widehat{\mathbf{U}}_g \widehat{\mathbf{U}}_g^\top - \hat{\mathbf{U}} \hat{\mathbf{U}}^\top) \widehat{\mathbf{M}}\|_{\max} &\leq r_{2,\infty} \times (\widehat{\sigma}_1 \tilde{r}_{2,\infty} + \|\widehat{\mathbf{V}}\|_{2,\infty} \times \widehat{\sigma}_1) + \|\widehat{\mathbf{U}}\|_{2,\infty} \times \widehat{\sigma}_1 \tilde{r}_{2,\infty} \\
&\leq \widehat{\sigma}_1 (r_{2,\infty} \tilde{r}_{2,\infty} + \|\widehat{\mathbf{U}}\|_{2,\infty} \tilde{r}_{2,\infty} + \|\widehat{\mathbf{V}}\|_{2,\infty} r_{2,\infty})
\end{aligned}$$

with probability at least $1 - 4\tilde{k}(m\delta + n\gamma) - \vartheta - 2e^{-n/2}$. □

S6.5 Proof of Corollary 2

For ease of notations we will omit the index k_0 from our matrices. If $\text{rk}(\mathbf{M}) = k_0$ then $\sigma_{k_0+1} = 0$ and, by the Davis-Kahan theorem (Davis and Kahan, 1970), $d_2(\widehat{\mathbf{U}}, \mathbf{U}) \leq E_n/\sigma_{k_0}$. Next, from

Corollary 1 with $k = k_0$ and $\vartheta = n^{-3}$ we have

$$d_2(\hat{\mathbf{U}}_g, \hat{\mathbf{U}}) \leq d_2(\hat{\mathbf{U}}, \mathbf{U}) + 3\sqrt{2}c_{\text{gap}}^{-1}(n/\tilde{k})^{1/2}\zeta_{k_0}^g \leq \left\{1 + 3\sqrt{2}c_{\text{gap}}^{-1}(n/\tilde{k})^{1/2}\zeta_{k_0}^{g-1}\right\} \frac{E_n}{\sigma_{k_0}}$$

with probability at least $1 - 2n^{-3}$, provided that $\tilde{k} \geq (1 - c_{\text{gap}})^{-2}\{k_0 + \sqrt{24k_0 \log n} + 6 \log n\}$.

Let $g_\iota = \frac{\log\{3\sqrt{2}c_{\text{gap}}^{-1}(n/\tilde{k})^{1/2}\iota^{-1}\}}{\log(1/\zeta_{k_0})}$. Then

$$3\sqrt{2}c_{\text{gap}}^{-1}(n/\tilde{k})^{1/2}\zeta_{k_0}^{g-1} = \iota \cdot \iota^{-1} 3\sqrt{2}c_{\text{gap}}^{-1}(n/\tilde{k})^{1/2} \cdot \zeta_{k_0}^{g-1} = \iota \cdot \zeta_{k_0}^{-g_\iota} \cdot \zeta_{k_0}^{g-1} = \iota \cdot \zeta_{k_0}^{g-1-g_\iota},$$

which yields (2.13).

Eq. (2.14) for the strong signal regime $\sigma_{k_0}/E_n \gtrsim n^\epsilon$ can be shown using the same argument as described above. First we have for some $c \in (0, 1)$, $\zeta_{k_0}^{-1} \geq \sigma_{k_0}/(2E_n) \geq cn^\epsilon$ when n is sufficiently large. Thus we have

$$g_* = \frac{\log(n) - \log(\tilde{k})}{2 \log(1/\zeta_{k_0})} \leq \frac{\log(n) - \log(\tilde{k})}{2\epsilon \log(n) + 2 \log c} \leq (2\epsilon)^{-1}$$

for sufficiently large n , where the final inequality follows from the fact that $\log(\tilde{k}) \gtrsim \log \log n$.

Let $\iota = 3\sqrt{2}c_{\text{gap}}^{-1}$ in (2.13), then we have

$$g_\iota = \frac{\log(n/\tilde{k})}{2 \log(1/\zeta_{k_0})} = g_*,$$

and when $g \in [g_*, 1 + g_*]$,

$$\begin{aligned} (1 + \iota \cdot \zeta_{k_0}^{g-g_\iota-1}) \frac{E_n}{\sigma_{k_0}} &= \frac{E_n}{\sigma_{k_0}} + 3\sqrt{2}c_{\text{gap}}^{-1} \cdot \zeta_{k_0}^{g-g_*-1} \cdot \frac{E_n}{\sigma_{k_0}} \\ &\leq \frac{E_n}{\sigma_{k_0}} + 6\sqrt{2}c_{\text{gap}}^{-1} \cdot \zeta_{k_0}^{g-g_*} \leq \frac{E_n}{\sigma_{k_0}} + 12\sqrt{2}c_{\text{gap}}^{-1} \cdot \left(\frac{E_n}{\sigma_{k_0}}\right)^{g-g_*} = O\left\{\left(\frac{E_n}{\sigma_{k_0}}\right)^{g-g_*}\right\}. \end{aligned}$$

When $g \geq 1 + g_* + \Delta$ for any $\Delta = \omega(\log^{-1} n)$, we have

$$\begin{aligned} (1 + \iota \cdot \zeta_{k_0}^{g-g_\iota-1}) \frac{E_n}{\sigma_{k_0}} &\leq \frac{E_n}{\sigma_{k_0}} + 6\sqrt{2}c_{\text{gap}}^{-1} \cdot \zeta_{k_0}^{g-g_*} = \frac{E_n}{\sigma_{k_0}} + 6\sqrt{2}c_{\text{gap}}^{-1} \cdot \zeta_{k_0}^{1+\Delta} \\ &\leq \frac{E_n}{\sigma_{k_0}} + 12\sqrt{2}c_{\text{gap}}^{-1} \cdot c^{-\Delta} n^{-\Delta\epsilon} \frac{E_n}{\sigma_{k_0}} = (1 + o(1)) E_n / \sigma_{k_0}. \end{aligned}$$

Combining the above results yield (2.14).

□

S6.6 Proof of Corollary 3

Similar to the proof of Corollary 2, we will omit the index k_0 from our matrices. From Corollary 1 with $k = k_0$ and $\vartheta = n^{-3}$ and $\delta = n^{-5}$ we have

$$d_{2,\infty}(\hat{\mathbf{U}}_g, \mathbf{U}) \leq C_* \left(\frac{(k \log n)^{1/2} \zeta_{k_0}^g}{\tilde{k}^{1/2}} + \frac{nu_{2,\infty} \zeta_{k_0}^{2g}}{\tilde{k}} + \frac{n(\log n)^{1/2} \zeta_{k_0}^{3g}}{\tilde{k}} \right) := r_{2,\infty}$$

with probability at least $1 - 5n^{-3} - 2e^{-n/2}$, where $\zeta_{k_0} = E_n/(\sigma_{k_0} - E_n)$ and C_* is a constant depending only on c_{gap} ; recall that, from the statement of Corollary 2 we already assume $c_{\text{gap}} > 0$ is a fixed but arbitrary constant. Now define

$$t_1 = 1 + \frac{\log(nk/\tilde{k}) + \log \log n}{2 \log(1/\zeta_{k_0})}, \quad t_2 = \frac{1}{2} + \frac{\log(n^{3/2} \|\mathbf{U}\|_{2,\infty}/\tilde{k})}{2 \log(1/\zeta_{k_0})}, \quad t_3 = \frac{1}{3} + \frac{\log(n^{3/2}/\tilde{k}) + \frac{1}{2} \log \log n}{3 \log(1/\zeta_{k_0})}.$$

Then for $g \geq t_1$ we have

$$g \log(1/\zeta_{k_0}) \geq \log(1/\zeta_{k_0}) + \frac{1}{2} \left\{ \log(nk/\tilde{k}) + \log \log n \right\}$$

which then implies

$$\zeta_{k_0}^g \leq \zeta_{k_0} \times \frac{\tilde{k}^{1/2}}{(kn \log n)^{1/2}} \implies \frac{(k \log n)^{1/2} \zeta_{k_0}^g}{\tilde{k}^{1/2}} \leq n^{-1/2} \zeta_{k_0} = O(n^{-1/2} E_n / \sigma_{k_0}).$$

Similarly, if $g \geq t_2$ then

$$\frac{nu_{2,\infty} \zeta_{k_0}^{2g}}{\tilde{k}} \leq \zeta_{k_0} \times u_{2,\infty} \times \frac{1}{n^{1/2} \|\mathbf{U}\|_{2,\infty}} \leq 2n^{-1/2} \zeta_{k_0} = O(n^{-1/2} E_n / \sigma_{k_0})$$

where the second inequality follows from the assumption $d_{2,\infty}(\widehat{\mathbf{U}}, \mathbf{U}) \leq \|\mathbf{U}\|_{2,\infty}$ in the statement of Corollary 3. If $g \geq t_3$ then

$$\frac{n(\log n)^{1/2} \zeta_{k_0}^{3g}}{\tilde{k}} \leq n^{-1/2} \zeta_{k_0} = O(n^{-1/2} E_n / \sigma_{k_0}).$$

As $\sigma_{k_0} > 2E_n$, we have $(\sigma_{k_0} - E_n)/E_n \geq \sigma_{k_0}/(2E_n)$ and thus

$$t_1 = 1 + \frac{\log(nk/\tilde{k}) + \log \log n}{2 \log(1/\zeta_{k_0})} \leq 1 + \frac{\log(nk/\tilde{k}) + \log \log n}{2 \log(\frac{1}{2} \sigma_{k_0}/E_n)},$$

and similarly for t_2 and t_3 . In summary, if $g \geq g_* \geq \max\{t_1, t_2, t_3\}$ then

$$d_{2,\infty}(\widehat{\mathbf{U}}_g, \widehat{\mathbf{U}}) = O(n^{-1/2} E_n / \sigma_{k_0})$$

with probability at least $1 - 5n^{-3} - 2e^{-n/2}$.

Furthermore, as \mathbf{M} and $\widehat{\mathbf{M}}$ are both symmetric, we have $u_{2,\infty} = v_{2,\infty} \leq 2\|\mathbf{U}\|_{2,\infty}$ and $r_{2,\infty} = \tilde{r}_{2,\infty}$. Then by Eq. (2.12), for $g \geq g_*$ we have

$$\begin{aligned} \|\widehat{\mathbf{U}}_g \widehat{\mathbf{U}}_g^\top \widehat{\mathbf{M}} - \mathbf{M}\|_{\max} &\leq \|\widehat{\mathbf{U}} \widehat{\mathbf{U}}^\top \widehat{\mathbf{M}} - \mathbf{M}\|_{\max} + (\sigma_1 + E_n)(r_{2,\infty}^2 + 4\|\mathbf{U}\|_{2,\infty} r_{2,\infty}) \\ &\leq \|\widehat{\mathbf{U}} \widehat{\mathbf{U}}^\top \widehat{\mathbf{M}} - \mathbf{M}\|_{\max} + O((\sigma_1 + E_n)(n^{-1}(E_n/\sigma_{k_0})^2 + n^{-1/2}(E_n/\sigma_{k_0})\|\mathbf{U}\|_{2,\infty})) \\ &\leq \|\widehat{\mathbf{U}} \widehat{\mathbf{U}}^\top \widehat{\mathbf{M}} - \mathbf{M}\|_{\max} + O(\kappa n^{-1/2} E_n \|\mathbf{U}\|_{2,\infty}) \end{aligned}$$

with probability at least $1 - 9n^{-3} - 2e^{-n/2}$, where the last inequality follows from the fact that $\|\mathbf{U}\|_{2,\infty} \geq k_0^{1/2} n^{-1/2}$. Finally, if $\sigma_{k_0} = \omega(E_n)$ and $g \geq g_* + c$ for any fixed but arbitrary $c > 0$ then $d_{2,\infty}(\widehat{\mathbf{U}}_g, \widehat{\mathbf{U}}) = O(n^{-1/2}(E_n/\sigma_{k_0})^{1+c}) = o(n^{-1/2} E_n / \sigma_{k_0})$ which also implies

$$\begin{aligned} \|\widehat{\mathbf{U}}_g \widehat{\mathbf{U}}_g^\top \widehat{\mathbf{M}} - \mathbf{M}\|_{\max} &\leq \|\widehat{\mathbf{U}} \widehat{\mathbf{U}}^\top \widehat{\mathbf{M}} - \mathbf{M}\|_{\max} + o((\sigma_1 + E_n)(n^{-1}(E_n/\sigma_{k_0})^2 + n^{-1/2}(E_n/\sigma_{k_0})\|\mathbf{U}\|_{2,\infty})) \\ &\leq \|\widehat{\mathbf{U}} \widehat{\mathbf{U}}^\top \widehat{\mathbf{M}} - \mathbf{M}\|_{\max} + o(\kappa n^{-1/2} E_n \|\mathbf{U}\|_{2,\infty}) \end{aligned}$$

S7 Proofs for Section 3, Section S2 and Section S3.1

S7.1 Proof of Theorem 3

As $d_{2,\infty}(\hat{\mathbf{U}}_g, \mathbf{U}) \geq n^{-1/2}d_2(\hat{\mathbf{U}}_g, \mathbf{U})$ always holds, we will only derive the lower bound for $d_2(\hat{\mathbf{U}}_g, \mathbf{U})$.

It is sufficient to lower bound $\|(\mathbf{I} - \hat{\mathbf{U}}\hat{\mathbf{U}}^\top)\hat{\mathbf{U}}_g\hat{\mathbf{U}}_g^\top\|$, which serves as a lower bound for $d_2^2()$. Note that

$$(\mathbf{I} - \hat{\mathbf{U}}\hat{\mathbf{U}}^\top)\hat{\mathbf{U}}_g\hat{\mathbf{U}}_g^\top = \hat{\mathbf{U}}_\perp\hat{\mathbf{U}}_\perp^\top\widehat{\mathbf{M}}^g\mathbf{G}\mathbf{T}(\mathbf{T}^\top\mathbf{G}^\top\widehat{\mathbf{M}}^{2g}\mathbf{G}\mathbf{T})^{-1}\mathbf{T}^\top\mathbf{G}^\top\widehat{\mathbf{M}}^g$$

where \mathbf{T} is a $\tilde{k} \times k$ matrix with orthonormal columns such that the column space of $\widehat{\mathbf{M}}^g\mathbf{G}\mathbf{T}$ is the same as that for $\hat{\mathbf{U}}_g$. Such \mathbf{T} always exists as the column space of $\widehat{\mathbf{M}}^g\mathbf{G}\mathbf{T}$ must include the column space of $\hat{\mathbf{U}}_g$ with $\tilde{k} \geq k$. We then have

$$\begin{aligned} \|(\mathbf{I} - \hat{\mathbf{U}}\hat{\mathbf{U}}^\top)\hat{\mathbf{U}}_g\hat{\mathbf{U}}_g^\top\| &= \lambda_{\max}(\hat{\mathbf{U}}_\perp^\top\widehat{\mathbf{M}}^g\mathbf{G}\mathbf{T}(\mathbf{T}^\top\mathbf{G}^\top\widehat{\mathbf{M}}^{2g}\mathbf{G}\mathbf{T})^{-1}\mathbf{T}^\top\mathbf{G}^\top\widehat{\mathbf{M}}^g\hat{\mathbf{U}}_\perp) \\ &= \lambda_{\max}(\hat{\mathbf{\Lambda}}_\perp^g\hat{\mathbf{U}}_\perp^\top\mathbf{G}\mathbf{T}(\mathbf{T}^\top\mathbf{G}^\top\widehat{\mathbf{M}}^{2g}\mathbf{G}\mathbf{T})^{-1}\mathbf{T}^\top\mathbf{G}^\top\hat{\mathbf{U}}_\perp\hat{\mathbf{\Lambda}}_\perp^g) \\ &\geq \frac{\lambda_{\max}(\hat{\mathbf{\Lambda}}_\perp^g\hat{\mathbf{U}}_\perp^\top\mathbf{G}\mathbf{T}\mathbf{T}^\top\mathbf{G}^\top\hat{\mathbf{U}}_\perp\hat{\mathbf{\Lambda}}_\perp^g)}{\|\mathbf{T}^\top\mathbf{G}^\top\widehat{\mathbf{M}}^{2g}\mathbf{G}\mathbf{T}\|} \\ &\geq \frac{\lambda_{\max}(\mathbf{T}^\top\mathbf{G}^\top\hat{\mathbf{U}}_\perp\hat{\mathbf{\Lambda}}_\perp^{2g}\hat{\mathbf{U}}_\perp^\top\mathbf{G}\mathbf{T})}{\|\mathbf{G}^\top\widehat{\mathbf{M}}^{2g}\mathbf{G}\|}. \end{aligned}$$

Now $\hat{\mathbf{U}}_\perp\hat{\mathbf{\Lambda}}_\perp^{2g}\hat{\mathbf{U}}_\perp^\top = \widehat{\mathbf{M}}^{2g} - \hat{\mathbf{U}}\hat{\mathbf{\Lambda}}^{2g}\hat{\mathbf{U}}^\top$ and hence

$$\begin{aligned} \|(\mathbf{I} - \hat{\mathbf{U}}\hat{\mathbf{U}}^\top)\hat{\mathbf{U}}_g\hat{\mathbf{U}}_g^\top\| &\geq \frac{\lambda_{\max}(\mathbf{T}^\top\mathbf{G}^\top\widehat{\mathbf{M}}^{2g}\mathbf{G}\mathbf{T}) - \|\hat{\mathbf{\Lambda}}\|^{2g} \times \|\mathbf{T}^\top\mathbf{G}^\top\hat{\mathbf{U}}\|^2}{\|\mathbf{G}^\top\widehat{\mathbf{M}}^{2g}\mathbf{G}\|} \\ &\geq \frac{\lambda_{\max}(\mathbf{G}^\top\widehat{\mathbf{M}}^{2g}\mathbf{G}) - \|\hat{\mathbf{\Lambda}}\|^{2g} \times \|\mathbf{G}^\top\hat{\mathbf{U}}\|^2}{\|\mathbf{G}^\top\widehat{\mathbf{M}}^{2g}\mathbf{G}\|} \end{aligned}$$

where the last inequality follows from the fact that \mathbf{T} is a partial isometry mapping the column space of $\widehat{\mathbf{M}}^g\mathbf{G}$ to $\hat{\mathbf{U}}_g$ and hence $\lambda_{\max}(\mathbf{T}\mathbf{G}^\top\widehat{\mathbf{M}}^{2g}\mathbf{G}\mathbf{T}) = \lambda_{\max}(\mathbf{G}^\top\widehat{\mathbf{M}}^{2g}\mathbf{G})$. Furthermore, as the diagonal entries of a matrix is majorized by its eigenvalues, we have

$$\|(\mathbf{I} - \hat{\mathbf{U}}\hat{\mathbf{U}}^\top)\hat{\mathbf{U}}_g\hat{\mathbf{U}}_g^\top\| \geq \frac{(\max_i \mathbf{g}_i^\top\widehat{\mathbf{M}}^{2g}\mathbf{g}_i) - \|\hat{\mathbf{\Lambda}}\|^{2g} \times \|\mathbf{G}^\top\hat{\mathbf{U}}\|^2}{\|\mathbf{G}^\top\widehat{\mathbf{M}}^{2g}\mathbf{G}\|}$$

where \mathbf{g}_i is the i th column of \mathbf{G} and the maximum is taken over all $i \leq \tilde{k}$. We next recall our assumption on $\widehat{\mathbf{M}}$, namely that $\mathbb{E}[\text{tr} \widehat{\mathbf{M}}^{2g}] \geq c_g(n^{g+1}\rho_n^g + (n\rho_n)^{2g})$ for some constant $c > 0$ and $n\rho_n \gtrsim n^\beta$ for some $\beta > 0$. Fix a $g < \beta^{-1}$. By Markov's inequality, there exists a constant $C > 0$ such that

$$\text{tr} \widehat{\mathbf{M}}^{2g} \geq C c_g n^{1+\beta g} \quad (\text{S7.1})$$

with probability at least $1 - p_0$. Furthermore, recall that we had assumed $\|\mathbf{M}\| \asymp n\rho_n$ and $\lambda_{k_0}/E_n \asymp (n\rho_n)^{1/2}$, which together implies $\|\widehat{\mathbf{M}}\| \asymp n\rho_n$ with probability at least $1 - n^{-3}$. Let \mathcal{E} be the event that Eq. (S7.1) holds together with $\|\widehat{\mathbf{M}}\| \asymp n\rho_n$; note that $\mathbb{P}(\mathcal{E}) \geq 1 - p_0 - n^{-3}$. Then by the Hanson-Wright inequality (Hanson and Wright, 1971), we have

$$\begin{aligned} \mathbb{P}(\mathbf{g}_i^\top \widehat{\mathbf{M}}^{2g} \mathbf{g}_i \geq \text{tr} \widehat{\mathbf{M}}^{2g} - t \mid \mathcal{E}) &\geq 1 - \exp \left\{ -C_2 \min \left(\frac{t^2}{\|\widehat{\mathbf{M}}^{2g}\|_{\text{F}}^2}, \frac{t}{\|\widehat{\mathbf{M}}^{2g}\|} \right) \right\} \\ &\geq 1 - \exp \left\{ -C_3 \min \left(\frac{t^2}{n^{2g+1}\rho_n^{2g}}, \frac{t}{(n\rho_n)^{2g}} \right) \right\}, \end{aligned}$$

for any $t \geq 0$; here $C_2 \geq 0$ and $C_3 \geq 0$ are constants not depending on n . We thus have, by a union bound over all $i \leq \tilde{k}$ that

$$\mathbb{P}(\max_i \mathbf{g}_i^\top \widehat{\mathbf{M}}^{2g} \mathbf{g}_i \geq \text{tr} \widehat{\mathbf{M}} - t \mid \mathcal{E}) \geq 1 - \tilde{k} \exp \left\{ -C_3 \min \left(\frac{t^2}{n^{2g+1}\rho_n^{2g}}, \frac{t}{(n\rho_n)^{2g}} \right) \right\}.$$

We now choose $t = C_4 n^{g+1/2} \rho_n^g \log^{1/2} n$ for some sufficiently large $C_4 \geq 0$. Then, conditional on \mathcal{E} , we have for sufficiently large n that

$$\max_{i \leq \tilde{k}} \mathbf{g}_i^\top \widehat{\mathbf{M}}^{2g} \mathbf{g}_i \geq \text{tr} \widehat{\mathbf{M}}^{2g} - C_4 n^{g+1/2} \rho_n^g \log^{1/2} n \geq \frac{1}{2} \text{tr} \widehat{\mathbf{M}}^{2g} \quad (\text{S7.2})$$

with high probability. Furthermore, from Lemma S3 we have

$$\begin{aligned} \|\mathbf{G}^\top \widehat{\mathbf{M}}^{2g} \mathbf{G}\| &\leq \|\mathbf{G}^\top \widehat{\mathbf{U}}\|^2 \times \|\widehat{\mathbf{\Lambda}}\|^{2g} + \|\mathbf{G}\|^2 \times \|\widehat{\mathbf{\Lambda}}_\perp\|^{2g} \\ &\lesssim \tilde{k} \|\mathbf{\Lambda}\|^{2g} + n \hat{\lambda}_{k+1}^{2g} \\ &\lesssim \tilde{k} (n\rho_n)^{2g} + n^{g+1} \rho_n^g \\ &\lesssim (\log n) (n\rho_n)^{2g} + n^{g+1} \rho_n^g \end{aligned}$$

with probability at least $1 - n^{-3}$, where the final inequality is because $\tilde{k} \asymp \log n = o(n^\epsilon)$ for any $\epsilon > 0$. Combining the above bounds we have (conditional on \mathcal{E}),

$$\|(\mathbf{I} - \hat{\mathbf{U}}\hat{\mathbf{U}}^\top)\hat{\mathbf{U}}_g\hat{\mathbf{U}}_g^\top\| \geq \frac{\frac{1}{2}\text{tr}\hat{\mathbf{M}}^{2g} - C_0\tilde{k}\|\hat{\mathbf{A}}\|^{2g}}{C_1n^{g+1}\rho_n^g + C_1(\log n)(n\rho_n)^{2g}} \quad (\text{S7.3})$$

with probability at least $1 - 2n^{-3}$. Finally, we also have for sufficiently large n that

$$\frac{1}{2}\text{tr}\hat{\mathbf{M}}^{2g} - C_0\tilde{k}\|\hat{\mathbf{A}}\|^{2g} \geq \frac{1}{4}\text{tr}\hat{\mathbf{M}}^{2g} \geq \frac{1}{4}c_gn^{g+1}\rho_n^g \quad (\text{S7.4})$$

Substituting Eq. (S7.4) into Eq. (S7.3), and unconditioning with respect to \mathcal{E} , we have for all $g < \beta^{-1}$, $(\log n)(n\rho_n)^{2g} < n^{g+1}\rho_n^g$ and thus

$$\|(\mathbf{I} - \hat{\mathbf{U}}\hat{\mathbf{U}}^\top)\hat{\mathbf{U}}_g\hat{\mathbf{U}}_g^\top\| \geq \frac{\text{tr}\hat{\mathbf{M}}^{2g} - C_0\tilde{k}\|\hat{\mathbf{A}}\|^{2g}}{C_5n^{g+1}\rho_n^g} \geq \frac{c_gn^{g+1}\rho_n^g}{4C_5n^{g+1}\rho_n^g} \geq C_{LB}c_g$$

with probability at least $1 - p_0 - 2n^{-3}$, where C_{LB} is a constant depending only on p_0 . Similarly, if $\beta^{-1} \leq g < 1 + \beta^{-1}$, we have $(\log n)(n\rho_n)^{2g} > n^{g+1}\rho_n^g$ and thus

$$\|(\mathbf{I} - \hat{\mathbf{U}}\hat{\mathbf{U}}^\top)\hat{\mathbf{U}}_g\hat{\mathbf{U}}_g^\top\| \geq \frac{\text{tr}\hat{\mathbf{M}}^{2g} - C_0\tilde{k}\|\hat{\mathbf{A}}\|^{2g}}{C_6(\log n)(n\rho_n)^{2g}} \geq \frac{c_gn^{g+1}\rho_n^g}{(\log n)(n\rho_n)^{2g}} \geq C_{LB}c_g(\log n)^{-1}(n)^{1-g\beta}.$$

Note that C_{LB} and c_g written in the theorem are the squared roots of the corresponding constants written here. □

S7.2 Proof of Theorem S6 and Corollary S4

Let $\hat{\mathbf{M}} = p^{-1}\hat{\mathbf{T}}$ and $\mathbf{M} = \mathbb{E}[p^{-1}\hat{\mathbf{T}}] = \mathbb{E}[p^{-1}\{\mathcal{P}_\Omega(\mathbf{T} + \mathbf{N})\}] = \mathbf{T}$. Now define \mathbf{U} , $\hat{\mathbf{U}}$ and $\hat{\mathbf{U}}_g$ accordingly, where, for simplicity of notations we have dropped the index k_0 from these matrices. Finally let $\hat{\mathbf{T}}_g = p^{-1}\hat{\mathbf{U}}_g\hat{\mathbf{U}}_g^\top\hat{\mathbf{T}}$.

S7.2.1 Bounding $\|\mathbf{E}\|$

We have

$$\mathbf{E} = \widehat{\mathbf{M}} - \mathbf{M} = \underbrace{\frac{1}{p}\{\mathcal{P}_{\Omega}(\mathbf{T}) - p\mathbf{T}\}}_{\mathbf{E}_1} + \underbrace{\frac{1}{p}\mathcal{P}_{\Omega}(\mathbf{N})}_{\mathbf{E}_2}. \quad (\text{S7.5})$$

Now \mathbf{E}_1 is a random symmetric matrix whose upper triangular entries are independent mean 0 random variables with

$$\frac{1}{\|\mathbf{T}\|_{\max}} \max_{(i,j) \in [n]^2} |p[\mathbf{E}_1]_{ij}| = \frac{1}{p\|\mathbf{T}\|_{\max}} \max_{(i,j) \in [n]^2} \left\{ (1-2p)|[\mathbf{T}]_{ij}|, p|[\mathbf{T}]_{ij}| \right\} \leq 1.$$

Furthermore we also have

$$\begin{aligned} \max_i \sum_{j=1}^n \frac{\mathbb{E}|p[\mathbf{E}_1]_{ij}|^2}{\|\mathbf{T}\|_{\max}^2} &= \max_i \sum_{j=1}^n \frac{p\{[\mathbf{T}]_{ij} - p[\mathbf{T}]_{ij}\}^2 + (1-p)\{-p[\mathbf{T}]_{ij}\}^2}{\|\mathbf{T}\|_{\max}^2} \\ &\leq \max_i \sum_{j=1}^n [p(1-p)^2 + (1-p)p^2] \leq np. \end{aligned} \quad (\text{S7.6})$$

By Remark 3.13 in [Bandeira and Van Handel \(2016\)](#), there exists a universal constant $c > 0$ such that for $t = (np)^{1/2}$,

$$\mathbb{P}\left[\frac{p}{\|\mathbf{T}\|_{\max}} \|\mathbf{E}_1\| \geq 4(np)^{1/2} + t\right] \leq ne^{-t^2/c}$$

which immediately implies, $\|\mathbf{E}_1\| \lesssim (n/p)^{1/2} \|\mathbf{T}\|_{\max}$ with probability at least $1 - \frac{1}{2}n^{-3}$. On the other hand, $p^{-1}\|\mathbf{E}_2\| \leq \|\mathcal{P}_{\Omega}(\mathbf{N})\| \lesssim \sigma(n/p)^{1/2}$, with probability at least $1 - \frac{1}{2}n^{-3}$, see e.g., Lemma 13 in [Abbe et al. \(2020\)](#). Eq. (S7.5) therefore implies

$$\|\mathbf{E}\| \lesssim (\sigma + \|\mathbf{T}\|_{\max})(n/p)^{1/2} \quad (\text{S7.7})$$

with probability at least $1 - n^{-3}$. We can thus choose $E_n = C_{\text{MC}}(\sigma + \|\mathbf{T}\|_{\max})(n/p)^{1/2}$ for some finite constant $C_{\text{MC}} > 2$. In summary we have

$$\frac{E_n}{|\lambda_{k_0}(\mathbf{T})|} \lesssim \frac{n^{1/2}(\sigma + \|\mathbf{T}\|_{\max})}{p^{1/2}|\lambda_{k_0}(\mathbf{T})|} \lesssim \kappa^{-1}(\log n)^{-1/2} \quad (\text{S7.8})$$

where the last inequality follows from the assumption in Eq. (S2.2).

S7.2.2 Bounding $d_2(\hat{\mathbf{U}}_g, \mathbf{U})$, $d_{2 \rightarrow \infty}(\hat{\mathbf{U}}_g, \mathbf{U})$ and $\|\hat{\mathbf{T}}_g - \mathbf{T}\|_{\mathbf{F}}$

Eq. (S7.8) implies $|\lambda_{k_0}(\mathbf{T})|/E_n \rightarrow \infty$ as $n \rightarrow \infty$. Let $g \geq \frac{\log n}{\log(|\lambda_{k_0}(\mathbf{T})|/E_n)}$. Then by Corollary 2 and Corollary 3 we have

$$\begin{aligned} d_2(\hat{\mathbf{U}}_g, \mathbf{U}) &\leq d_2(\hat{\mathbf{U}}, \mathbf{U}) + o\left(\frac{E_n}{|\lambda_{k_0}(\mathbf{T})|}\right) \\ d_{2,\infty}(\hat{\mathbf{U}}_g, \mathbf{U}) &\leq d_{2,\infty}(\hat{\mathbf{U}}, \mathbf{U}) + o\left(\frac{n^{-1/2}E_n}{|\lambda_{k_0}(\mathbf{T})|}\right) \end{aligned} \quad (\text{S7.9})$$

with probability at least $1 - n^{-3}$. Similarly, by Eq. (2.17), we have

$$\|\hat{\mathbf{T}}_g - \mathbf{T}\|_{\max} \leq \|\hat{\mathbf{T}}_S - \mathbf{T}\|_{\max} + o(n^{-1/2}E_n\kappa\|\mathbf{U}\|_{2,\infty}) \quad (\text{S7.10})$$

with probability at least $1 - n^{-3}$, where $\hat{\mathbf{T}}_S = p^{-1}\hat{\mathbf{T}}^{(k_0)}$ is the truncated rank- k_0 SVD of $\hat{\mathbf{T}}$. Eq. (S2.3) follows directly from Eq. (S7.9) together with the bounds for $d_{2,\infty}(\hat{\mathbf{U}}_g, \mathbf{U})$ and $\|\hat{\mathbf{T}}_S - \mathbf{T}\|_{\max}$ given in Theorem 3.4 of Abbe et al. (2020).

S7.2.3 Entrywise limiting distribution

Fix $g \geq g_* := \frac{\log n}{\log(|\lambda_{k_0}(\mathbf{T})|/E_n)}$. For ease of exposition we say that an event \mathcal{E} happens with high probability (whp) if \mathcal{E} happens with probability at least $1 - Cn^{-3}$. Here $C > 0$ is an arbitrary constant that can change from line to line. First recall the definition of v_{ij}^* in Eq. (S2.6). As the entries of \mathbf{T} are homogeneous, the $\{[\mathbf{T}^2]_{ii}\}$ also homogeneous. Now $[\mathbf{T}^2]_{ii} = \|[\mathbf{U}\mathbf{\Lambda}]_i\|^2$ and hence (as \mathbf{T} has bounded condition number), $\min_i \|[\mathbf{U}]_i\|^2 \asymp \max_i \|[\mathbf{U}]_i\|^2$ where $\|[\mathbf{U}]_i\|^2$ is the squared ℓ_2 norm of the i th row of \mathbf{U} . We therefore have

$$\begin{aligned} v_{ij}^* &\geq p^{-1}\{\min_{k\ell}(1-p)T_{k\ell}^2 + \sigma^2\}(\|[\mathbf{U}]_i\|^2 + \|[\mathbf{U}]_j\|^2) \\ &\gtrsim p^{-1}\{\min_{k\ell}(1-p)T_{k\ell}^2 + \sigma^2\}\|\mathbf{U}\|_{2,\infty}^2 \asymp p^{-1}(\|\mathbf{T}\|_{\max}^2 + \sigma^2)\|\mathbf{U}\|_{2,\infty}^2 \end{aligned} \quad (\text{S7.11})$$

where the final “equality” is due to the assumption that p is bounded away from 1. Recalling the expression for E_n given after Eq. (S7.7), we have

$$\begin{aligned} (v_{ij}^*)^{-1/2} \times o(n^{-1/2} E_n \kappa \|\mathbf{U}\|_{2,\infty}) &= o(n^{-1/2} p^{1/2} (\|\mathbf{T}\|_{\max}^2 + \sigma^2)^{-1/2} E_n) \\ &= o(\|\mathbf{T}\|_{\max}^2 + \sigma^2)^{-1/2} (\|\mathbf{T}\|_{\max} + \sigma) = o(1) \end{aligned}$$

Therefore, by Eq. (S7.10), we obtain

$$(v_{ij}^*)^{-1/2} ([\hat{\mathbf{T}}_g - \mathbf{T}]_{ij}) = (v_{ij}^*)^{-1/2} ([\hat{\mathbf{T}}_S - \mathbf{T}]_{ij}) + o(1) \rightsquigarrow \mathcal{N}(0, 1) \quad (\text{S7.12})$$

where the convergence in distribution of $[\hat{\mathbf{T}}_S - \mathbf{T}]_{ij}$ is precisely Theorem 4.12 in [Chen et al. \(2021\)](#).

S7.2.4 Confidence interval

We now derive Eq. (S2.9). This is equivalent to showing that $\hat{v}_{ij}/v_{ij}^* \rightarrow 1$ in probability where \hat{v}_{ij} is defined in Eq. (S2.8). Our derivations will proceed in three steps.

Step 1. We first consider a truncated version of $\hat{\mathbf{T}}$. Recall that the (upper triangular) entries of \mathbf{N} , denoted η_{ij} , are iid $\mathcal{N}(0, \sigma^2)$. Let $\tilde{\eta}_{ij} := \eta_{ij} \mathbb{I}\{|\eta_{ij}| \leq 5\sigma(\log n)^{1/2}\}$ and let $\tilde{\mathbf{N}}$ be the matrix whose entries are the $\tilde{\eta}_{ij}$. Now define

$$\tilde{\mathbf{T}} := \mathcal{P}_{\Omega}(\mathbf{T} + \tilde{\mathbf{N}}) \text{ and } \tilde{\mathbf{E}} = \tilde{\mathbf{T}}/p - \mathbf{T}. \quad (\text{S7.13})$$

By standard tail bounds for Gaussian distribution, we have

$$\mathbb{P}\left(\max_{ij} |\eta_{ij}| \leq 5\sigma(\log n)^{1/2}\right) \geq 1 - n^2 \mathbb{P}(|\eta_{ij}| > 5\sigma(\log n)^{1/2}) \geq 1 - n^{-10}.$$

We thus have $\tilde{\mathbf{E}} = \mathbf{E}$ and $\tilde{\mathbf{T}} = \hat{\mathbf{T}}$ whp. See ([Chen et al., 2021](#), Section 3.2.3) for more details. Next let v_{ij} be the variance of $[\mathbf{U}\mathbf{U}^\top \tilde{\mathbf{E}}]_{ij} + [\tilde{\mathbf{E}}\mathbf{U}\mathbf{U}^\top]_{ij}$. We can then use a similar argument to the proof of Theorem 4.12 in [Chen et al. \(2021\)](#), to bound v_{ij} from below. More specifically, for

all k, ℓ we have

$$\zeta_{k\ell}^2 = ([\mathbf{U}]_k^\top [\mathbf{U}]_\ell)^2 \leq \|[\mathbf{U}]_k\|^2 \times \|[\mathbf{U}]_\ell\|^2$$

and hence, following the proof of Lemma 4.19 in [Chen et al. \(2021\)](#), we have

$$\begin{aligned} v_{ij} &= \sum_{\ell \neq j} \mathbb{E}([\tilde{\mathbf{E}}]_{i\ell}^2) \zeta_{k\ell}^2 + \sum_{\ell \neq i} \mathbb{E}([\tilde{\mathbf{E}}]_{\ell j}^2) \zeta_{i\ell}^2 + \mathbb{E}([\tilde{\mathbf{E}}]_{ij}^2) \{\zeta_{ii} + \zeta_{jj}\}^2 \\ &\geq \left\{ \min_{(k, \ell) \in [n^2]} \mathbb{E}([\tilde{\mathbf{E}}]_{k\ell}^2) \right\} \left\{ \|[\mathbf{U}]_i\|^2 + \|[\mathbf{U}]_j\|^2 \right\}. \end{aligned} \quad (\text{S7.14})$$

As the distribution of η_{ij} is symmetric around 0, the distribution of $\tilde{\eta}_{ij}$ is also symmetric around 0 and $\mathbb{E}[\tilde{\eta}_{ij}] = 0$. We therefore have

$$\begin{aligned} \mathbb{E}([\tilde{\mathbf{E}}]_{ij}^2) &= p^{-1} \mathbb{E}\{([\mathbf{T}]_{ij} - p[\mathbf{T}]_{ij} + [\tilde{\mathbf{N}}]_{ij})^2\} + (1-p)[\mathbf{T}]_{ij}^2 \\ &= \frac{1-p}{p} [\mathbf{T}]_{ij}^2 + \frac{1}{p} \mathbb{E}[\tilde{\eta}_{ij}^2] \geq \frac{1-p}{p} \min_{k\ell} |T_{k\ell}|^2 + \frac{1}{2p} \sigma^2, \end{aligned} \quad (\text{S7.15})$$

provided that n is sufficiently large. The inequality in the above display is derived as follows.

By the Cauchy–Schwarz inequality we have

$$\frac{1}{\sigma^2} \mathbb{E}[\eta_{ij}^2 \mathbb{I}(|\eta_{ij}| > 5\sigma(\log n)^{1/2})] \leq \left(\mathbb{E}[(\eta_{ij}/\sigma)^4] \mathbb{P}[|\eta_{ij}/\sigma| > 5(\log n)^{1/2}] \right)^{1/2} = o(1), \quad (\text{S7.16})$$

and hence

$$\mathbb{E}([\tilde{\mathbf{N}}]_{ij}^2 / \sigma^2) = \sigma^{-2} \mathbb{E}[\eta_{ij}^2 \{1 - \mathbb{I}(|\eta_{ij}| > 5\sigma(\log n)^{1/2})\}] = 1 + o(1).$$

Under the conditions of Theorem [S6](#) we have that p is bounded away from 1 and \mathbf{T} is homogeneous, and thus

$$v_{ij} \gtrsim p^{-1} (\|\mathbf{T}\|_{\max}^2 + \sigma^2) \{ \|[\mathbf{U}]_i\|^2 + \|[\mathbf{U}]_j\|^2 \} \quad (\text{S7.17})$$

We next show that $v_{ij}/v_{ij}^* \rightarrow 1$ in probability and hence v_{ij} can be replaced by v_{ij}^* in without changing the limit result in Eq. [\(S2.7\)](#); here v_{ij}^* is defined in [\(S2.6\)](#). By Eq. [\(S7.15\)](#) and

Eq. (S7.16), we have

$$|\mathbb{E}[\mathbf{E}]_{k\ell}^2 - \mathbb{E}[\tilde{\mathbf{E}}]_{k\ell}^2| = \left| \frac{1}{p} \mathbb{E}[\eta_{kl}^2] - \frac{1}{p} \mathbb{E}[\tilde{\eta}_{kl}^2] \right| \leq \frac{\sigma^2}{p} \left(\mathbb{E}[(\eta_{kl}/\sigma)^4] \mathbb{P}(|\eta_{kl}| > 5\sigma(\log n)^{1/2}) \right)^{1/2}$$

and thus

$$\max_{(k,\ell) \in [n]^2} |\mathbb{E}[\mathbf{E}]_{k\ell}^2 - \mathbb{E}[\tilde{\mathbf{E}}]_{k\ell}^2| = o(p^{-1}\sigma^2). \quad (\text{S7.18})$$

Combining Eq. (S7.15), Eq. (S7.17) and Eq. (S7.18), we obtain

$$\begin{aligned} \left| \frac{v_{ij}^* - v_{ij}}{v_{ij}} \right| &\leq \left\{ \max_{(k,\ell) \in [n]^2} |\mathbb{E}[\mathbf{E}]_{k\ell}^2 - \mathbb{E}[\tilde{\mathbf{E}}]_{k\ell}^2| \right\} \cdot \frac{\left[\sum_{\ell \neq j} \zeta_{\ell j}^2 + \sum_{\ell \neq i} \zeta_{i\ell}^2 + \{\zeta_{ii} + \zeta_{jj}\}^2 \right]}{v_{ij}} \\ &\leq \frac{2 \max_{(k,\ell) \in [n]^2} |\mathbb{E}[\mathbf{E}]_{k\ell}^2 - \mathbb{E}[\tilde{\mathbf{E}}]_{k\ell}^2| \cdot \left\{ \|\mathbf{U}\|_i^2 + \|\mathbf{U}\|_j^2 \right\}}{\min_{(k,\ell) \in [n]^2} \mathbb{E}([\tilde{\mathbf{E}}]_{k\ell}^2) \cdot \left\{ \|\mathbf{U}\|_i^2 + \|\mathbf{U}\|_j^2 \right\}} = o(1), \end{aligned}$$

as desired. **Step 2.** We now consider an unbiased estimator for v_{ij} , namely

$$\tilde{v}_{ij} := \sum_{\ell \neq j} [\tilde{\mathbf{E}}]_{i\ell}^2 \zeta_{\ell j}^2 + \sum_{\ell \neq i} [\tilde{\mathbf{E}}]_{\ell j}^2 \zeta_{i\ell}^2 + [\tilde{\mathbf{E}}]_{ij}^2 (\zeta_{ii} + \zeta_{jj})^2.$$

Then by a standard application of Bernstein's inequality, we have $|\tilde{v}_{ij} - v_{ij}| = o(v_{ij}^*)$ with high probability. See the derivation of Eq. (4.171) in [Chen et al. \(2021\)](#) for more details. Next let

$\check{\mathbf{E}} := \hat{\mathbf{U}}_g \hat{\mathbf{U}}_g^\top \tilde{\mathbf{T}}/p - p^{-1} \hat{\mathbf{T}}$ where $\tilde{\mathbf{T}}$ is defined in Eq. (S7.13) and let

$$\check{v}_{ij} = \sum_{\ell \neq j} [\check{\mathbf{E}}]_{i\ell}^2 \zeta_{\ell j}^2 + \sum_{\ell \neq i} [\check{\mathbf{E}}]_{\ell j}^2 \zeta_{i\ell}^2 + [\check{\mathbf{E}}]_{ij}^2 (\zeta_{ii} + \zeta_{jj})^2.$$

Then whp $\check{\mathbf{E}} = \hat{\mathbf{E}} = \hat{\mathbf{T}}_g - p^{-1} \hat{\mathbf{T}}$ and $\check{v}_{ij} = \hat{v}_{ij}$. As $\tilde{\mathbf{E}} = \mathbf{E}$ whp, we have by Eq. (S2.3) that

$$\|\check{\mathbf{E}} - \tilde{\mathbf{E}}\|_{\max} = \|\hat{\mathbf{E}} - \mathbf{E}\|_{\max} = \|\hat{\mathbf{T}}_g - \mathbf{T}\| \lesssim p^{-1/2} (\|\mathbf{T}\|_{\max} + \sigma) (n \log n)^{1/2} \|\mathbf{U}\|_{2,\infty}^2$$

whp. Therefore, by standard tail bounds for Gaussian random variables, we have

$$\begin{aligned}
\|\check{\mathbf{E}}\|_{\max} &\lesssim \|\tilde{\mathbf{E}}\|_{\max} + \|\check{\mathbf{E}} - \tilde{\mathbf{E}}\|_{\max} \\
&\lesssim p^{-1/2}(\|\mathbf{T}\|_{\max} + \sigma)(n \log n)^{1/2} \|\mathbf{U}\|_{2,\infty} + p^{-1} \left\{ \|\mathbf{T}\|_{\max} + \sigma \sqrt{\log n} \right\} \\
&\lesssim \frac{1}{p} \left\{ \|\mathbf{T}\|_{\max} + \sigma \sqrt{\log n} \right\},
\end{aligned}$$

whp. Furthermore, we have by Eq. (S7.9) that

$$\|\hat{\mathbf{U}}_g\|_{2,\infty} \leq \|\mathbf{U}\|_{2,\infty} + d_{2,\infty}(\hat{\mathbf{U}}_g, \mathbf{U}) = (1 + o(1)) \|\mathbf{U}\|_{2,\infty}$$

whp and hence

$$\|\hat{\mathbf{U}}_g \hat{\mathbf{U}}_g^\top - \mathbf{U} \mathbf{U}^\top\|_{\max} \leq \|\hat{\mathbf{U}}_g \hat{\mathbf{U}}_g^\top - \hat{\mathbf{U}} \hat{\mathbf{U}}^\top\|_{\max} + \|\hat{\mathbf{U}} \hat{\mathbf{U}}^\top - \mathbf{U} \mathbf{U}^\top\|_{\max} = (1 + o(1)) \|\hat{\mathbf{U}} \hat{\mathbf{U}}^\top - \mathbf{U} \mathbf{U}^\top\|_{\max}$$

whp. In summary we have whp that

$$\|\hat{\mathbf{U}}_g \hat{\mathbf{U}}_g^\top\|_{\max} \leq \|\hat{\mathbf{U}}_g \hat{\mathbf{U}}_g^\top - \mathbf{U} \mathbf{U}^\top\|_{\max} + \|\mathbf{U} \mathbf{U}^\top\|_{\max} \lesssim \|\mathbf{U}\|_{2,\infty}^2.$$

Step 3. Finally we bound $|\hat{v}_{ij} - v_{ij}^*|$ using the same arguments as that presented in Eq. (4.176)–Eq. (4.177) of [Chen et al. \(2021\)](#), but with terms depending on $\hat{\mathbf{U}}$ replaced by terms depending

on $\hat{\mathbf{U}}_g$. More specifically let $\hat{\zeta}_{k\ell} = [\hat{\mathbf{U}}_g \hat{\mathbf{U}}_g]_{k\ell}^\top$. We then have, after some tedious algebra, that

$$\begin{aligned}
|\hat{v}_{ij} - \tilde{v}_{ij}| &= |\check{v}_{ij} - \tilde{v}_{ij}| \\
&\leq \left| \sum_{\ell \neq j} ([\check{\mathbf{E}}]_{i\ell}^2 \hat{\zeta}_{\ell j}^2 - [\tilde{\mathbf{E}}]_{i\ell}^2 \zeta_{\ell j}^2) \right| + \left| \sum_{\ell \neq i} ([\check{\mathbf{E}}]_{\ell j}^2 \hat{\zeta}_{i\ell}^2 - [\tilde{\mathbf{E}}]_{\ell j}^2 \zeta_{i\ell}^2) \right| + 2 \left| [\check{\mathbf{E}}]_{ij}^2 \hat{\zeta}_{ii} \hat{\zeta}_{jj} - [\tilde{\mathbf{E}}]_{ij}^2 \zeta_{ii} \zeta_{jj} \right| \\
&\lesssim (\|\check{\mathbf{E}}\|_{\max} + \|\tilde{\mathbf{E}}\|_{\max}) \|\check{\mathbf{E}} - \tilde{\mathbf{E}}\|_{\max} \|\hat{\mathbf{U}}_g \hat{\mathbf{U}}_g^\top\|_{\max} \\
&\quad + (\|\hat{\mathbf{U}}_g \hat{\mathbf{U}}_g^\top\|_{\max} + \|\mathbf{U} \mathbf{U}^\top\|_{\max}) \|\hat{\mathbf{U}}_g \hat{\mathbf{U}}_g^\top - \mathbf{U} \mathbf{U}^\top\|_{\max} \|\tilde{\mathbf{E}}\|^2 \\
&\quad + (\|\check{\mathbf{E}}\|_{\max} + \|\tilde{\mathbf{E}}\|_{\max}) \|\check{\mathbf{E}} - \tilde{\mathbf{E}}\|_{\max} \|\hat{\mathbf{U}}_g \hat{\mathbf{U}}_g^\top\|_{\max}^2 \\
&\quad + \|\tilde{\mathbf{E}}\|_{\max}^2 (\|\hat{\mathbf{U}}_g \hat{\mathbf{U}}_g^\top\|_{\max} + \|\mathbf{U} \mathbf{U}^\top\|_{\max}) \|\hat{\mathbf{U}}_g \hat{\mathbf{U}}_g^\top - \mathbf{U} \mathbf{U}^\top\|_{\max} \\
&\lesssim \|\tilde{\mathbf{E}}\|_{\max} \|\hat{\mathbf{T}}_S - \mathbf{T}\|_{\max} \|\mathbf{U} \mathbf{U}^\top\|_{\max} + \|\mathbf{U} \mathbf{U}^\top\|_{\max} \|\hat{\mathbf{U}} \hat{\mathbf{U}}^\top - \mathbf{U} \mathbf{U}^\top\|_{\max} \|\tilde{\mathbf{E}}\|^2 \\
&\quad + \|\tilde{\mathbf{E}}\|_{\max} \|\mathbf{T}_S - \mathbf{T}\|_{\max} \|\mathbf{U} \mathbf{U}^\top\|_{\max}^2 + \|\tilde{\mathbf{E}}\|_{\max}^2 \|\mathbf{U} \mathbf{U}^\top\|_{\max} \|\hat{\mathbf{U}} \hat{\mathbf{U}}^\top - \mathbf{U} \mathbf{U}^\top\|_{\max}
\end{aligned} \tag{S7.19}$$

Now define

$$B = \|\tilde{\mathbf{E}}\|_{\max} \lesssim p^{-1} \{\|\mathbf{T}\|_{\max} + \sigma \log^{1/2} n\}, \quad \sigma_E^2 = \max_{k\ell} \mathbb{E}([\tilde{\mathbf{E}}]_{k\ell}^2) \lesssim p^{-1} (\|\mathbf{T}\|_{\max}^2 + \sigma^2).$$

Then, following the same steps as that for bounding Eq. (4.177) in [Chen et al. \(2021\)](#) (where we had assumed that $k_0 \lesssim 1$ and $\kappa \lesssim 1$, which then implies $\|\mathbf{U}\|_{2,\infty} \asymp n^{-1/2}$) we have

$$\begin{aligned}
|\hat{v}_{ij} - v_{ij}| &\lesssim \frac{B \sigma_E (\log n)^{1/2}}{n^{3/2}} + \frac{\sigma_E^3 (\log n)^{1/2}}{|\lambda_{k_0}(\mathbf{T})| n^{1/2}} \\
&\lesssim \frac{(\log n) \{\|\mathbf{T}\|_{\max} + \sigma\}^2}{(np)^{3/2}} + \frac{(\log n)^{1/2} \{\|\mathbf{T}\|_{\max} + \sigma\}^3}{n^{1/2} p^{3/2} |\lambda_{k_0}(\mathbf{T})|}
\end{aligned} \tag{S7.20}$$

Combining Eq. (S7.20) and Eq. (S7.11) we obtain

$$\frac{|\hat{v}_{ij} - v_{ij}|}{v_{ij}} \lesssim \frac{\log n}{(np)^{1/2}} + \frac{(n \log n)^{1/2} \{\|\mathbf{T}\|_{\max} + \sigma\}}{p^{1/2} |\lambda_{k_0}(\mathbf{T})|} = o(1)$$

where the final equality follows from the assumptions C3 and C4 in Theorem S6. Therefore, by Slutsky's Theorem and Eq. (S7.12), we have

$$\frac{[\hat{\mathbf{T}}_g - \mathbf{T}]_{ij}}{\hat{v}_{ij}^{1/2}} = \left(\frac{v_{ij}}{\hat{v}_{ij}} \right)^{1/2} \frac{[\hat{\mathbf{T}}_g - \mathbf{T}]_{ij}}{v_{ij}^{1/2}} \rightsquigarrow \mathcal{N}(0, 1),$$

as desired.

S7.3 Proof of Theorem S7

Let $\mathbf{Q}^* = \mathbf{BF}(\mathbf{BF})^\top$. Then with probability at least $1 - d^{-10}$, we have

$$|\lambda_i(\mathbf{Q}^*)| \asymp m\lambda_i \text{ for } i \in [k_0]. \quad (\text{S7.21})$$

and conditional on a given \mathbf{Q}^* , with probability at least $1 - d^{-10}$,

$$\|\mathbf{Q} - \mathbf{Q}^*\| \lesssim m\lambda_{k_0}\mathcal{E}. \quad (\text{S7.22})$$

See Eq. (33) and Eq. (37) in the supplementary material of [Cai et al. \(2021\)](#) for derivations of the above bounds; note that the quantities n, r and \mathcal{E}_{ce} in [Cai et al. \(2021\)](#) corresponds to the quantities m, k_0 and \mathcal{E} in the current paper. Let $E_n = m\lambda_k\mathcal{E}$. Then, recalling the condition for m in Eq. (S3.5), we have $\lambda_{k_0}(\mathbf{Q}^*)/E_n \asymp \mathcal{E}^{-1} \gtrsim \log^2(m + d)$ with probability at least $1 - d^{-6}$. Therefore, by applying Corollary 2 and Corollary 3 with $\mathbf{M} = \mathbf{Q}^*$, $\widehat{\mathbf{M}} = \mathbf{Q}$, $\tilde{k} \geq (1 + c_{\text{gap}}) \max\{k_0, \log n\}$ and $g \geq g_* = \frac{\log d}{\log(1/\mathcal{E})}$, we have with probability at least $1 - d^{-5}$ that

$$d_2(\widehat{\mathbf{U}}_g, \mathbf{U}) \leq d_2(\widehat{\mathbf{U}}, \mathbf{U}) + \mathcal{E}, \quad \text{and} \quad d_{2,\infty}(\widehat{\mathbf{U}}_g, \mathbf{U}) \leq d_{2,\infty}(\widehat{\mathbf{U}}, \mathbf{U}) + o(d^{-1/2}\mathcal{E}) \quad (\text{S7.23})$$

Eq. (S3.7) follows directly from Eq. (S7.23) together with bounds for $d_2(\widehat{\mathbf{U}}, \mathbf{U})$ and $d_{2,\infty}(\widehat{\mathbf{U}}, \mathbf{U})$ given in Corollary 4.3 of [Cai et al. \(2021\)](#). \square